TUMOR-HOSTING ORGANS DIFFERENTIALLY INFLUENCE TUMOR GROWTH AND RESPONSE TO THERAPY

by

YAHYA SAEED Y AL HAMHOOM

(Under the Direction of Dexi Liu)

ABSTRACT

Tumor microenvironment plays an essential role in tumor growth and drug resistance. Accumulated evidence during recent years suggest the existence of environmental heterogeneity among different organs. We hypothesized that solid tumors growing in different organs have different microenvironments and, therefore, tumors may exhibit different growth and sensitivities to anticancer therapy. In this project, we established a multi-organ tumor model using the hydrodynamic cell delivery method to seed identical tumor cells in different organs: lung, liver, and kidneys. The multi-organ tumor model allowed us to assess the contributions of the stroma of different organs to tumor growth and its response to antitumor therapies. Ultrastructural analysis with electron microscopy demonstrated different tumor cell-stroma interactions in different organs. In the lung, tumor cells proliferated intravascularly, causing expansion of the capillaries diameter and loss of the mesh-like structure formed by the alveoli. In the liver and kidneys, tumor cells proliferated extravascularly, as evidenced by hepatic cords disruption and renal tubules disorganization, respectively. Another evidence of extravascular tumor growth in the liver and kidneys is the vascular damage that resulted from tumor cell intravasation. Moreover, tumor growth rate analysis demonstrated that renal cell carcinoma tumors grew more rapidly in the

kidneys, whereas tumor growth in the lung was the slowest. Additionally, tumors in different organs responded differentially to 5-fluorouracil and cytokine gene therapy. 5-fluorouracil significantly suppressed tumor growth in the lung and liver, while tumors in the kidneys were resistant to the treatment. IL-12 gene therapy resulted in whole-body tumor suppression and prolonged animal survival. IFN-β gene therapy was effective in suppressing tumor growth in the liver but not effective for those in the lung and kidneys. Our results suggested that cancer cells, once metastasized in different organs, have different growth patterns and respond differently to treatment. This project highlights the differential influences of the stroma of different organs on the tumor growth and the need to consider this when designing anticancer therapies. Our data also imply that an animal model with multi-organ tumor growth is critical for the development of a new strategy for cancer metastasis treatment.

INDEX WORDS: Cancer metastasis, Cancer treatment, Tumor heterogeneity, Tumor microenvironment, Multi-organ tumor model, Hydrodynamic delivery, Preclinical tumor metastatic model, Tumor growth, Tumor resistance.

TUMOR-HOSTING ORGANS DIFFERENTIALLY INFLUENCE TUMOR GROWTH AND RESPONSE TO THERAPY

by

YAHYA SAEED Y AL HAMHOOM

B.S., King Khalid University, Abha, Saudi Arabia, 2007

A Dissertation Submitted to the Graduate Faculty of The University of Georgia in Partial Fulfillment of the Requirements for the Degree

DOCTOR OF PHILOSOPHY

ATHENS, GEORGIA

2017

© 2017

YAHYA SAEED Y AL HAMHOOM

All Rights Reserved

TUMOR-HOSTING ORGANS DIFFERENTIALLY INFLUENCE TUMOR GROWTH AND RESPONSE TO THERAPY

by

YAHYA SAEED Y AL HAMHOOM

Major Professor:	Dexi Liu
Committee:	Michael Bartlett
	James Franklin
	Mandi Murph
	Rajgopal Govindarajan

Electronic Version Approved:

Suzanne Barbour
Dean of the Graduate School
The University of Georgia
August 2017

DEDICATION

I dedicate this dissertation to….

…. to my parents, **Saeed** and **Khayria**.

The fountain of love, optimism and support.

You are always there to clear the thorns from my path of seeking knowledge.

….to my soulmate, **Wedad**.

A burning candle to illuminate my life.

You are always there when I need a sympathetic ear to share my pains and frustrations. You always make the obstacles easier and enjoyable to overcome.

….to my children, **Thamer**, **Hatem** and **Shaden**.

Angels fluttering in my life spreading love and joy.

Thamer, thank you for staying by your mother's side whenever I am away from home.

….to my siblings, **Ali**, **Zhoor**, **Halimah**, **Abeer** and **Azhar.**

The immaculate hearts that kept me in their prayers.

ACKNOWLEDGEMENTS

First, all gratefulness and appreciation go to Allah (God) for his favors both seen and unseen.

I would like to express my appreciation to my advisor, Dr. Dexi Liu, for his guidance and support for my PhD work. He encouraged me to think critically when I read literature, develop my own hypotheses and ideas, and design my experiments. I am thankful for his advice on how to communicate effectively.

I would like to thank my committee members, Dr. Michael Bartlett, Dr. James Franklin, Dr. Rajgopal Govindarajan and Dr. Mandi Murph, for their advice and guidance. I would like to thank Dr. Shanta Dhar for serving on my committee and her support while she was at the University of Georgia. I would like to thank Dr. Robert D Arnold for serving as my advisor during my first 2.5 years in the graduate program.

My appreciation also goes to the previous and current members of Dr. Liu's lab for their companionship, and for the memories of life in graduate school, doing research and having fun together. I would like to express my gratitude to Sary Alsanea for his friendship and help, both in academics and personal life.

I would like to thank Dr. Megan Morgan for proofreading this dissertation.

Finally, I would like to thank King Khalid University in Abha, Saudi Arabia, for the financial support to pursue the PhD.

PREFACE

The purpose of this dissertation is to present the findings of my dissertation project, which demonstrated the influence of different anatomical sites on tumor growth and response to therapy. This project was presented as the main body of the dissertation and formatted in regular chapter style. Part of this project was previously published as a research paper (Alhamhoom *et. al*, *In vivo* growth and responses to treatment of renal cell carcinoma in different environments, 2017, American Journal of Cancer Research, Volume 7(2), pp 301-311).

In addition to the dissertation research work, this dissertation includes additional work I carried out in Dr. Dexi Liu's lab. As the lab is interested in identifying new genes for prevention and treatment of obesity, I took a chance to investigate the role of sPLA2G5 in HFD-induced obesity. In addition, I participated in writing a book chapter on targeted delivery of oligonucleotides (Alhamhoom *et. al*, Future perspective: toward targeting at the cellular level, 2015, in "Advances and Challenges in the Delivery of Nucleic Acid Therapeutics, Volume 2", edited by Olivia Merkel & Mansoor M. Amiji, Future Medicine, London, UK, pp 2-17). Since these works were side projects and out of the scope of the dissertation project, both works were included as separate appendices at the end of the dissertation.

Of note, during my first 2.5 years in the PBS graduate program, I was in Dr. Robert D. Arnold's lab. My major project focused on developing a novel liposome formulation of topotecan-carboxylate (TPT-carboxylate) and a HPLC method to analyze the amount of both carboxylate and lactone forms of TPT simultaneously. Besides working on my main project in Dr. Arnold's lab, I was also involved in other projects that were collaborations between Dr. Arnold's lab and other

labs in the College of Pharmacy and School of Veterinary Medicine. My participation in these projects involved fabrication of liposome formulation and LC-MS/MS analyses of small molecules and lipids in biological samples. The results of these projects were published as research papers and not included in this dissertation. My participation in these projects was discontinued when Dr. Arnold left for Auburn University and I shifted to Dr. Liu's lab.

TABLE OF CONTENTS

Page

LIST OF TABLES

Page

LIST OF FIGURES

Page

ABBREVIATIONS

5-FU	5-Fluorouracil
ADAMTS1	A disintegrin and metalloproteinase with thrombospondin motifs
ANGPTL4	Angiopoietin-like 4
BBB	Blood brain barrier
BH3	Bcl-2 Homology 3
BMSCs	Bone marrow stromal cells
BRCA	Breast cancer susceptibility gene
CCR9	Chemokine receptor type 9
CKB	Creatine kinase brain-type
CNS	Central nervous system
COX-2	Cyclooxygenase-2
CSF1	Colony-stimulating factor 1
CTLA-4	Cytotoxic T-lymphocyte-associated protein 4
CXCL12	Chemokine ligand 12
CXCR4	Chemokine receptor type 4
DMEM	Dulbecco’s Modified Eagle’s Medium
DPBS	Dulbecco's phosphate-buffered saline
ECM	Extracellular matrix
EDTA	Ethylenediaminetetraacetic acid
EGF	Epidermal growth factor

EGFR	Epidermal growth factor receptor
EM	Electron microscopy
EMT	Epithelial-mesenchymal transition
FABP4	Fatty acid–binding protein 4
FasL	Fas ligand
FBS	Fetal bovine serum
FDA	Food and Drug Administration
FOV	Field of view
GEMM	Genetically engineered mouse model
GFP	Green fluorescent protein
GP100	Glycoprotein 100
H&E	Hematoxylin and eosin
HGF/c-Met	Hepatocyte growth factor/ tyrosine-protein kinase Met pathway
HH	Hedgehog
HIF-1	Hypoxia-inducible factor 1
i.p.	Intraperitoneal
i.v.	Intravenous
IFN-β	Interferon beta
IL	Interleukin
IVC	Inferior vena cava
JAM-B	Junctional adhesion molecule B
KRAS	Kirsten rat sarcoma
L1CAM	L1 cell adhesion molecule

Luc	Luciferase
mAb	Monoclonal antibody
MM	Multiple myeloma
MMP-1	Matrix metalloproteinase-1
MMP-9	Matrix metalloproteinase-9
MQ	Milli-Q
Nf2	Neurofibromatosis type 2 gene
NK	Natural killer
NSCLC	Non-small cell lung cancer
OD	Optical density
OPN	Osteopontin
p/s/cm^2/sr	Photons/second/cm^2/steradian
PARP	Poly ADP ribose polymerase
PBS	Phosphate buffered saline
PD-1	Programmed cell death protein 1
PD-L1	Programmed death-ligand 1
PDK1	Pyruvate dehydrogenase kinase-1
PGC-1α	Peroxisome proliferator-activated receptor gamma coactivator 1-alpha
RANK	Receptor activator of nuclear factor kappa-B
RCC	Renal cell carcinoma
RFP	Red fluorescent protein
RLU	Relative light units
rpm	Revolutions per minute

RPMI-1640	Roswell Park Memorial Institute medium 1640
SD	Standard deviation
SDS	Sodium dodecyl sulfate
SEAP	Secreted embryonic alkaline phosphatase
SEM	Scanning electron microscope
ST6GALNAC5	Beta-N-acetylgalactosaminide alpha 2,6 sialyltransferase
TGF-β	Transforming growth factor beta
Th1	Type 1 T helper
TnC	Tenascin C
VEGF	Vascular endothelial growth factor
WHO	World Health Organization

CHAPTER 1

INTRODUCTION

1.1. Cancer Metastasis

The breaking away of tumor cells from a tumor mass, localized in a specific organ, and their spread to other anatomical sites forming new tumor masses is called cancer metastasis. The majority of patients who demonstrate tumor metastasis at the time of diagnosis have a high risk of death. According to the most recent cancer statistical analysis, the five-year survival rates for patients with tumor metastasis range between 3%, as in the case of pancreatic cancer, to around 29% for prostatic cancer metastasis [1]. While patients with primary tumors are commonly treated surgically and have a high chance to survive, patients with metastatic tumors need systemic therapy to target metastatic nodules, in addition to surgical dissection of the primary tumors.

Research has offered a variety of options with different mechanisms of action for treatment of cancer metastasis. The current list of approaches includes chemotherapy, hormone therapy, radiation therapy, immunotherapy and the recently developed targeted therapy, such as gefitinib, which targets epidermal growth factor receptor (EGFR) [2-4]. Unfortunately, all conventional treatments do not show satisfactory improvement in the survival of patients [1], with the exception of recently FDA approved immunotherapy, which extended patients' survival for a few months compared to chemotherapy [5-7]. Unfortunately, targeted therapies do not produce detectable improvement [8-11]. Clinically, cancer metastasis is the leading cause of death for cancer patients [12].

1.2. Translational Gap Between Preclinical Studies and Clinical Trials

The comprehensive preclinical investigation over the past several decades to understand cancer metastasis biology and to develop effective anticancer drugs does not match the outcomes of treating patients with cancer metastasis. For example, targeted small molecules and antibodies, which are considered cutting-edge therapies, demonstrated excellent antitumor activity *in vitro* and *in vivo*. Targeted therapies effectively eradicate the tumor metastasis and improve survival of model animals [13-15]. However, oncologists are facing a major obstacle in translating the excellent antitumor outcomes from preclinical research to the clinic [11, 15-17]. Only around 6.7% of antitumor agents that were selected based on preclinical animal studies show activity in clinic [18].

Many reasons can account for these undesirable outcomes, including toxicity, low bioavailability, and undesirable pharmacokinetics and pharmacodynamics between mice and humans [19-25]. One critical factor, in our opinion, is the use of improper animal models for therapeutic evaluation. For an extended period in the past, cancer research has relied on using animal models that overlook essential characteristics of tumor metastasis, such as tumor cell-stroma communication and the influence of environment on tumor growth in different organs. For instance, the subcutaneous tumor model ignores the contribution of the visceral organs, which are the natural sites of metastasis, to drug resistance [26]. Moreover, the orthotopic tumor model represents the communication between the tumor cells and the stroma at the primary organ where the tumor is initiated.

1.3. Tumor Cell and Stroma Communication

Tumor metastasis does not rely solely on the intrinsic properties of the tumor cells but rather on the complex interplays between the tumor cells and the surrounding stroma, consisting of non-malignant cells and extracellular matrix. The stroma supports tumor cells throughout different stages of the metastasis, such as during the escape from the primary tumor, intravasation, hematogenous spread, extravasation and metastatic nodule growth. The stroma helps tumor cells escape from both innate and adaptive immunity [27] and plays a major role in shaping tumor response to therapy. For example, it has been shown that breast tumor cells responded to doxorubicin when the surrounding stroma losses the production of MMP9 and CCR2 better than tumors growing in the presence of these factors [28].

Tumor cells forming metastatic nodules in a specific organ are tumor-type specific. The tumor growth in the secondary organs is governed by the organ-specific and bidirectional communication between tumor cells and the surrounding environment. Thus, disseminated tumor cells are only able to survive in a new organ when it provides the necessary and supporting environment [29].

Cumulative evidence suggests that each organ has unique characteristics to facilitate tumor cell colonization. For example, it was shown that neuroblastoma tumors growing orthotopically in the adrenal gland are surrounded by more immunosuppressive M2 macrophages compared to the same tumor growing subcutaneously [30]. Therefore, stroma in various organs would influence the therapeutic outcomes of tumor therapy. Results from a few recent studies agree with this view, showing that the ectopic factors influence drug sensitivity of the tumor cells differently when compared to that of cells at an orthotopic site. Comparing kidney tumor cells growing subcutaneously to those growing orthotopically, Devaud *et al*. have shown a significantly better

suppression of subcutaneous tumors when treated with Tri-mAb immunotherapy [31]. As far as cancer research is concerned, subcutaneous tumor growth was established for the convenience of monitoring tumor growth [32, 33]. The subcutaneous environment is significantly different from that of organs or tissues in which tumor metastasis takes place. Thus, an animal model that represents the real situation of tumor metastasis needs to be developed.

1.4. Multi-organ Tumor Model to Evaluate the Impact of Stroma

A hallmark of tumor metastasis is tumor growth at multiple distant sites from the site of primary tumor [34]. It is possible that tumor cells, once metastasized, grow differently in the new environments and would have different responses to the same treatment. An unmet need in research is to examine and assess the impact of stroma in different organs on tumor growth. As far as anticancer drug development is concerned, therapeutic assessments of drug candidates will require animals with tumor growth in different organs, mimicking clinical situations. To this end, a previous study in this laboratory developed a method using hydrodynamic delivery to implant tumor cells into mouse lung, liver and kidneys [35]. The multi-organ tumor growth achieved, compared to other preclinical metastatic models, offering the possibility to assess how tumor cells grow in the unique environment of different organs and how tumors growing in these organs respond to therapeutic treatment.

1.5. Hypothesis and Objectives

The overall goal of this dissertation research is to evaluate the impact of different organs on tumor growth and response to treatments. The dissertation hypothesis is that different organs have differential influences on tumor growth and response to therapy. The results generated can

address the importance of evaluating systemic antimetastatic therapies in multi-organ preclinical tumor models to improve the translational research and develop more efficient antimetastatic drugs. It might be necessary to combine different anticancer drugs based on the efficacy of each drug in a particular organ in order to eradicate metastatic nodules in different anatomical sites. The following are the dissertation research objectives:

Objective 1: To establish and characterize tumor growth in multi-organ tumor models of breast cancer and renal cell carcinoma:

Aim 1: Establish multi-organ tumor models of 4T1 breast cancer and Renca renal cell carcinoma.

Aim 2: Analyze structural interactions of the tumor cells with the stroma in the lung, liver, and kidney using a multi-organ tumor model of 4T1 breast cancer.

Aim 3: Quantify tumor growth in each organ using a multi-organ tumor model of Renca renal cell carcinoma.

Objective 2: To examine the influence of stroma of different organs on tumor cell response to anticancer therapy:

Aim 1: Evaluate response of tumors growing in different organs to 5-fluorouracil chemotherapy.

Aim 2: Assess the impact of cytokine gene therapy on tumors growing in various organs.

This dissertation consists of six chapters including this introduction chapter. Chapter two provides a literature review on cancer metastasis, current treatment options for cancer treatment and their limitations. The literature review discusses advantages and limitations of the recently developed animal models. Chapter three details experimental designs and procedures utilized in the dissertation research. Chapter four reports findings of differential growth of tumors in different organs and the

existence of tumor heterogeneity between various metastatic organs in response to therapy. Chapter five provides a discussion on the results with concluding remarks. Chapter six discusses the remaining challenges in treating tumor metastasis in the clinic and provides future perspectives focusing on opportunities offered by the multi-organ tumor model to advance cancer research.

CHAPTER 2

LITERATURE REVIEW: PROGRESS IN MODELING THE ENVIRONMENTAL HETEROGENEITY OF THE ORGANS FOR PRECISE ANTIMETASTATIC TREATMENT

2.1. Cancer and Cancer Metastasis

2.1.1. *Cancer*

Cancer is a complicated disease that involves genetic mutations and gene expression alterations that cause cells to undergo uncontrolled proliferation and exert abnormal functions [36]. *Tumor* and *neoplasm* are other terms used instead of *cancer*. Research suggested that intrinsic DNA replication errors or external factors, such as smoking and infectious microbes, initiate DNA mutation and cause the cell to lose control of its programmed proliferation and death machinery [37-39]. Because of cancer cell infinite growth, the cancer mass invades adjacent healthy tissue and disrupts the physiological homeostasis of the organ. Cancer cells with different genetic mutation profiles share common features called hallmarks. Hallmarks of cancer include uncontrolled proliferation, growth signal production self-dependency, antigrowth signal resistance, cell death escape, immunosurveillance escape, angiogenesis, altered cellular metabolism, and metastasis (spread) [40]. Besides these hallmark traits, cancer cells hijack the surrounding healthy stromal cells and recruit non-malignant cells to the tumor site to enhance cancer cell growth [41].

Cancer arises from all body tissues, which has led the World Health Organization (WHO) to categorize different cancer types into six main categories based on the tissue of origin. Carcinoma is considered the most common category and includes epithelium tissue-derived

cancers. Carcinoma cancers initiate from the cells that form the internal and external surfaces of the body, such as breast adenocarcinoma. Sarcoma is another category that includes cancers originating from the bone and connective tissues. Leukemia and myeloma are two separate categories that include cancers of immature white blood cells and plasma cells, respectively. Lymphoma is for cancer developed in the lymph glands and nodes. Finally, the mixed cancer category includes cancers that have a mixture of different types of cancers within the same category or from the above-mentioned categories, such as adenosquamous carcinoma or carcinosarcoma [42].

Cancer is also classified based on the cancer stage. A TNM staging system specifies the size of the primary tumor (T), the involvement of lymph nodes (N), and metastasis to distant organs (M). Clinicians use different strategies to identify cancer stages that include: physical examination, biopsy procedures, imaging techniques and surgical staging. The TNM staging system is beneficial since it allows clinicians to determine the treatment options and assess the treatment outcomes [43].

2.1.2. *Cancer Metastasis*

Cancer metastasis is the last step of cancer progression. Cancer metastasis is defined as the process whereby cancer cells travel from the organ where they initiated to other, not necessarily neighboring, organs and develop new nodules. The presence of the metastasis feature allows the oncologist to distinguish a malignant tumor from a benign one. Many tumor cells detach from the primary tumors, but only a very few tumor cells can form metastatic foci in specific organs [44, 45]. The metastatic process commonly begins when the primary tumors are large enough, as evident by the prevention of metastasis when the primary tumor is removed by surgery soon after

formation. In rare cases, however, metastasis can initiate when the primary tumor is still a small nodule [46].

The metastatic process is composed of sequential rate limiting steps, so an interruption in any step prevents the establishment of tumor nodules in secondary organs. When the primary tumor grows to a mass with a diameter of more than 1 mm, tumor cells and surrounding host cells release proangiogenic factors. Vascular endothelial growth factor (VEGF) and epidermal growth factor (EGF) are among many proangiogenic factors that initiate the formation of new vasculature [47, 48]. Metastasis starts when tumor cells lose their attachment to adjacent cells and the extracellular matrix and gain the traits of mesenchymal cells, including the ability to remodel their cytoskeleton and migrate through a process called epithelial-mesenchymal transition (EMT). Detached tumor cells secrete enzymes, such as matrix metalloproteinases, to enhance the degradation of the extracellular matrix and facilitate tumor cells to travel toward and penetrate new blood or lymphatic vasculature [49]. Cells that reach circulation will be transported to various organs, and with help from platelets, tumor cells can escape immune system recognition [50, 51]. Tumor cells that survive the shear stress of blood flow and arrive at distant organs extravasate into the new organ parenchyma and start forming metastatic nodules [52]. Research estimates that only 0.01% of metastatic tumor cells that detach from primary tumor can successfully form micrometastasis in secondary sites [44].

2.1.3. *Organotropism of Metastasis*

Cancer metastases grow in predictable organs based on the type of cancer. Stephen Paget was the first to observe that there was a pattern for metastatic nodule distribution after studying tumor tissue samples collected from patients with metastatic breast cancer [53]. Paget found that

breast cancer metastasized to the lung, liver, ovary and bone. Based on his findings, Paget proposed the "seed and soil" hypothesis. An alternative hypothesis states that metastasis results from the entrapment of tumor cells in the first capillary that the tumor cells encounter. However, Paget believed that was not enough. He claimed that tumor cell "seeds" can reach various organs, including distant ones, but it is the "congenial soil" that provides a supporting environment for the extravasated tumor cells to proliferate [29]. Decades later, research revived Paget's hypothesis when radiolabeled melanoma cells, injected *iv* into mice, formed metastatic nodules in the subcutaneous and intramuscular grafted tissues of the lung and ovary but not in the grafted tissue of the kidney [54]. Furthermore, the incapability of colon cancer to form metastatic lesions in the thyroid gland while it can in the liver indicates that the blood circulation pattern is not the central regulator for secondary site metastasis. Instead, an interaction between tumor cells and the surrounding stroma, non-malignant cells and extracellular matrix (ECM), is the key mediator for a successful metastasis [55].

The concept of organotropism describes the propensity of tumor cells to grow in specific secondary sites. After Paget's remarkable observation with breast cancer colonization in particular organs, others have studied the common metastatic sites for different types of cancer. A study has demonstrated that lung cancer commonly metastasizes to the brain, liver, lymph nodes and bone. Additionally, it was observed that colon cancer mainly spreads to the liver and lung, while ovarian cancer commonly spreads to the abdominal cavity and liver [56]. Melanoma commonly metastasizes to the lung, brain, bone and liver [34]. Moreover, research has demonstrated the development of neuroblastoma metastases in the lung, liver, skin and bone [57].

2.2. Tumor Cell-Stroma Communications at Metastatic Sites

2.2.1. *Organ-specific Support for Extravasation*

Tumor metastasis is not a random process, as mentioned previously. It is predictable for tumor cells to form metastatic nodules in specific organs depending on the type of cancer. Studies to understand why tumor cells possess a tendency to colonize specific organs have been carried out during the last several decades [58-60]. The current findings do not clearly explain this phenomenon. However, organ-specific architecture, the presence of a unique receptor or ligand, secretion of signaling molecules and ECM support tumor cells' attachment and extravasation [61, 62]. Research has indicated that the blood vessel architecture in the new environment contributes to the attachment and extravasation of tumor cells at the new site. The different structure of blood vessels in different organs had a differential impact on tumor cell extravasation. In the liver and bone, the presence of fenestra in the blood vessel walls makes the extravasation process easier in these organs compared to the tight junctions between the endothelial cells lining the pulmonary vasculature [63]. In the brain, the presence of the blood-brain barrier creates a challenge for tumor cells to extravasate. Tumor cells cannot colonize the brain without receptor-mediated extravasation, such as extravasation by ST6GALNAC5, as will be explained later [59, 61, 62, 64].

Additionally, the expression of unique ligands or receptors in the secondary organs is another mechanism by which stroma can support attachment and extravasation. Thus, only metastatic tumor cells that upregulate specific proteins for these specific ligands or receptors can take advantage of these proteins for seeding in specific organs. In the lung and lymph nodes, for example, chemokine ligand CXCL12 that overexpressed in these sites attracted circulating breast cancer cells that expressed CXCR4, a receptor for CXCL12 [65]. Similarly, the vasculature of the lung possessed the ligand for metadherin, a cell surface protein overexpressed in breast tumor

cells, which allowed tumor cells to attach to the pulmonary blood vessels. Blocking this ligand in the vasculature or suppressing the expression of metadherin in tumor cells prevented breast cancer colonization in the lung [66]. In the bone, a study found that metastatic cells of breast, prostate and lung cancers that colonize the bone upregulated the receptor activator of nuclear factor kappa-B (RANK). RANK allowed tumor cells to colonize bone tissues through binding with its ligand RANKL that was expressed by osteoblasts [67]. In the brain, research found beta-N-acetylgalactosaminide alpha 2,6 sialyltransferase (ST6GALNAC5) expressed in the brain metastasis of breast cancer. ST6GALNAC5 helped breast cancer cells to extravasate into the brain tissue. Inhibition of ST6GALNAC5 destroyed the ability of breast cancer to pass through the BBB [59, 64]. Angiopoietin-like4 (ANGPTL4) is another cell surface protein that played a role in both brain and lung colonization. The research found that ANGPTL4 is overexpressed and helped breast cancer cells to metastasize to these organs [59, 61, 62, 68].

Moreover, research observed that specialized stromal cells release signaling molecules and proteins upon or before the arrival of the disseminated tumor cells to the receptive organs. A study reported that the proteins secreted by stromal cells in the liver mediated pancreatic cancer colonization in the liver. Kupffer cells and hepatic stellate cells produced transforming growth factor β (TGF-β) and fibronectin, respectively, in response to the stimulation by pancreatic cancer-derived exosomes [69]. In the brain, astrocytes have displayed dual roles in promoting or blocking metastasis. Plasminogen activator released from astrocytes blocks L1CAM-dependent extravasation by cleaving L1CAM, which is expressed on tumor cell surface. Moreover, plasminogen activator cleaves the Fas ligand (FasL) that acts as a death signal in a paracrine fashion [70]. Conversely, the release of IL-6 by astrocytes can prevent the death of breast cancer cells expressing the IL-6 receptor that have been isolated from brain tissue [71]. Cathepsin S,

secreted from macrophages in brain tissue, cleaves junctional adhesion molecule B (JAM-B) in the BBB and contributes to tumor cell extravasation into brain tissue [61, 62, 72].

2.2.2. *Organ-specific Support for Tumor Cell Survival and Growth*

The extravasation of the tumor cells into the stroma of the secondary organ does not guarantee the establishment of the metastatic nodule in this site. It is critical that the stroma secretes growth factors and provides the infiltrated tumor cells with the necessary requirements for their growth to form micrometastasis and then macrometastasis. A clinical study demonstrated that half of the patients who had presented detectable bone micrometastasis of breast cancer at the time of diagnosis developed macrometastasis after dissection of the primary tumor [73]. An *in vivo* study to quantify the number of B16F1 melanoma cells that extravasated and formed metastatic nodules in the liver, after injecting them into the portal vein, has been performed. Results indicated that while 80% of the injected tumor cells extravasated, around 2.5% of the cells formed micrometastasis [74, 75].

Besides its contribution to the tumor cell extravasation process, the stroma can support or hinder metastatic tumor cell growth. In the lung, an *in vivo* study demonstrated that myofibroblasts became the second source, besides tumor cells, for producing tenascin C (TnC) at a later stage of the outgrowth of breast cancer micrometastasis [76]. In the bone, proteolytic activity of both matrix metalloproteinase-1 (MMP-1) and a disintegrin and metalloproteinase with thrombospondin motifs (ADAMTS1), which are secreted from the bone stromal cells, stimulated tissue remodeling and facilitated osteolytic bone metastasis of breast cancer [77]. Moreover, osteopontin (OPN) and periostin secreted from the stromal cells promote metastatic breast cancer cell growth in the bone [61, 62, 78, 79].

The metabolism of disseminated tumor cells is another feature that is modified based on the metabolic status of the new environment. Circulating tumor cells demonstrated enhanced mitochondrial biogenesis and oxidative phosphorylation through upregulation of peroxisome proliferator-activated receptor gamma coactivator 1-alpha (PGC-1α) to survive in circulation. Loss of this adaptation prevented tumor cells from forming distant metastasis [80]. Research demonstrated that metastatic ovarian cancer cells in the omentum, an organ in which the majority of the cells are adipocytes, upregulated fatty acid–binding protein 4 (FABP4). FABP4 helped tumor cells import the abundant fatty acids that are released from adipocytes to be used as a source of energy. The loss of FABP4 blocked omental metastasis of ovarian cancer [61, 81].

In the liver, there is a shortage of oxygen compared to its abundance in the lung, and a possible competition with hepatocytes for the available glucose in the interstitial space [82-84]. Therefore, tumor cells adapted a different mechanism than aerobic glycolysis to supply their energy. Colon cancer cells that metastasized to the liver took advantage of the high level of creatine, which is produced and secreted by hepatocytes in the milieu as a carrier for energy that existed extracellularly. The process consisted of two steps. First, tumor cells secreted creatine kinase brain-type (CKB) that catalyzed the phosphorylation of the creatine in the extracellular space. Then, tumor cells shuttled the phosphocreatine into the cells and utilized it as a source of energy [85]. Similarly, breast cancer cells extravasated into the liver struggled with this hypoxic environment, so they activated pyruvate dehydrogenase kinase-1 (PDK1)-mediated glycolysis to survive in the liver [61, 86].

In the brain, a study demonstrated that tumor cells adapted a different mechanism for fueling their survival. Tumor cells consumed glutamine and branched-chain amino acids that are abundant in the brain tissue. Breast cancer cells isolated from the brain metastasis demonstrated

minimal glucose consumption when compared to the same tumor cells isolated from the primary tumor site [61, 87].

2.2.3. *Stroma Alters Tumor Cell Response to Therapy*

The environment that exists in the receptive organ not only governs the colonization and growth of the disseminated tumor cells, but also the environment is considered an obstacle to the oncological therapist attempting to kill metastatic tumors. The environment contributes to the resistance of tumor cells to therapy. Breast cancer cells that were sensitive to several alkylating agents *in vitro* showed no response to the same drugs when treated *in vivo* [88]. The research demonstrated the impact of different types of non-malignant stromal cells and ECM on the development of tumor resistance to therapy in several types of cancer, including solid cancer, leukemia, and myeloma both *in vitro* and *in vivo* [89-92]. For example, the interaction between astrocytes and different cancer types in the presence of Taxol caused endothelin secretion from astrocytes. Endothelin bound and activated its receptor on the surface of the tumor cells leading to the activation of the protein kinase B (AKT)/mitogen-activated protein kinase (MAPK) pathway that protected tumor cells from death [93].

Not only can stroma lead to the development of drug resistance, but also, the stroma can improve the antitumor activity of certain agents. The acidic pH in the tumor mass is considered a double-edged sword. While the cellular uptake of weakly basic cytotoxic compounds is decreased in the low pH environment leading to drug resistance, weakly acidic cytotoxic compounds showed enhanced accumulation inside tumor cells due to the ionization and subsequent entrapment of these molecules, leading to an improved antitumor activity [94]. Another example is reversine, which

showed no activity in a subcutaneous xenograft model of multiple myeloma (MM), yet reversine significantly reduced the tumor burden in an orthotopic tumor model [89].

The stroma can influence tumor cells' response to therapy through various mechanisms. The stroma can alter the genomic stability and proliferation capability of tumor cells, the accessibility of medication to the tumor site and tumor escape from immune response [28, 89, 95-97]. A study found alteration in various cellular pathways and processes such as cytokines secretion, chromatin remodeling, cell cycle regulation, and antiapoptotic pathways in multiple myeloma cells after being cocultured with (BMSCs) stromal cells [89].

The ability of the stroma to restrict the accessibility of the medication to the tumor nodules is another mechanism that leads to treatment failure. The presence of a condensed ECM and elevated interstitial pressure inside the tumor mass limits the penetration of cytotoxic drugs. Consequently, tumor did not respond to the therapy and developed acquired drug resistance due to prolonged exposure to low amounts of the drug [95]. Conversely, degrading the ECM by targeting hyaluronic acid with the enzyme hyaluronidase improved drug penetration [98]. Moreover, the treatment options for brain metastasis are particularly limited. The brain environment creates an accessibility challenge for surgeons trying to remove metastatic tumors. Additionally, the BBB forms a natural barrier, restricting the accessibility of many antitumor drugs [99].

Finally, the stroma can induce an immunosuppressive tumor microenvironment that renders cancer cells resistant to treatment. An *in vivo* study demonstrated that the increased production of interleukin-34 and colony-stimulating factor 1 (CSF1) in the tumor microenvironment stimulated macrophage infiltration into the tumor mass. When macrophage infiltration was inhibited, T lymphocytes infiltration increased, which contributed to tumor suppression [97].

2.2.4. *Different Anatomical Sites Displayed Different Impacts on Tumor Response to Therapy*

Research has demonstrated different cellular regulation between various anatomical sites, which creates microenvironmental heterogeneity among organs. Immune cells, for example, are recognized for their involvement in the establishment of metastatic tumors and the development of drug resistance [100, 101]. A study demonstrated that IL-34 was responsible for the differentiation of microglia and Langerhans cells in the central nervous system (CNS) and epidermis. Conversely, CSF-1 was responsible for the differentiation of macrophages and dendritic cells in other anatomical sites [102]. Therefore, different anatomical sites may possess differential effects on the development of drug resistance in metastatic tumors.

Recently, several studies have assessed the influence of ectopic and orthotopic sites on the development of drug resistance when genetically similar tumor cells were implanted. A study demonstrated that neuroblastoma tumor growing orthotopically in the adrenal gland displayed more accumulation of the immunosuppressive phenotype of M2 macrophages compared to the same tumor growing subcutaneously [30]. Tumors that display more infiltration of immunosuppressive cells are recognized as resistant to immunotherapy [103]. Other types of cancer demonstrated differential responses to therapy when implanted in the ectopic and orthotopic sites. Renal cell carcinoma tumors growing orthotopically in the kidney were more resistant to Tri-mAb immunotherapy when compared to the same tumors growing subcutaneously, which showed significant tumor inhibition [31].

The heterogeneity in tumor response to therapy between tumors growing in ectopic and orthotopic sites attracted additional studies to assess the differences in tumor response to therapy between tumors in metastatic site and the ones in ectopic or orthotopic sites. A mouse model of colon cancer demonstrated discrepancies in the response to doxorubicin treatment between

subcutaneous tumor and liver metastasis [104]. Additionally, a study demonstrated a discrepancy in the response between tumor cells that had been isolated from the primary site in the colon and tumor cells isolated from the livers of patients with metastatic colon cancer. Tumor cells isolated from the liver possessed more resistance to different chemotherapeutic agents when compared to those isolated from colon tissue [105].

Several lines of evidence indicated that tumor cells metastasized to secondary sites are associated with gene expression alterations and mutations. For example, primary and metastatic tumors in breast cancer patients demonstrated significant variability in the expression levels of cyclooxygenase-2 (COX-2), epidermal growth factor receptor (EGFR), MET and mesothelin between tumors in these locations [106]. Another study showed heterogeneity between primary and metastatic tumors in the lymph nodes of patients with metastatic colon cancer. The results demonstrated EGFR gene deregulation in 25 out of 36 (69.4%) and 29 out of 36 (80.5%) primary and metastatic tumors, respectively. Conversely, KRAS mutations were found in 16 out of 37 (43.2%) and 15 out of 37 (40.5%) of the primary and metastatic tumors, respectively [107]. The evidence collected from tumors in ectopic, orthotopic and metastatic sites suggested that the stroma in different organs had different influences on the tumor cells response to treatment.

2.3. Cancer Metastasis Treatment

2.3.1. *Current Antimetastatic Therapies in Clinic*

Developing antimetastatic drugs that eliminate metastatic tumors from secondary organs remains the most appropriate strategy to fight tumor metastasis and should be the focus for the future advances. Research has demonstrated that drugs targeting the early stages of metastatic cascade were not efficient in preventing cancer metastasis since a considerable percentage of

cancer patients presented tumor metastases at the time of diagnosis [108, 109]. Platelet inhibitors that prevent the clustering of circulating cancer cell with platelets, a strategy for tumor cells to escape immune response, decreased the number of metastatic foci in mice. However, platelet inhibitors were not able to improve the overall survival of patients with existing metastases [110]. Even patients who do not present detectable metastatic tumors at the time of diagnosis have a high chance that tumor cells have already metastasized to distant organs, where these tumor cells might remain dormant [111]. The current treatment options for cancer patients with metastasis include radiotherapy, chemotherapy, hormone therapy, immunotherapy and targeted therapy.

Radiotherapy relies on using ionizing radiation to damage the DNA and kill cancer cells. Radiotherapy is not selective and can affect both malignant and non-malignant cells. However, the non-malignant cells can repair themselves better, while malignant cells are significantly less efficient, which causes their death. While radiotherapy can effectively eliminate the primary tumor, oncologists use radiotherapy as a palliative therapy in metastatic tumors to minimize the symptom intensities, such as bone pain, and slow down tumor growth. Clinicians apply radiotherapy to metastatic tumors using single or combined strategies, which include: applying an external source that directs the beam toward the tumor mass, such as whole-brain radiation therapy for brain metastases, or injecting radioisotopes locally into or near the tumor mass or systemically in the circulation [112, 113]. For systemic administration, microsphere or antibody formulations allow for targeted delivery of the radioisotopes to metastatic tumors [114, 115]. Combination of radiotherapy with a chemotherapeutic agent, immunotherapy or targeted therapy improves the effectiveness of the radiation therapy. Based on the administrated dose, radiotherapy toxicity can range from minor damage, such as alopecia, to serious toxicities such as organ damage [112, 113, 116].

The second treatment option is chemotherapy, which uses drugs to inhibit DNA synthesis or cell division of the cancer cells, leading to the activation of apoptosis and cell death. Drugs in this class have different mechanisms of action, including substitution for the DNA building blocks, inhibition of enzymes required for DNA synthesis, formation of crosslinks with DNA strands, or inhibition of the cell division. Chemotherapy includes subclasses such as antimetabolites, topoisomerase inhibitors, alkylating agents, antitumor antibiotics, and antimicrotubule agents [117].

Oncologists give patients with metastatic cancer a combination of chemotherapeutic agents with different mechanisms of action. For example, breast cancer patients take a combination of cyclophosphamide, methotrexate and fluorouracil, or doxorubicin and cyclophosphamide. The advantages of using multiple chemotherapeutic agents are improved efficacy by killing cancer cells in different phases of the cell cycle thereby overcoming tumor resistance to the therapy [118]. Clinical trials have demonstrated that incorporating targeted therapy with a combination of chemotherapeutic agents increased the median survival of patients. For example, bevacizumab increased the median survival of the patients to 25.6 months when combined with 5-FU and irinotecan, compared to the median survival of 17 months when patients were treated with a combination of 5-FU and irinotecan [117].

The clinical use of chemotherapeutic agents is associated with drawbacks. First, chemotherapeutic agents cause systematic toxicities, as they are not selective and target both malignant and non-malignant cells. The toxicities can be acute during the treatment, such as myelosuppression and immunosuppression, or chronic, such as lung fibrosis and cardiomyopathy. Thus, oncologists restrict chemotherapeutic agent use to patients with good response. Supportive medications such as antibiotics and drug delivery systems such as liposomes are often used to

minimize toxicities. Another drawback of chemotherapy is that tumors commonly develop resistance to chemotherapeutic agents through different mechanisms that involve processes such as drug transport, DNA repair and drug metabolism [117, 118].

Hormone therapy is a treatment option to shrink tumors that are hormonal-dependent, such as prostate and breast cancers that express progesterone and estrogen receptors, respectively. Hormone therapy relies on the use of receptor antagonists (e.g., antiandrogens), drugs that inhibit the production of endogenous hormones (e.g., aromatase inhibitors) or exogenous synthetic hormones (e.g., fluoxymesterone). Additionally, surgical removal of the endocrine glands, such as the ovaries and prostate, are alternative strategies to treat breast and prostate cancers, respectively [119, 120]. The majority of the patients who underwent hormone therapy developed tumor resistance to hormone therapy through mechanisms that involve hormone receptors, growth factors, epigenetic alterations, and activation of other cellular pathways [121, 122]. Clinical studies demonstrated that patients with estrogen receptor-positive breast cancer metastasis developed resistance after a couple of years of treatment [122].

Since tumor growth results from the ability of cancer cells to escape the immune response, oncologists employ immunotherapy, which aims to stimulate the body's immune system to kill cancer cells. Immunotherapy is preferred in immunogenic tumors such as melanoma and renal cell carcinoma. Oncologists use different strategies of immunotherapy, which include cytokine immunotherapy, cell-based immunotherapy, vaccination, and monoclonal and immunomodulating antibodies [123]. These immunotherapy strategies stimulate the immune system through three discrete mechanisms: cancer cell antigen presentation, T cell activation, and blockage of tumor cell-mediated immunosuppression [124]. The low response rate and severe toxicity in patients with metastatic tumors who underwent interferon and interleukin therapies led to the FDA approval of

many antibody and vaccine therapies. Currently, IL-2 is restricted to patients with favorable response [116].

While immunotherapy strategies are promising due to their target specificity, these new immunotherapies are not without challenges. Immunotherapy normally has a low response rate, and tumor recurrence occurs. Thus, there is a growing interest in a strategy combining immunotherapeutic agents with different classes of drugs to increase the efficacy. In fact, a clinical study used the gp100 peptide vaccine in combination with ipilimumab (anti-CTLA4) and demonstrated a significant increase in the overall survival of patients (10 months) compared to gp100 monotherapy (6 months) [116]. Clinical study (ClinicalTrials.gov Identifier: NCT01844505) on combination therapy of ipilimumab with nivolumab (anti-PD-1) is ongoing. The early outcomes demonstrated that the progression-free survival of patients with PD-L1-negative metastatic melanoma increased significantly in the combination group [125]. As a new therapy, other side effects of immunotherapy may be observed in the future. For example, around 20% of patients treated with ipilimumab demonstrated autoimmune reactions in the form of hypophysitis, pituitary gland inflammation, and colitis [116, 123, 124]. Continuous efforts to improve therapeutic outcomes of immunotherapy are needed.

Finally, an extraordinary revolution in the field of cancer treatment occurred two decades ago, when the FDA approved the first targeted therapy, rituximab, in 1997 [126]. Targeted therapies, including small molecules and antibodies, are specifically designed to target oncoproteins or cellular pathways that support tumor cell growth. The selection of a targeted therapy is based on the pathway involved in the initiation and promotion of the cancer and can be personalized. For example, clinicians are giving vemurafenib, a BRAF inhibitor, to patients with metastatic NSCLC and melanoma that have the BRAF V600E mutation [127].

Targeted therapies that received FDA approval or are currently being examined in the clinic target cancer hallmarks: uncontrolled proliferation, genetic instability, sustained oncogenic signals, oncosuppressor signal escape, death resistance, angiogenesis, dysregulated metabolism, immune escape, tumor-promoting inflammation, and invasion [40]. Targeted therapies are categorized into different classes based on the therapeutic intervention, such as telomerase inhibitors, poly ADP ribose polymerase (PARP inhibitors), epidermal growth factor receptor (EGFR) inhibitors, cyclin-dependent kinase inhibitors, proapoptotic BH3 mimetics, vascular endothelial growth factor (VEGF) inhibitors, aerobic glycolysis inhibitors, antibody immunotherapy, anti-inflammatory drugs, and hepatocyte growth factor/ tyrosine-protein kinase Met pathway HGF/c-Met inhibitors [7, 40].

Although targeted therapies have higher safety profiles when compared to other anticancer strategies due to their specificity, targeted therapies also face challenges [128]. First, current targeted therapies did not produce satisfactory antitumor activity in patients with cancer metastasis. For example, bevacizumab, a humanized antibody capable of blocking VEGF, failed to demonstrate significant efficacy against triple-negative breast cancer, ovarian cancer and non-small-cell lung cancer [8-10]. Although clinical response in some cancer types has been observed with an increase of patients' survival for an extra few months, no complete tumor eradication was achieved. Around 10% of the patients with metastatic renal cell carcinoma demonstrated complete eradication when treated with cytokine immunotherapy, yet no complete eradication was obtained with the targeted therapies [129]. Thus, clinicians tend to use a combination of targeted therapy and other classes of cancer treatment to improve the efficacy of the treatment [7].

Genetic instability and mutations is another challenge. The same tumor might have different oncogenic pathways involved and exhibit variability in resisting the targeted therapy.

Research has demonstrated drug resistance to targeted therapy beginning within a few months to a few years. Recent study has shown that patients with non-small-cell lung cancer treated with EGFR inhibitors developed resistance within 12-18 months [7, 130].

2.3.2. *Translational Gap between Preclinical Research and Clinical Trials*

Although cancer research has introduced many therapeutic agents to treat metastasis, it remains the cause for 90% of cancer patients' deaths [12]. Recent statistical analysis revealed that the five-year survival rates for patients with distant metastasis at the time of diagnosis for 13 cancer types were less than 30%. More than 85% of patients with distant metastasis of liver, pancreatic, lung, esophageal, urinary bladder, kidney and colorectal cancers died within five years from the time of diagnosis [1]. Compared to the rates a decade ago, the five-year survival rates for patients with metastatic gastric, breast and pancreatic cancers remained the same or slightly improved [11, 131-133]. **Figure 2.1** shows the most recent data on five-year survival rates of the 15 most common types of cancer [1].

Historical data demonstrates that the development of a new antitumor drug requires 10-15 years from the time of isolating a natural product or synthesizing a chemical molecule to examining its efficacy in clinical trials, with a total cost of hundreds of millions of dollars [134]. The process involves assessment of the activity of the new entity in tumor-bearing animals. Unfortunately, the massive investment made by government agencies and the pharmaceutical industry in the development of new therapies has resulted in limited return. More than 90% of the drugs selected from animal studies and tested in clinical trials fail to gain FDA approval [18]. As shown in **Figure 2.2**, the success rate of anticancer drugs that eventually receive FDA approval is less than 7%. Evidently, there is a discrepancy in drug efficacy between animals and cancer patients.

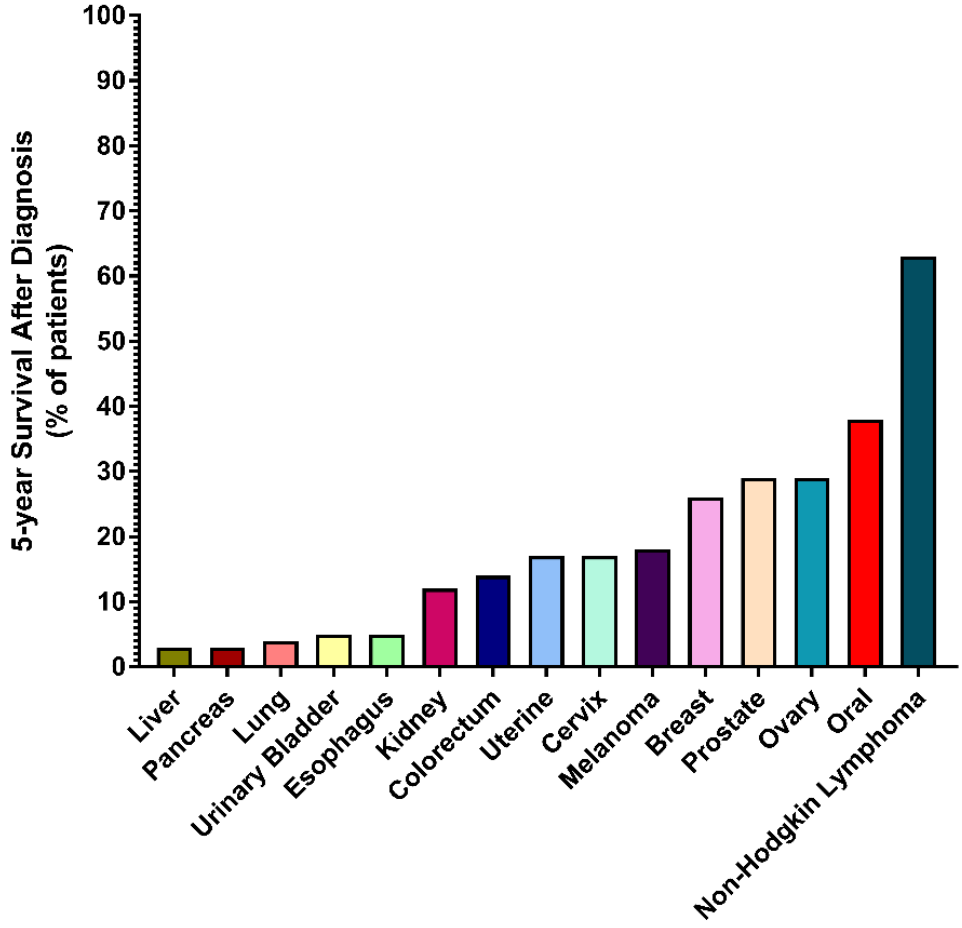

Figure 2.1: Five-year survival of patients with distant metastasis. The figure demonstrates that the five-year survival rates at the time of diagnosis for patients with distant metastasis of 13 cancer types are less than 30%. Figure was generated based on the data in reference [1].

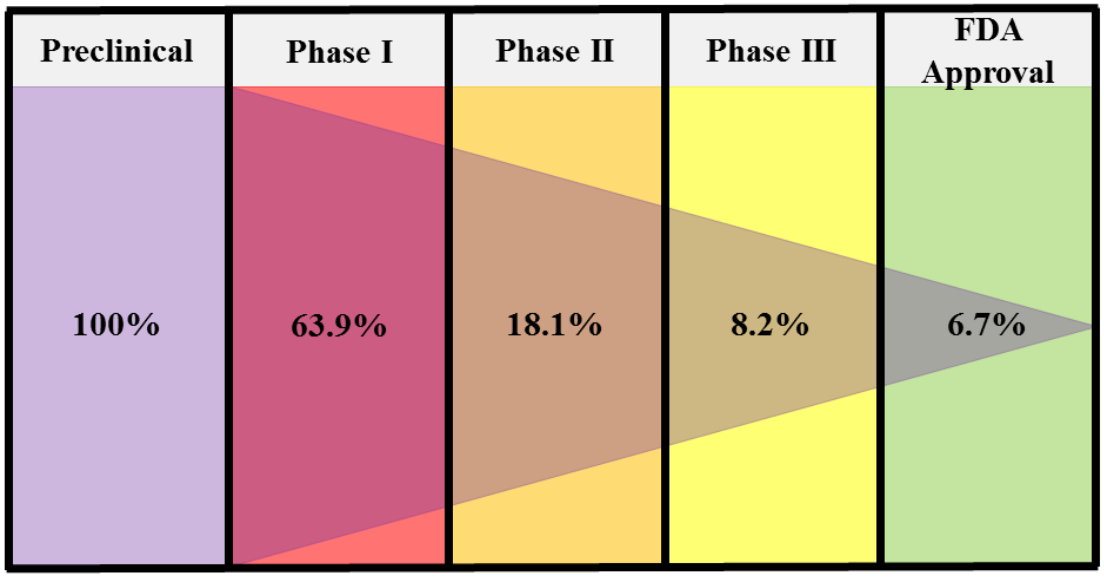

Figure 2.2: Percentage of drugs successfully finishing each phase compared to preclinical stage. The success rates of anticancer drugs, from entering phase I clinical trials to receiving FDA approval. Figure was generated based on data in reference [18].

Translation of preclinical results to clinical success has been a focus in recent years in cancer therapy. The insufficient antitumor activities of dasatinib and IPI-926 in clinical trials are examples of translational failure. The proto-oncogene tyrosine-protein kinase Src is upregulated in many types of cancer and leads to cancer progression through activation of cellular pathways [135]. Dasatinib, a Src inhibitor, demonstrated a significant inhibition of tumor growth in animal models of many types of cancer [13, 136-138]. However, dasatinib showed no activity when examined in patients with cancer metastasis of similar cancer types [11, 16, 17, 139-141]. The research observed similar failure with the hedgehog (HH) signaling pathway inhibitor, IPI-926, also known as saridegib. The HH pathway is involved in the development of neoplasia and tumor metastasis of bone, prostate, colon, lung, brain and skin [15, 142-145]. IPI-926 was successful in inhibiting tumor growth in preclinical models of solid tumors [14, 15]. However, it displayed no activity in clinical trials [15].

The scientific community recognizes several differences between animal models and humans. Differences in the genetic background, the pharmacodynamics of the drugs at the molecular and cellular levels, pharmacokinetics, and immune system function could make animal models less effective in predicting the efficacy of therapeutic agents [25, 146-148]. Although these variances are justifiable, animal models remain a vital component in drug development as they overcome ethical and practical challenges. However, as far as tumor metastasis is concerned, it is difficult to justify using animal models without a full representation of the pathological condition of tumor growth in different organs.

For a long period of time, drugs were evaluated for their efficacy using tumors growing in non-natural sites, i.e., subcutaneous, or in the original organ of the tumor, i.e., orthotopic, which

is considered as the primary tumor, but not in metastatic sites. Conversely, clinical trials examined the antitumor activity of new drugs in patients with detectable metastatic tumors in one or more secondary organs. Considering the environmental heterogeneity when modeling the metastasis in preclinical studies is of great importance to obtain a more reliable assessment. This approach would enhance the efficiency of the drug discovery and development processes with a higher success rate.

2.4. Animal Models for Preclinical Drug Efficacy Evaluation

2.4.1. *Traditional in vivo Models*

The development of novel anticancer drugs is accompanied by a preclinical drug efficacy evaluation to predict the drug ability to shrink metastatic tumors in patients. Preclinical assessment of novel antitumor drugs is accomplished through utilization of the cell-based *in vitro* system and *in vivo* animal models. The cell-based *in vitro system* offers a high throughput screening for drug discovery. Additionally, molecular biologists use the *in vitro* system, due to its controllable environment, to study the drug's mechanism of action. Recently, many research laboratories have developed three-dimensional *in vitro* systems to imitate the tumor microenvironment architecture and overcome limitations of two-dimensional *in vitro* systems [149]. However, tumor mass is considered a complex tissue composed of different types of cells and an extracellular matrix that exists side-by-side with the cancer cells. Unfortunately, the incorporation of all different types of cells and the extracellular matrix that form the tumor microenvironment has not been achieved in a cell-based *in vitro* system [149-151]. Additionally, the *in vitro* system does not replicate the true levels of cytokines and growth factors that are present in the tumor in the clinic [149, 152].

Efforts have been made to overcome the limitations of the *in vitro* system. The simplest method is to implant cancer cells into an animal model and allow tumors to develop. This i*n vivo* model offers comprehensive consideration of the tumor microenvironment, which improves preclinical prediction of drug efficacies, especially for medications that target the tumor microenvironment [153]. The early generation of mouse models is established by subcutaneously implanting a mouse cell line or tissue (allograft) or human tumor cell line or tissue (xenograft) in an immunocompetent or immunocompromised mouse, respectively. The subcutaneous tumor model allows simple evaluation of the drug efficacy by measuring tumor volume, using calipers to monitor tumor growth [32, 33]. The subcutaneous xenograft model offers the opportunity to evaluate individualized medications or targeted therapies that react with human targets, such as monoclonal antibodies that target human epitopes [154, 155]. Unfortunately, the subcutaneous tumor model has the limitation that the tumor is growing on a site that is not natural for tumor growth, i.e., the subcutaneous tissue. Subcutaneous tissue does not possess the same cells and ECM that are present in the organs where metastatic tumor cells spread, such as the brain, liver, lung, kidney, and bone. Moreover, the xenograft model necessitates the utilization of immunocompromised mice to avoid the natural rejection of tumor growth by the immune system [26]. Therefore, the subcutaneous xenograft model does not replicate the interaction between the immune system and the tumor cells that occurs in metastatic tumors [156].

The orthotopic tumor model, in which tumor cells are injected into the natural site of tumor growth, was introduced to overcome the limitations of the subcutaneous tumor model. The orthotopic tumor model provides a more realistic environment for tumor cells to grow since the model accounts for the organ architecture, preexisting blood and lymphatic vasculatures, organ-specific extracellular matrix, secreted molecules and proteins [156-158]. Tumor cells need to be

labeled with a reporter gene such as luciferase or green fluorescent protein (GFP) to allow quantification of tumor growth [159]. Intravascular tail-vein injection of the tumor cells leads to the development of tumor nodules in the lung. However, the development of orthotopic tumor nodules in other organs, such as the liver and kidneys, requires surgery, which is considered a drawback. The surgery creates a challenging task for the investigator and might disrupt the body homeostasis of the model.

2.4.2. *Advanced in vivo Metastatic Tumor Models: Types and Principles*

There is a need to examine the effectiveness of antimetastatic drugs against tumors growing in a more precise condition that imitates metastasis in the clinic. Several *in vivo* models that incorporate a more relevant tumor-stroma interaction at the metastatic sites have been developed including: 1) the genetically engineered mouse model; 2) the experimental metastasis model; 3) the spontaneous metastasis model; and 4) the multi-organ tumor model [35, 160, 161]. The multi-organ tumor model is discussed in detail later in a separate section. In the genetically engineered mouse model (GEMM), tumor cells initiate in situ in a particular organ, and then tumor cells metastasize to different organs. The GEMM depends on overexpressing oncogenes or mutated forms of tumor suppressor genes or knocking in or knocking out tumor suppressor genes that are altered in human malignancies [160, 162-164]. The GEMM is considered a highly valuable model to study the early development of cancer and the various steps of metastasis in the presence of a functionally active immune system [157]. The GEMM has been established for different types of cancer [163, 165-171]. Recently, preclinical studies used GEMM as a model for drug screening and development, especially for evaluating drugs that prevent tumor metastasis or target the early steps of the metastasis process [161, 167, 172]. The preclinical assessment of antitumor drugs

using GEMM demonstrated comparable pharmacokinetics and antitumor efficacy for the same drugs when tested in the clinic, which suggested that the GEMM is an accurate representation of cancer in patients [161, 173, 174].

The experimental metastasis model, which simulates the later steps of metastatic cascades, is the most widely exploited among the four advanced models for preclinical drug evaluation. The experimental metastasis model relies on injecting the tumor cells into circulation and allows the blood flow to deliver the cells to the first organ they meet. Based on which blood vessel is being injected with the tumor cells, tail-vein injection causes lung metastasis, intraportal injection produces liver metastasis, and intracardiac injection initiates bone metastasis. The development of the experimental metastasis model is faster with a controllable number of cells [175].

Another advanced model that develops cancer metastasis in secondary sites is the spontaneous tumor metastasis model [161]. The principle of the spontaneous metastasis model is that human or murine metastatic tumor cells or tissues are implanted orthotopically, based on the type of cancer in the immunocompromised or immunocompetent mouse, respectively. After the primary tumor reaches a measurable size, a surgical procedure is performed to dissect the tumor. The removal of primary tumor allows the mice to survive and gain enough time for disseminated tumor cells to form detectable metastatic nodules in the secondary organs. Tumor cells are then isolated from the secondary organs and again re-implanted orthotopically in a new animal. The *in vivo* selection procedure is repeated several times to select the most aggressive and highly metastatic tumor cell variants. This approach has developed spontaneous tumor metastasis models for many types of cancer [176-181]. Preclinical drug evaluation for both cytotoxic and monoclonal antibody agents have been performed using this model [161, 182, 183].

2.4.3. *Limitations of Current Metastatic Animal Models*

While the GEMM, experimental and spontaneous metastasis models enhance the ability to predict the efficacy of antimetastatic agents in the clinic, these advanced *in vivo* models suffer from critical drawbacks that limit their use. First, the incidence of cancer metastases in the GEMM is low compared to the percentage of patients with metastasis of the same type of cancer and gene mutation. For example, breast cancer metastasis in $Brca^{+/-}$ mice occurred in less than 10% of the mice compared to the occurrence of metastasis in breast cancer patients, which reached 67% of the patients with brain metastasis [184, 185]. Similarly, the spontaneous tumor metastasis model does not guarantee the formation of secondary metastases in all animals nor the development of metastatic tumors in multiple organs. A study demonstrated that the spontaneous melanoma model developed lung metastases in 50%-100% of mice, while the incidence of the liver, brain and kidney metastases was low or none based on the tumor cell variant used to establish the model [177]. The experimental tumor metastasis model forms tumor metastasis in a single organ only and needs a surgical procedure to implant tumor cells, with the exception of the lung metastasis model [186, 187].

Moreover, the GEMM and spontaneous metastasis models require a long time, ranging from several months to more than a year to allow the tumor cells to disseminate from the primary site until they can form detectable metastatic lesions in the distant organs. For example, the c-Met autocrine activation-induced spontaneous melanoma metastasis model and the Nf2 heterozygous mouse model needed an average time of 15.6 and 22.4 months, respectively, until the formation of tumors [188, 189]. Similarly, the WM239 spontaneous melanoma model needed almost a year to generate a highly metastatic variant of this cell line using the *in vivo* selection procedure [177]. The long time needed makes the GEMM and spontaneous metastasis models impractical for

preclinical drug assessment if the tumor grows too slowly. Housing the mice for an extended period until tumor development is costly. Moreover, expensive bioimaging techniques are needed in the GEMM to confirm the initiation of the primary tumor, monitor tumor growth and metastasis and assess response to therapy.

2.5. Multi-organ Tumor Model for Drug Evaluation

2.5.1. *The Need for Simultaneous Drug Evaluation in Multiple Anatomical Sites*

One of the hallmarks of metastasis is the development of tumor growth in more than one organ. A clinical study to investigate the incidence of multiple organ metastases demonstrated that around 95% of the patients with melanoma metastases exhibited the formation of metastases in multiple organs [34]. The presence of metastases worsens the systemic therapy outcome. RCC patients with metastases in multiple organs demonstrated that patients with more than two organs affected had the poorest overall survival. The median survival time of patients with more than two organ metastases is 6.8 months, compared to 9.7 months for patients with two organ metastases or 32 months with one organ metastasis [190]. The study suggested that the establishment of metastases in multiple anatomical sites might cause tumors to become resistant to therapy. Similarly, an animal model with kidney tumors grown simultaneously in the subcutaneous and orthotopic sites demonstrated a poorer survival rate compared to the animals with tumor growth in a single site. The orthotopic tumor of RCC caused the subcutaneous tumor to become an immunosuppressive environment, leading to the loss of tumor sensitivity to immunotherapy [191]. The study suggests that there was an interaction between tumors in multiple sites.

Although the advanced *in vivo* metastatic tumor models allow an evaluation of tumor response to therapy in the metastatic site, the advanced *in vivo* models do not allow simultaneous

drug evaluation on tumors growing in multiple sites. First, the primary and metastatic tumors in the advanced *in vivo* models do not grow at the same time. Practically, when the primary tumor in the GEMM or spontaneous tumor models becomes large, the researcher needs to dissect the primary tumor to prevent animal mortality. The animal that survives for a prolonged period allows tumor cells to disseminate from the primary tumor and grow in the metastatic sites. Second, the tumor metastases do not develop simultaneously in multiple sites [161]. Therefore, it is difficult to evaluate antitumor efficacy in a preclinical model of metastasis that imitates the metastasis in patients with multiple visceral organs involved. Evidence in support of efficacy of a treatment strategy in animals with multi-site tumor metastasis will be most desirable for an oncologist and has the potential to influence the outcome of treatment.

2.5.2. *Hydrodynamic Cell Delivery to Establish Multi-organ Tumor Model*

Historically, our lab introduced the hydrodynamic delivery technique to the drug delivery field more than 15 years ago to deliver naked DNA to hepatocytes [192, 193]. The hydrodynamic delivery technique involves a rapid injection of a large volume of solution to change the flow dynamics and generate higher pressure. This pressure extends the fenestra present in the endothelial cells of the hepatic vasculature and creates temporary pores in the cell membrane of the hepatocytes to allow DNA entry into hepatocytes. Noteworthily, structural and functional assessments of the liver showed that the effect of the hydrodynamic impact on the liver stromal cells is temporary and reversible. The liver returns to its normal physiological status in two days. To date, research has used hydrodynamic delivery technique to deliver various macromolecules to cells in different organs in both small and large animals [194-196]. This procedure has been used

for the purpose of gene functional analysis, discovery of a therapeutic gene, and establishment of disease animal models [194, 197-199].

Recently, our lab has extended the application of hydrodynamic delivery technique to the establishment of a multi-organ tumor model by implanting tumor cells simultaneously to the lung, liver, and kidney [35]. The procedure is nonsurgical and accomplished by a hydrodynamic tail vein injection of a tumor cell suspension. The high hydrodynamic pressure pushes tumor cells to the liver and kidney through the hepatic and renal veins and results in the seeding of the tumor cells in both organs. Tumor cells remaining in circulation move through the heart and are then trapped in the lung [200]. Consequently, tumor cells in the liver, kidneys and lung grow simultaneously and establish an animal with tumor growth in three organs.

This tumor model offers remarkable benefits. Firstly, the liver, lung, and kidney are the most common sites of metastasis for many types of cancer in patients [201], and there are at least 16 types of cancer that are known to form metastases in the lung, liver and kidneys (**Figure 2.3**). Secondly, the simultaneous seeding of the tumor cells in these three different anatomical sites offers the opportunity to examine the influence of the distinctive stroma in each anatomical site on the therapeutic response to a therapeutic treatment. Thirdly, this model offers the opportunity to study how the different environment in these three organs influences tumor growth, formation of microenvironment, and interaction of tumor cells with the stroma, and, finally, how these influences affect the outcome of a treatment. Lastly, this animal model with multi-organ tumor growth would offer the opportunity to evaluate and establish new treatment strategies with higher relevance to patients.

2.6. Conclusion

The last few decades have witnessed remarkable comprehensive research in cancer metastasis, including studying tumor cell-stroma communications. However, the development of preclinical models that incorporate these complex interactions from the metastatic sites of patients is still lagging. *In vivo* animal models will remain a critical tool to identify and validate the efficacies of novel antimetastatic therapies. Minimizing the differences between preclinical studies and clinical trials will improve our ability to select the most effective drugs. The heterogeneity in tumor biology and therapeutic response that exists between tumors of the same type but growing in different anatomical sites, i.e., subcutaneous, primary organ, and secondary organ, is increasingly being recognized. Evidence indicates that the stroma of various organs is a major determinant of the effectiveness of anticancer drugs. These findings suggest that once tumor cells metastasize to different secondary organs, their response to antimetastatic therapies might be different.

Here, we proposed that tumor-site based drug evaluation is the most suitable strategy to develop antimetastatic drugs with high efficiencies to eradicate metastatic tumors. A multi-organ tumor model using the hydrodynamic delivery technique is a highly suitable model that provides the ability to assess the influence of different anatomical sites on the growth of metastatic tumors and their response to antitumor drugs.

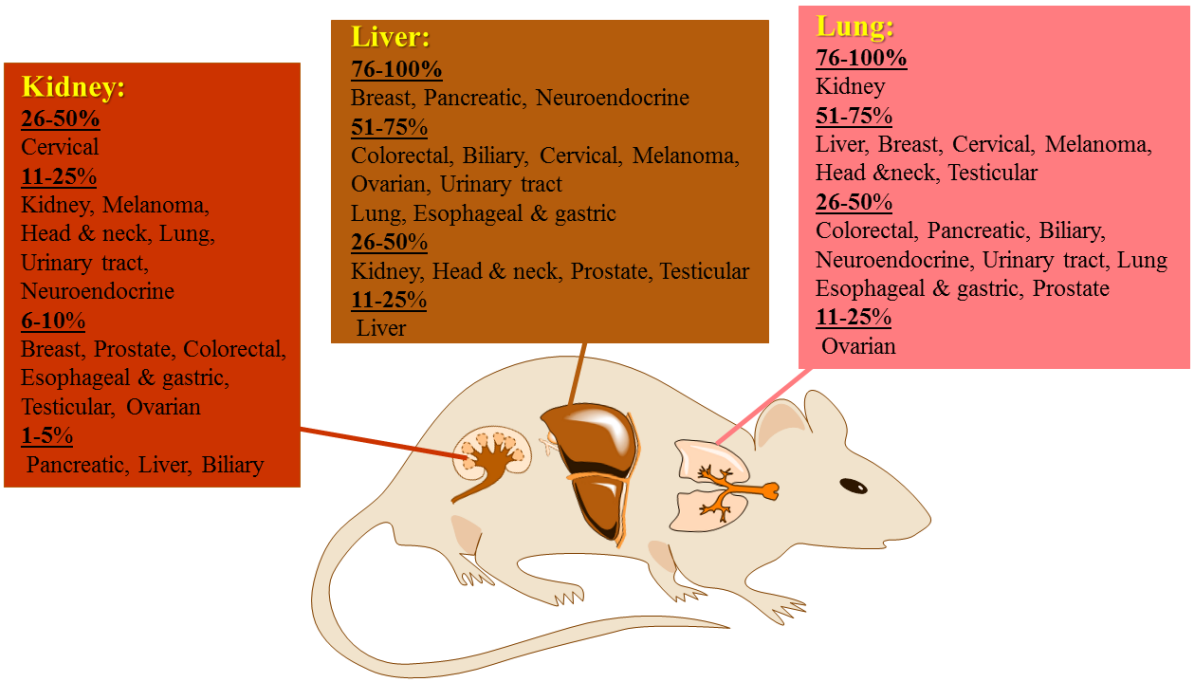

Figure 2.3: Multi-organ tumor model for tumor metastasis research. It offers opportunity to assess the therapeutic response of at least 16 types of cancer that metastasize to the lung, liver, and kidney in patients. Figure was generated using ChemDraw® and based on the clinical data in reference [183].

CHAPTER 3

MATERIALS AND METHODS

3.1. Materials

3.1.1. *Chemicals, Plasmids and Cell Culture Supplies*

5-Fluorouracil with a purity of 99% and Kanamycin were purchased from Sigma-Aldrich (St. Louis, MO). Neutral buffered formalin (10%) and hematoxylin and eosin staining kit were purchased from BBC Biochemical (Atlanta, GA). Firefly D-Luciferin kit was purchased from Perkin-Elmer (Akron, OH). Luciferase activity assay kit was purchased from Promega (Madison, WI). Pierce™ Coomassie Blue Plus (Bradford) Protein Assay kit was obtained from Thermo Fisher Scientific, Inc. (Waltham, MA). NaCl was obtained from Alfa Aesar (Tewksbury, MA). Glycerol, anhydrous LiCl were obtained from ACROS. Glutaraldehyde aqueous solution (70%) EM-grade was obtained from Electron Microscopy Sciences (Hatfield, PA). NaOH was obtained from J.T.Baker (Phillipsburg, NJ). Sodium cacodylate trihydrate, ethidium bromide solution, n-butanol, lysozyme from chicken egg white, KCl, potassium acetate, KH_2PO_4, Na_2HPO_4, NaCl, glucose, sucrose, 37% (v/v) HCl, and osmium tetroxide 4% for EM were purchased from Sigma-Aldrich (St. Louis, MO). Tryptone and yeast extract were purchased from BD biosciences (San Jose, CA). Agarose and SDS were purchased from Bio-Rad Laboratories (Hercules, CA). CsCl was obtained from bioWORLD© (Dublin, OH). The pLIVE® plasmid vector, containing an albumin promoter and the kanamycin resistance gene, was purchased from Mirus Bio (Madison, WI). The pCMV-IL-2 and pCMV-mIL-12 were kindly provided by Dr. Shulin Li (The University of Texas MD Anderson Cancer Center, Houston, TX). pUMVC3-mIL-7 was purchased from

Aldevron (Fargo, ND). pORF9-mIL-21 and pORF9-mIL-24 were purchased from InvivoGen (San Diego, CA). pCMV6-mIFN-β and pCMV6-mIL-27 were purchased from OriGene (Rockville, MD). Ethanol, isopropanol, chloroform, glacial acetic acid, Tris base and EDTA were obtained from Fisher Scientific (Madison, WI). 4T1 (breast tumor) and Renca (renal cell carcinoma) cells were purchased from ATCC (Manassas, VA). Dulbecco's Modified Eagle's Medium (DMEM) (ATCC® 30-2002™), RPMI-1640 medium (ATCC® 30-2001™) and freezing medium (ATCC® 30-2600™) were purchased from ATCC (Manassas, VA). Fetal bovine serum (FBS) was obtained from Atlanta Biologics (Atlanta, GA), while penicillin/streptomycin was purchased from Life Technologies (Carlsbad, CA). Trypsin/EDTA solution (0.25 % (w/v) Trypsin, 2.21 mM EDTA) was purchased from Mediatech (Herndon, VA). Membrane filters with an average pore size of 40 µm were obtained from BD Falcon (Franklin Lakes, NJ). Corning® culture dishes, multiple-well plates, and cryovial tubes were purchased from Sigma-Aldrich (St. Louis, MO).

3.1.2. *Solutions and Buffers*

A list of solutions and buffers used in the research project can be found in **Table 3.1**. The table includes amounts and volumes used to prepare the solutions and buffers.

3.2. Instruments

A list of the major instruments used in the research can be found in **Table 3.2**. Instruments were listed in front of the procedures.

Table 3.1. Solutions and buffers utilized in this project. Composition of washing and fixative solutions used in SEM analysis (*) were as described previously in reference [202].

Solution/buffer	Composition
Complete cell culture media	450 ml DMEM or RPMI-1640 medium + 50 ml FBS + 5 ml penicillin (10,000 U/ml)/streptomycin (10 mg/ml).
TB medium for bacteria culture	24 g yeast extract + 12 g tryptone + 4 ml glycerol + distilled water up to 900 ml. Then, the solution was autoclaved. Just before use, the previous solution was mixed with an autoclaved solution of (2.31 g KH_2PO_4 + 12.54 g K_2HPO_4 + distilled water up to 100 ml). 2 ml kanamycin (50 mg/ml) was added.
Solution I	4.9 g glucose + 12.5 ml 1M Tris-Cl, pH 8 + 10 ml 1M EDTA pH 8 + distilled water 472.5 ml.
Lysozyme solution	90 mg lysozyme + 9 ml Sol I.
Solution II	6.8 ml 5M NaOH + 17 ml 10% SDS + distilled water up to 170 ml.
Solution III	147 g potassium acetate + 200 ml distilled water. Mix until dissolved. Then, add 58.5 ml glacial acetic acid + distilled water up to 500 ml. The solution was kept at 4°C.
TE buffer	10 ml 1M Tris-HCl (12.1 g tris base in 100 ml distilled water, pH 7.5) + 2 ml 0.5M EDTA (18.6 g EDTA in 100 ml distilled water, pH 8) + 988 ml distilled water.

Phosphate buffered saline (PBS)	0.24 g KH_2PO_4 + 0.2 g KCl + 1.44 g Na_2HPO_4 + 8 g NaCl + 900 MQ water. Adjust pH to 7.4, then MQ water to 1 L.
Saturated butanol	50 ml n-butanol + 50 ml distilled water. Store at room temperature.
5M LiCl	212 g anhydrous LiCl + distilled water up to 1 L.
5M sodium acetate pH 5.2	680 g sodium acetate.3H2O + distilled water up to 1 L. Adjust pH with glacial acetic acid before the final volume is obtained.
D-Luciferin solution for *in vivo* bioluminescence imaging	D-Luciferin 15 mg/ml in Dulbecco's phosphate-buffered saline without Mg^{2+} and Ca^{2+} (DPBS). The solution was sterilized through a 0.2 µm syringe filter.
Lysis buffer: 100 mM Tris-HCl, 2 mM EDTA and 0.1% Triton X-100, pH 7.8	12.114 g Tris-base + 989.41 ml MQ water + 5.59 ml 37.2% HCl + 4 ml 0.5 M EDTA + 1 ml Triton X-100
0.2 M Cacodylate buffer pH 7.4	22.9 g sodium cacodylate trihydrate + 674.8 ml MQ water + 25.2 ml 0.2 M HCl.*
2.5% glutaraldehyde fixative in 0.075 M cacodylate buffer	61.6 ml glutaraldehyde solution 70% + 646.87 ml 0.2 M cacodylate buffer + 17.215 g sucrose + 1016.17 ml MQ water. Filter through 0.2 µm syringe filter.*
Washing buffer 1 for SEM	30 ml 0.2 M cacodylate buffer + 0.9 g sucrose + 60 ml MQ water.*
0.2 M Phosphate buffer pH 7.4	162 ml 0.2 M $Na_2HPO_4.2H_2O$ (17.8 g in 500 ml MQ water) + 38 ml 0.2 M $NaH_2PO_4.H_2O$ (13.8 g in 500 ml MQ water).*

Washing buffer 2 for SEM	45 ml 0.2 M phosphate buffer + 45 ml MQ water. Filter through 0.2 µm syringe filter.*
1% Osmium tetroxide in phosphate buffer	22.5 ml 4% osmium tetroxide + 45 ml 0.2 M Phosphate buffer + 22.5 ml MQ water. Filter through 0.2 µm syringe filter.*

Table 3.2. Major instruments used in the project.

Procedure	Instrument
Analytical balances	Mettler AE163 balance from Mettler-Toledo (Columbus, OH) and Scientech SL400 digital balance from Scientech Inc. (Boulder, CO).
Water bath	Precision™ Reciprocal Shaking Bath purchased from Thermo Fisher Scientific (Madison, WI) and VWR® Digital Dry Block Heaters from VWR (Radnor, PA).
Water purification	Millipore Direct-Q® 5UV-R Ultrapure Water Purification System from Millipore (Billerica, MA).
pH measurement	OAKTON pH 510 benchtop meter from OAKTON Instruments (Vernon Hills, IL).
Cell culture and tissue microscopy and imaging	Nikon Eclipse TS100 and an Eclipse T*i*-U inverted fluorescence microscopes purchased from Nikon Instruments (Melville, NY). Image processing carried out using NIS-Elements imaging platform.

Mammalian cell culture incubator	NAPCO Series 8000 Water-Jacketed CO_2 Incubator from Thermo Fisher Scientific (Madison, WI).
Bacteria cell culture incubator	Eppendorf™ Excella® E25 Incubator shaker from New Brunswick Scientific Inc. (Edison, NJ).
Cell culture	1300 Series A2 biological safety cabinet from Thermo Fisher Scientific (Madison, WI).
Polymerase chain reaction (PCR)	2720 Thermal Cycler was purchased from Applied Biosystems (Foster City, CA).
DNA agarose gel electrophoresis	OWL EasyCast™ horizontal gel electrophoresis chamber connected with EC105 power supply obtained from Thermo Electron Corporation. Gels were imaged using Gel Doc™ EZ Imager purchased from Bio-Rad Laboratories (Hercules, CA).
Measuring DNA and protein concentration	GENESYS 10S UV-Vis Spectrophotometer (DNA/protein) and NANODROP LITE Spectrophotometer (DNA) from Thermo Fisher Scientific (Madison, WI).
In vivo bioluminescence imaging	IVIS Imaging System from Perkin-Elmer (Akron, OH) located in the Coverdell Center for Biomedical and Health Sciences at the University of Georgia. Image processing was performed with the Living Image Software (Perkin-Elmer).
Tissue luciferase activity assay	Luminometer AutoLumat LB 953 from EG & G (Salem, MA).

Drying SEM samples by exchanging ethanol for liquid CO_2	Samdri-780A critical point dryer from Tousimis® (Rockville, MD) at the GEM facility at the University of Georgia.
Scanning electron microscopy	Zeiss 1450EP SEM from Carl Zeiss MicroImaging, Inc. (Thornwood, NY) coupled with a variable pressure sample chamber and equipped with Oxford INC EDS system, Georgia Electron Microscopy (GEM) facility at the University of Georgia.
Gold coating SEM samples	SPI-Module sputter coater from Structure Probe, Inc. (West Chester, PA) at the GEM facility at the University of Georgia.
Centrifugation	Optima™ L-100 XP Ultracentrifuge, Avanti® J-30I and Allegra® X-15R centrifuge from Beckman Coulter, Inc. (Brea, CA). Eppendorf™ Centrifuge 5424 and Centrifuge 5810R from Eppendorf (Hauppauge, NY).
Tissue paraffin embedding	LINDBERG BLUE M convection oven from Thermo Fisher Scientific (Madison, WI) and Leica EG1160 Tissue Embedding Station from Leica Microsystems, Inc. (Buffalo Grove, IL).
Tissue section processing	RM2235 rotary microtome from Leica Microsystems, Inc. (Buffalo Grove, IL).
Mixer	Vortex-Genie 2 Variable Speed Vortex Mixer from Scientific Industries, Inc. (Bohemia, NY).
Tissue homogenization	Tissue-Tearor homogenizer from Dremel (Racine, WI).

3.3. *In Vivo* Research Design

Experimental design of *in vivo* studies performed in the research can be found in **Figure 3.1**. Female Balb/c (6-8 weeks old, 18-22 g) mice from Charles River Laboratories (Wilmington, MA) were used in all studies.

3.4. Procedures and Data Analysis

3.4.1. *Cell Culture*

Tumor cells were passaged when the cells reached 80-90% confluency. Cell culture medium was removed, and cells were trypsinized with 2.5 ml of Trypsin/EDTA solution at 37°C for 3 and 5 min for 4T1 and Renca cells, respectively. The trypsin solution containing the detached cells was mixed with 12.5 ml of the cell culture medium with FBS (10%). The cell suspension was aspirated 4-6 times to create a homogeneous single-cell suspension. Cell suspension (2 ml) was mixed with 10 ml of the appropriate cell culture medium and dispensed into a new dish. The cell culture dish was maintained in a humidified atmosphere at 37°C and 5% CO_2. The medium was renewed every two days.

For the long-term storage, detached cells suspended in the cell culture medium were centrifuged at 1,200 rpm for 5 min. The cell pellet was re-suspended in 2 ml of freezing medium, and then each 1 ml of the cell suspension was transferred to a cryovial. After being stored at -80° C for 24 hr, cryovials were transferred to a liquid nitrogen tank. For frozen cell recovery, cryovials were thawed by placing in a 37°C water bath for < 1 min. Cell suspensions (1 ml, 1.5-2×10^6 cells) were diluted dropwise with the complete cell culture medium (10 ml) and centrifuged at 1,200 rpm for 5 min. Cell pellets were re-suspended in cell culture medium and dispensed into a new 100 mm × 20 mm dish.

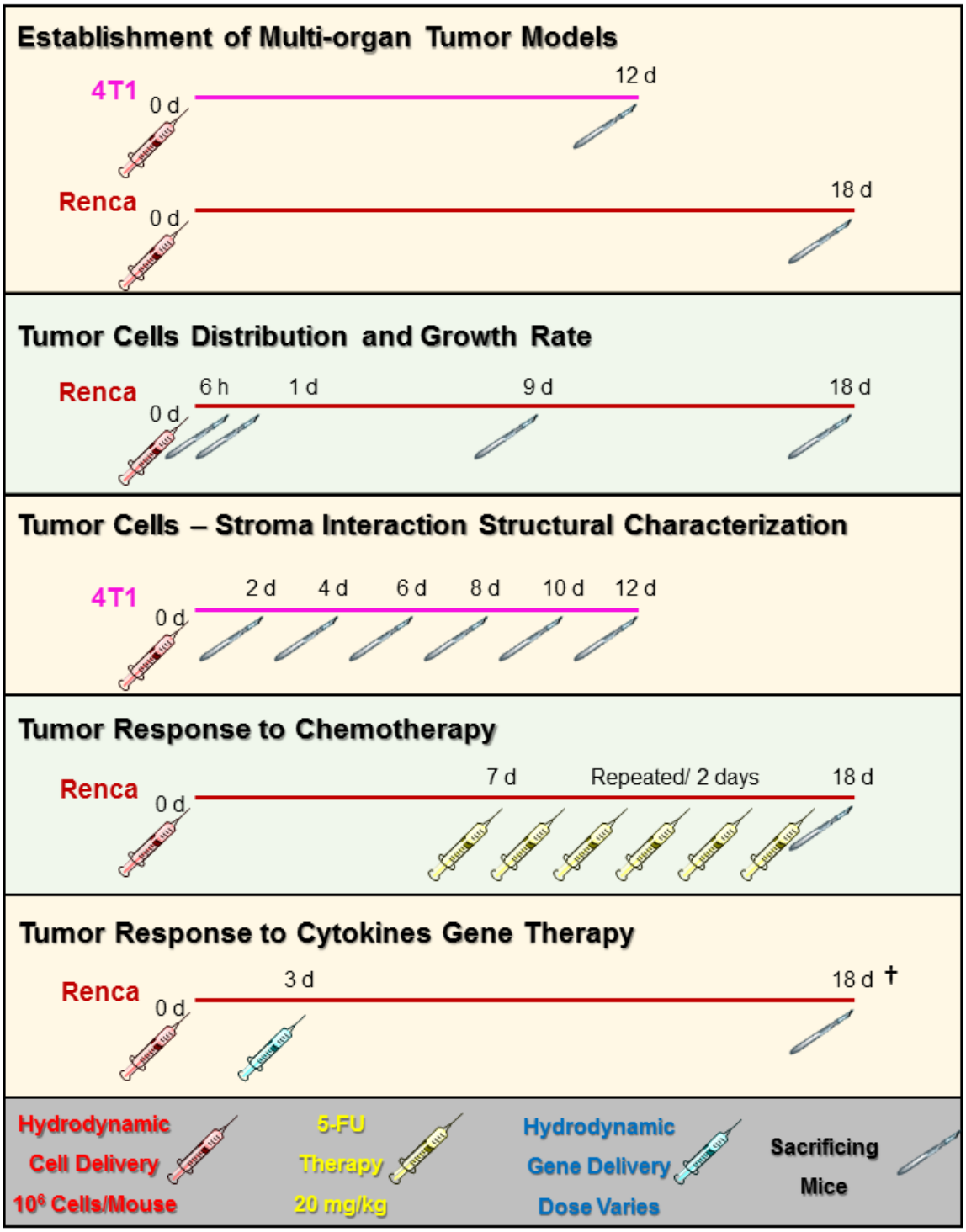

Figure 3.1. Experimental design of *in vivo* studies performed in the project. Tumor load was determined using *in vivo* bioluminescence imaging, histochemistry or/and luciferase assay. Scanning electron microscopy was used for structural characterization of tumor cell-stroma interaction. † IL-12 treated mice survived for 32 days. Detailed procedures can be found in Section IV, Procedures and Data Analysis.

To count the number of cells, an aliquot of the cell suspension was mixed with equal volume of trypan blue, and then 10 µl was transferred into a hemocytometer. The light microscope was used to count the number of live cells. The average number of cells counted within four gridded squares were multiplied by the dilution factor and 10^4 to obtain the number of cells per ml. The procedure was repeated, and the final cell number was averaged.

3.4.2. *Establishment of Renca$^{Luc/RFP}$ Cell Line*

To generate Renca$^{Luc/RFP}$ cells, a stable cell line expressing the luciferase and red fluorescent protein (RFP) genes, was generated by lentiviral transduction of the Renca cells. Luciferase and RFP genes were cloned into the FUCRW lentiviral vector and expressed under the regulation of the human ubiquitin promoter. Lentiviruses were made under the regulation of biosafety level 2 in Dr. Houjian Cai's lab at the University of Georgia, Athens, GA. When Renca cells reached 70-80% confluency, cells were harvested, and 2×10^4 cells were seeded in a 2-inch petri dish. On the following day, the medium was replaced, and 50 ul of a viral vector suspension was added. Cells were incubated for 48 h to assure cell transduction, and then the old media was replaced with fresh media. Viral infection was confirmed by the expression of RFP under an inverted fluorescence microscope.

A single-cell cloning procedure in a 96-well culture plate was performed to obtain a single clone. In brief, harvested Renca$^{Luc/RFP}$ cells suspended in a complete cell culture medium were counted and diluted to a final working solution with an estimated 1 Renca$^{Luc/RFP}$ cell/200 µl /well. Renca$^{Luc/RFP}$ cells were then dispensed into a 96-well plate, in which each well received 200 µl of the cell suspension. After 4 hr to allow tumor cells to attach, individual wells that received 1 Renca$^{Luc/RFP}$ cell were marked and monitored for 10 days. Wells that received multiple cells or showed growth of multiple clones were excluded. Then, the 6 colonies with the highest fluorescent

signal were transferred to a 6-well plate (1 clone/well) and cultured for a few days. Then, each colony was amplified in a 100 mm × 20 mm dish.

A single colony was then chosen for all the animal experiments, while other colonies were cryopreserved. The standard calibration curve of luciferase activity as a function of the number of Renca$^{Luc/RFP}$ cells was established using *in vitro* luciferase activity assay. Tumor cells were imaged using a Nikon Eclipse T*i*-U inverted fluorescence microscope. Image processing was carried out using the NIS-Elements imaging platform.

3.4.3. *DNA Plasmids Construction and Preparation*

The individual mouse cytokine genes: IFN-β (549 bp), IL-2 (509 bp), IL-7 (500 bp), IL-12 (fused p35 and p40 subunits; 2289 bp), IL-21 (440 bp), IL-24 (555 bp), or IL-27 (1975 bp), were subcloned into multiple cloning sites in a pLIVE vector. DNA constructed plasmids were confirmed by DNA sequencing. DNA purity was confirmed by agarose gel electrophoresis. DNA plasmid preparation for animal studies was performed by incubating the individual bacterial colony that contained the DNA plasmid of each gene in TB medium overnight at 37°C. Bacterial culture solution was centrifuged at 7,000 rpm for 10 min at 4°C. The bacterial pellet was stored at -80°C for 1 hr. The pellet was suspended in 10 ml of Solution I with vigorous shaking and then mixed with 2 ml of lysozyme solution and 8 ml of Solution I. After 10 min at room temperature, the solution was mixed with 40 ml of Solution II by gentle inversion. Then, 30 ml of Solution III was added to the mixture with gentle inversion, followed by centrifugation at 7,000 rpm for 20 min at 4°C. The supernatant was mixed with 0.6× volume of isopropanol. The mixture was spun at 7,000 for 20 min. Pellet was dissolved in 10 ml TE buffer and mixed with 1× volume of 5M

LiCl. The solution was spun at 10,000 rpm for 20 min, and the supernatant was washed with 0.5× volume of isopropanol. A pellet was obtained by spinning the mixture at 9,000 rpm for 25 min.

Plasmid DNA was purified using the method of cesium chloride-ethidium bromide gradient centrifugation. The pellet obtained previously was dissolved in TE buffer. Every 21 ml of the solution was mixed with 21 g CsCl. 500 µl ethidium bromide was added, and the solution was centrifuged at 62,000 rpm for 16 hr. The plasmid DNA band was separated and washed with saturated butanol until the solution became clear. DNA solution was dialyzed in new double-distilled water × 3 times overnight. The DNA solution was mixed with a 1/10 × volume of 5M sodium acetate pH 5.8 and 2 × volume of 100% ethanol. A DNA pellet was obtained by incubation at -20°C and spun at 10,000 rpm for 20 min. The pellet was washed again with 70% ethanol and centrifuged following the previous step. The DNA pellet was air dried, dissolved in saline and stored at -80°C until use. The purity of the purified plasmids was determined by $OD_{260/280}$ ratio and agarose gel electrophoresis. Plasmid DNA concentration was determined by absorbency at OD_{260}.

3.4.4. *Establishment of Multi-organ Tumor Models*

Female Balb/c (6-8 weeks old, 18-22 g) mice were purchased from Charles River Laboratories (Wilmington, MA) and housed in a pathogen-free environment in the Animal Facility of the University of Georgia. Mice were fed regular chow diets, and water was available *ad libitum*. All animal procedures performed were approved by the Institutional Animal Care and Use Committee of the University of Georgia in Athens, Georgia. Tumor cell suspensions for *in vivo* experiments were prepared by mixing the detached tumor cells with complete cell culture medium, and cells were collected by centrifugation (1,200 rpm for 5 min). Cell pellets were re-suspended and washed twice with serum-free medium, then passed through a membrane filter with an average

pore size of 40 μm (BD Falcon, Franklin Lakes, NJ). Cell pellets were obtained by centrifugation of tumor cell suspensions at 1,200 rpm for 5 min at room temperature, followed by resuspending the cells in serum-free medium at a desirable concentration determined by a hemocytometer.

To establish multi-organ tumor growth, we used hydrodynamic cell delivery as previously described [35]. A volume equivalent to 9% of the body weight and containing 10^6 4T1 or $Renca^{Luc/RFP}$ tumor cells were injected into the tail vein of a mouse over 5-8 s. To determine tumor growth in different organs, we sacrificed mice at desirable time points after cell injection, collected organs, and determined the tumor load using histochemistry or/and luciferase assay.

3.4.5. *Treatment of Tumor-bearing Mice*

For chemotherapy treatment, tumor-bearing mice were randomly divided into control and treatment groups. The treatment group received an intraperitoneal injection of 5-FU (20 mg/kg) [203], and the control animals received carrier solution on day 7. Treatment continued every other day for a total of 6 injections. Mice were euthanized 18 days after the tumor cell injection. For cytokine gene therapy, plasmids containing cytokine genes, including IFN-β, IL-2, IL-7, IL-12, IL-21, IL-24, or IL-27, were hydrodynamically injected into mice 3 days after tumor inoculation [192, 193]. Tumor growth in mice was assessed using *in vivo* bioluminescence imaging at different time points. To evaluate the response of tumors in different organs to 5-FU and IFN-β treatments, mice were sacrificed at day 18 post cancer cell injection, and the tumor load in different organs was determined by histochemistry or/and luciferase assay. Mice receiving injection of pLIVE empty vector served as a control.

3.4.6. *In vivo Bioluminescence Imaging*

On the day of examination, mice from the same group were intraperitoneally injected with 200 µl (150 mg/Kg) of Firefly D-luciferin in Dulbecco's phosphate buffered saline and anesthetized 2 min later with isoflurane inhalation (Abbott Lab, Irving, TX) in an induction chamber. To begin imaging, mice from the same group were transferred into the imaging chamber where they were placed on the dorsal position (abdomen facing up) and their noses were inserted in nosecones providing a continuous infusion of isoflurane to keep the mice anesthetized. Whole body imaging was performed 15 min after D-luciferin injection using an IVIS Imaging System (Perkin-Elmer). Imaging was acquired using 1 min acquisition time (binning 4, F-stop 1, FOV 12.5). The region of the area of interest was manually adjusted. Light intensity was calculated using Living Image Software with background subtraction and was expressed as photons/second/cm^2/steradian (p/s/cm^2/sr).

3.4.7. *Tissue Luciferase Activity Analysis*

Tissue samples collected from sacrificed mice were immediately frozen in liquid nitrogen and kept at -80°C until use. For luciferase assay, 1 ml of the lysis buffer was added to a piece of tissue (~100 mg) and homogenized using a tissue homogenizer (Dremel). Tissue homogenates were centrifuged for 10 min in an Eppendorf™ Centrifuge 5424 at 12,000 rpm at 4°C. 10 µl of supernatant was used to determine luciferase activity using a luminometer AutoLumant LB 953. The protein concentration of the supernatant was determined by the Bradford protein assay kit. Luciferase activity was expressed as the relative light units (RLU)/µg protein.

3.4.8. *Scanning Electron Microscopy*

Animals were sacrificed on days 2, 4, 6, 8, 10 or 12 post tumor cell injection. Samples were prepared according to the procedure described previously [202]. Lung, liver, and kidneys were immediately immersed in 2.5% glutaraldehyde in 0.075M cacodylate buffer overnight at 4°C. The tissues were cut into slices (less than 1 mm in thickness) using a clean razor blade. After being rinsed using washing buffer 1 (cacodylate buffer) (× 3 times, 15 min each), tissue slices were post-fixed in 1% OsO_4 in cacodylate buffer for 2 h at room temperature. Tissue slices were then washed with washing buffer 2 (× 3 times, 15 min each) and dehydrated in a series of graded ethanol (30%, 50%, 70%, 85%, 95% and 100% × 2 times, 15 min each) at room temperature, then dried in a Samdri-780A critical point dryer. Dried samples were mounted onto aluminum stubs and gold coated with SPI-Module sputter coater. Sections under vacuum pressure were examined with a Zeiss 1450EP scanning electron microscope. To identify the tumor nodules in different organs, the architectures of tumor-bearing organs were compared with the architectures of the surrounding healthy tissues of the same organs and organs from control mice. Different types of cells were identified based on the morphology of the same cells that reported in the literature.

3.4.9. *Histochemical Analysis by Hematoxylin and Eosin (H&E) Staining*

Samples were prepared as described previously [204]. Tissues from the lungs, liver, and kidneys were collected and fixed in neutrally buffered formalin (10%) for 3-5 days. Fixed tissue samples were washed with distilled water and dehydrated in a graded ethanol series (50%, 70%, 85%, 95%, for 30 min each, and then 100% × 2 times, 60 min each), followed by immersion in xylene (× 2 times, 60 min). Samples were incubated in paraffin overnight at 60°C. Embedded tissues were sectioned at 6 μm in thickness. Tissue sections were placed on glass slides and

incubated in xylene (× 3 times, 3 min each) followed by immersion in a graded ethanol series (100% × 2 times, 95% × 2 times, 75% for 3 min each). The slides were stained with H&E following the manufacturer's instructions (BBC Biochemical, Atlanta, GA). Tissue sections were examined under a regular microscope, and photo images were taken using the NIS-Elements imaging software from Nikon Instruments Inc. (Melville, NY).

3.4.10. *Statistical Analysis*

In vivo studies were carried out with three to four mice per treatment group. Results are expressed as the mean ± SD. Statistical significance was determined using an unpaired Student's *t*-test. A $P<0.05$ was considered significantly different. Statistical analysis was carried out using GraphPad Prism software purchased from GraphPad Software, Inc. (La Jolla, CA).

CHAPTER 4

RESULTS

4.1. Generation of Reporter-tagged Cell Line

Tumor growth in internal organs and tumor response to therapy cannot be assessed using caliper measurement as in the case of a subcutaneous tumor, nor can it be determined by measuring the wet weight of organs since variable tissue blood content can produce misleading results. Therefore, Renca tumor cells labeled with the luciferase gene allows for quantitative assessment of the tumor burden in each organ. Measurement can be obtained by direct *ex vivo* measurement of luciferase activity in dissected organs or *in vivo* by bioluminescence imaging of the whole animal after intraperitoneal injection of the substrate. To generate a Renca cell line stably expressing luciferase, we used viral transduction to integrate the luciferase gene into the tumor cells' genome. Viral vectors carrying red fluorescent protein (RFP) and firefly luciferase genes were obtained from Dr. Houjian Cai, who also assisted in the transduction of the Renca cells *in vitro*. Viral vectors were incubated with Renca cells for 2 days, with continued monitoring of the RFP expression, before changing cell culture medium with a fresh medium. **Figure 4.1** showed an image from an inverted fluorescence microscope confirming the expression of RFP and that the viral infection was successful.

However, viral transduction resulted in a heterogeneous population of cells that either had RFP expression or did not. Even those cells that expressed RFP showed variable expression of the RFP as indicated by different fluorescence intensities among tumor cells, suggesting some tumor cells were infected with more viral vectors than other cells. Therefore, a single-cell cloning

procedure (**Figure 4.1**) in a 96-well culture plate was used to obtain a pure colony derived from a single cell, so the colony would have similar gene expression. The Renca cell suspension was diluted so that each well would receive a single cell. After seeding, a single-cell colony was monitored for up to 10 days. A pure colony that showed a fluorescence signal, which indicated luciferase gene expression, was selected and transferred to a 6-well plate for expansion. We used this colony for all of the following experiments.

4.2. Establishment of Tumor Growth in the Lung, Liver, and Kidneys by Hydrodynamic Cell Delivery

A single colony of luciferase expression Renca$^{Luc/RFP}$ or 4T1 breast cancer cells were hydrodynamically injected into Balb/c mice (1×10^6 cells/mouse). Tumor nodules in the lung, liver, and kidneys were examined 12 and 18 days post cell injection for breast cancer and renal cell carcinoma, respectively. Photo images of the external appearance of the three organs showed multiple tumor nodules in the lung and the liver, but none in the kidneys (**Figure 4.2A**). However, H&E staining for Renca$^{Luc/RFP}$ tumor-bearing organs and SEM images of 4T1 tumor-bearing organs show tumor growth in all three organs (**Figures 4.2B** and **4.2C**). These results confirmed the effectiveness of the hydrodynamic procedure for establishing tumor growth in the lung, liver, and kidneys.

4.3. Tumor Cell Distribution by Hydrodynamic Cell Delivery

The presence of more tumor nodules in the lung and liver, and fewer in the kidneys (**Figure 4.2**), suggested a difference in the tumor load among the organs. Such a difference could be due to uneven delivery of tumor cells to the organs by tail vein hydrodynamic cell delivery,

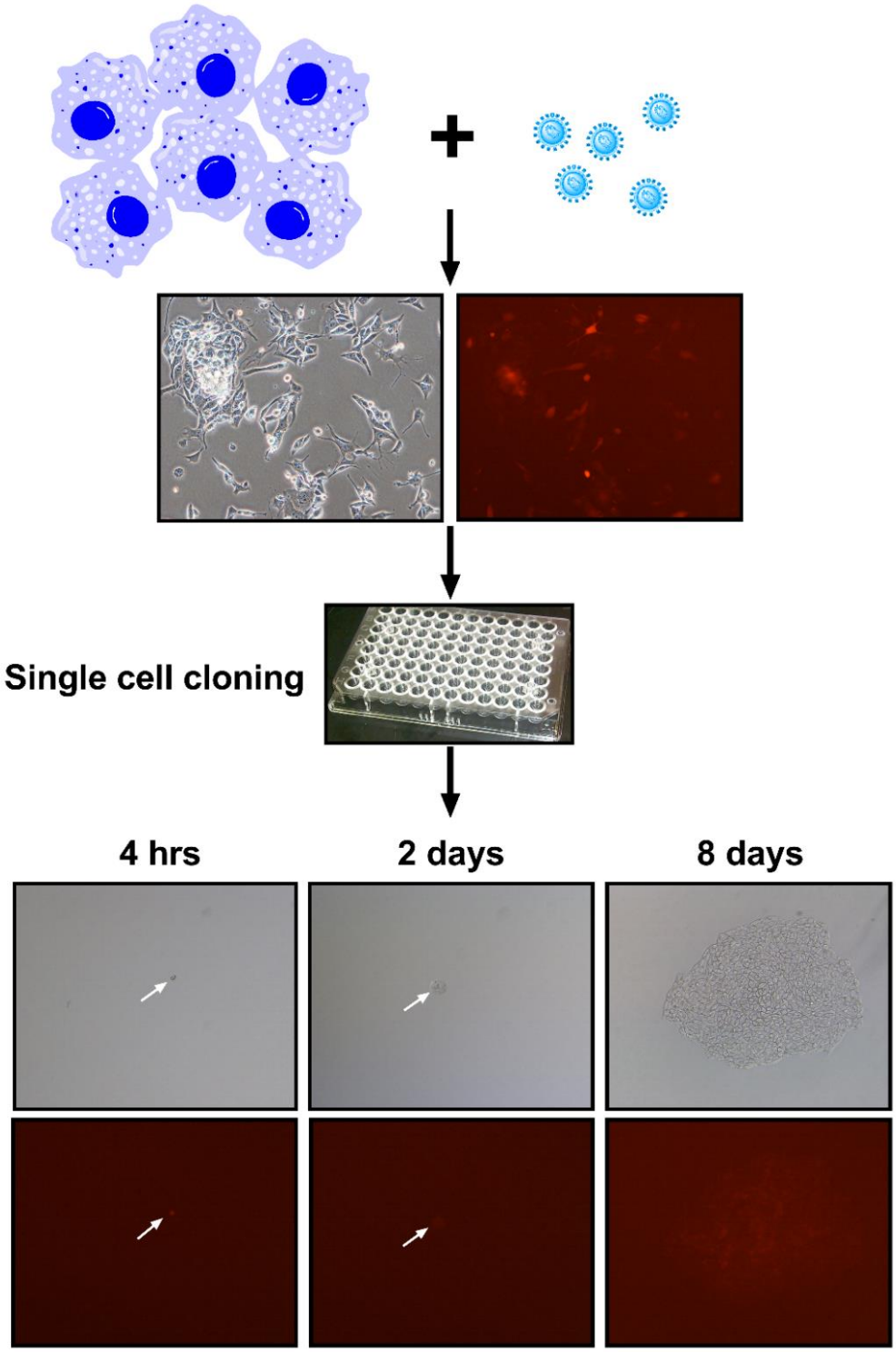

Figure 4.1. Establishment of Renca$^{Luc/RFP}$ cell line. A lentiviral vector carrying firefly luciferase and red fluorescent protein (RFP) genes was incubated with Renca cells. Two days later after viral infection, a single-cell cloning procedure using a 96-well plate was carried out to generate a pure colony. White arrows indicate the colony.

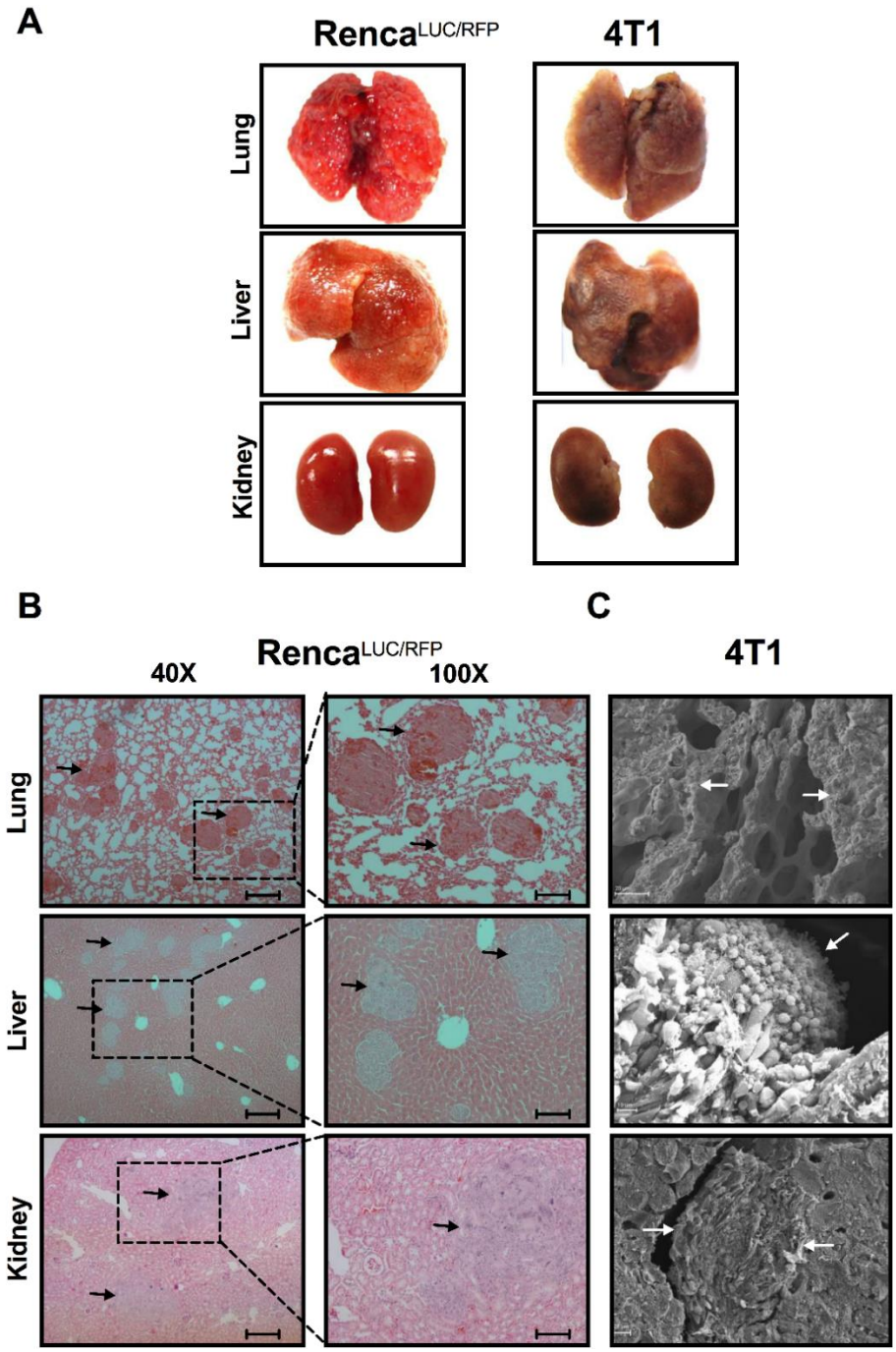

Figure 4.2. Establishment of tumor growth by hydrodynamic cell delivery. Balb/c mice were hydrodynamically injected with 1×10^6 Renca$^{Luc/RFP}$ or 4T1 cells/mouse. Mice were euthanized 12 or 18 days after injection of 4T1 or Renca cells, respectively, and the lung, liver and kidneys were collected and examined. A) Representative images of tumor-bearing lung, liver and kidneys. B) H&E staining of tissue sections of the organs collected from Renca model. Tumor nodules are indicated with arrows. Scale bars represent 250 μm (40×) and 100 μm (100×). C) SEM images of tissue sections of the same organs collected from 4T1 model. Tumor nodules are indicated with white arrows.

or to different growth rates of the tumor in different organs. To test these possibilities, we hydrodynamically injected Renca$^{Luc/RFP}$ cells into mice and examined their tissue distribution 6 h later, before possible proliferation could take place. *In vivo* bioluminescence imaging shows the expression of luciferase in injected Renca$^{Luc/RFP}$ cells 6 hr post injection (**Figure 4.3A**). Animals were then sacrificed and internal organs collected for luciferase assay. Quantification of luciferase activity in each of the three dissected organs shows 24.5% and 11.4% of the injected cells were distributed in the lung and liver (**Figure 4.3B**), respectively. Luciferase activity in the kidneys was below the detection limit of our luciferase assay, suggesting a minimal cell delivery for hydrodynamic injection to the kidneys. It appears that we lost about 65% of estimated luciferase activity, based on values derived from the standard curve of luciferase activity as a function of Renca$^{Luc/RFP}$ cell numbers. These results suggest that hydrodynamic injection created an uneven cell distribution among the three organs involved.

4.4. Tumor Growth Rate in Different Organs

Similar experiments were performed to examine the tumor load in different organs as a function of time. Results in **Figure 4.3C** show a slight decrease of luciferase activity in the lung between 6 to 24 hr, suggesting a loss of luciferase expressing cells in this organ. However, luciferase activity increased from day 1 on. At the end of the 18-day experiment after cell injection, a similar level of tumor load was seen in the lung and liver, with luciferase activity at approximately 10^5 RLU per microgram of proteins of the tissue homogenates (**Figures 4.3C** and **4.3D**). Interestingly, until day 9, luciferase activity in the kidneys was below our detection limit, indicating minimal tumor cell proliferation (**Figure 4.3E**).

Tumor growth rates in different organs were determined by the fold increase of luciferase activity in the lungs (**Figure 4.3F**), liver (**Figure 4.3G**), and kidneys (**Figure 4.3H**). The number of tumor cells in the lung increased 14- and 23-fold from days 1 to 9, and from days 9 to 18, respectively. Similarly, the increase in the liver was 66-fold from days 1 to 9, and 30-fold from days 9 to 18. Compared to the lung and liver, tumors in the kidneys expanded 557-fold between days 9 and 18, suggesting that tumor growth in the kidneys was slow initially and expanded rapidly once reaching a threshold level.

4.5. Structural Characterization of Tumor Cells-Stroma Interaction in Different Organs

One of the dissimilarities between the liver, lung, and kidneys is the distinction in organ architecture. Each organ has constituent cell types that arrange themselves in a unique structure. Therefore, tumor cells might interact differently with the structure of each organ. To test this possibility, we examined 4T1 tumor-bearing organs using scanning electron microscopy and analyzed the morphological alterations associated with tumor growth. As expected, tumor growth patterns were different among the organs. In the lung, tumor cells are confined inside the small capillaries surrounding the alveoli, with no signs of extravasation. The intravascular growth of tumor cells caused expansion of the pulmonary capillaries that leads to alveoli collapse (**Figure 4.4**). Therefore, the normal mesh-like structure of the interior of the lung, formed by alveoli, was lost, and the tumor mass rarely seen earlier gradually invaded the interior cavity throughout the lung.

Conversely, the tumor growth in the liver and kidneys took place with extravasation. In the liver, the tumor cells present at the border of the tumor nodule compressed the hepatocytes and disrupted the hepatic cords (**Figures 4.5A** and **4.5B**). Another piece of evidence for the

extravascular growth in the liver is the vascular invasion by tumor cells that entered the blood vessels, leading to tumor growth inside blood vessels (**Figures 4.5C** and **4.5D**). In the kidney, the tumor showed similar extravascular growth, as demonstrated by the disorganization of renal tubule arrangements (**Figures 4.6A** and **4.6B**) and the presence of tumor cell intravasation (**Figures 4.6C, 4.6D,** and **4.6E**). Structural alterations in the hepatic and renal vessels during tumor cell intravasation included loss of the endothelial cell-cell junction, leading to the formation of intercellular gaps, and accumulation of white blood cells in large numbers in the disrupted blood vessels.

4.6. Differential Responses to Chemotherapy

Two approaches were taken to examine how Renca$^{Luc/RFP}$ cells seeded in the lung, liver, and kidneys responded to treatment. The first approach employed 5-FU as an anticancer drug. Tumor-bearing mice were treated with 5-FU (20 mg/kg in 100 μl, *i.p.*) every other day for 12 days starting on day 7 post hydrodynamic cell delivery. The control animals received an injection of PBS, the carrier solution. Results in **Figure 4.7** show that 5-FU treatments suppressed tumor growth in the lung by 57.4%, compared to 43.1% in the liver and 38.6% in the kidneys. While significant antitumor activity was seen in the lung and liver, as quantified by luciferase activity, tumor nodules were observed in all three organs (data not shown). These results suggest that 5-FU has limited effectiveness in suppressing the growth of Renca$^{Luc/RFP}$ cells in mice.

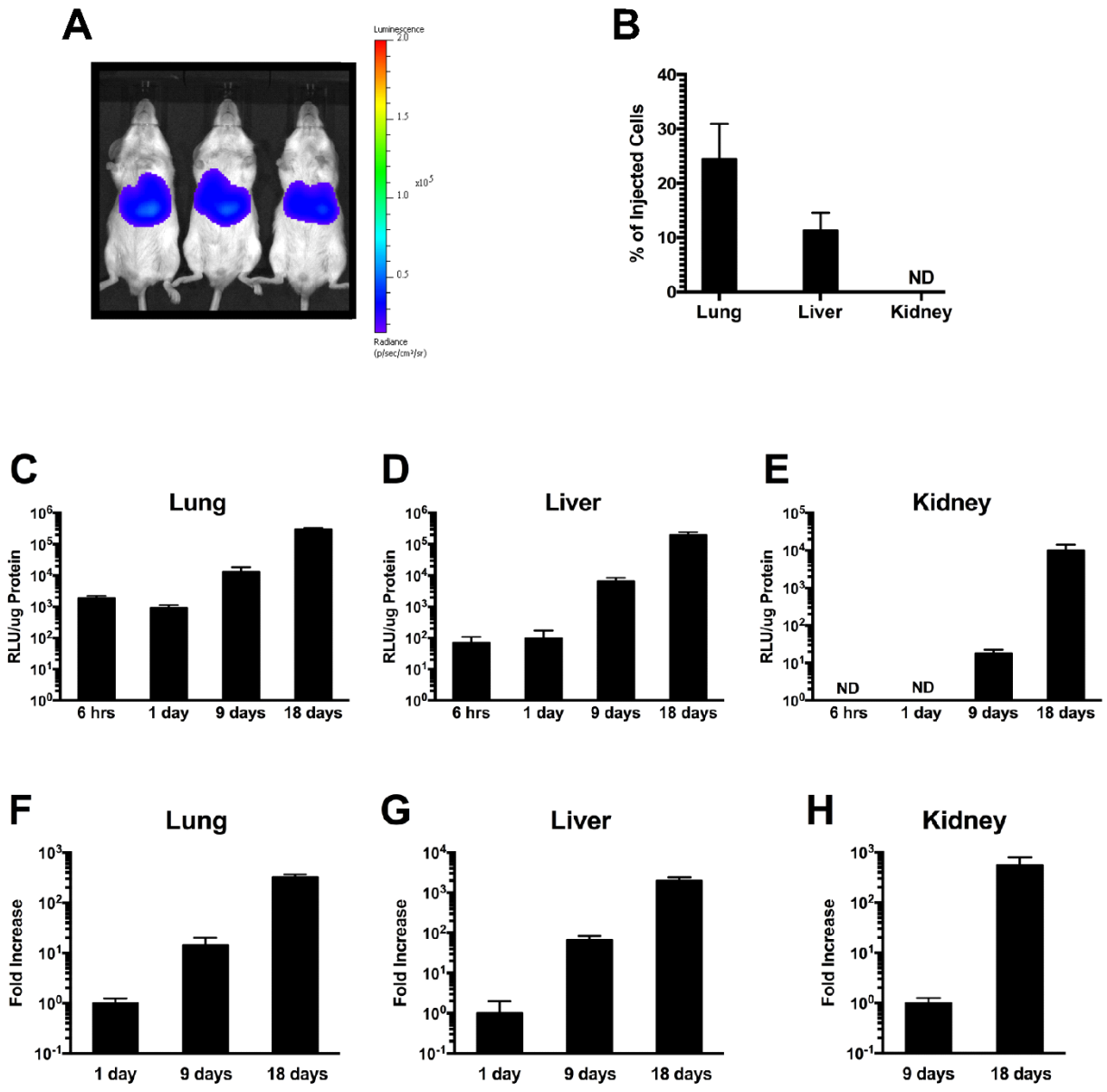

Figure 4.3. Renca$^{Luc/RFP}$ cell distribution and characterization of tumor growth rates in different organs. Balb/c mice were hydrodynamically injected with 1×10^6 Renca$^{Luc/RFP}$ cells/mouse. Mice were imaged using *in vivo* bioluminescence imaging at 6 hr after injection. Different groups of mice were euthanized on 6 hr, 1, 9, and 18 days, organs were collected and luciferase activity was determined. A) Ventral view of the *in vivo* bioluminescence image showing adequate light emitted from tumor cells 6 hr after hydrodynamic cell injection. B) Organ distribution of Renca$^{Luc/RFP}$ cells 6 hr after hydrodynamic injection of tumor cells. C-E) Estimation of tumor burden in different organs at different time points judging from luciferase activity (RLU/μg of protein). F-H) Increase of tumor mass on days 9 and 18 in the lung and liver compared to that of day 1, and folds of increase of tumor burden in kidneys between days 9 and 18. Values represent mean ± SD (n=3), **P*<0.05. ND: not detected.

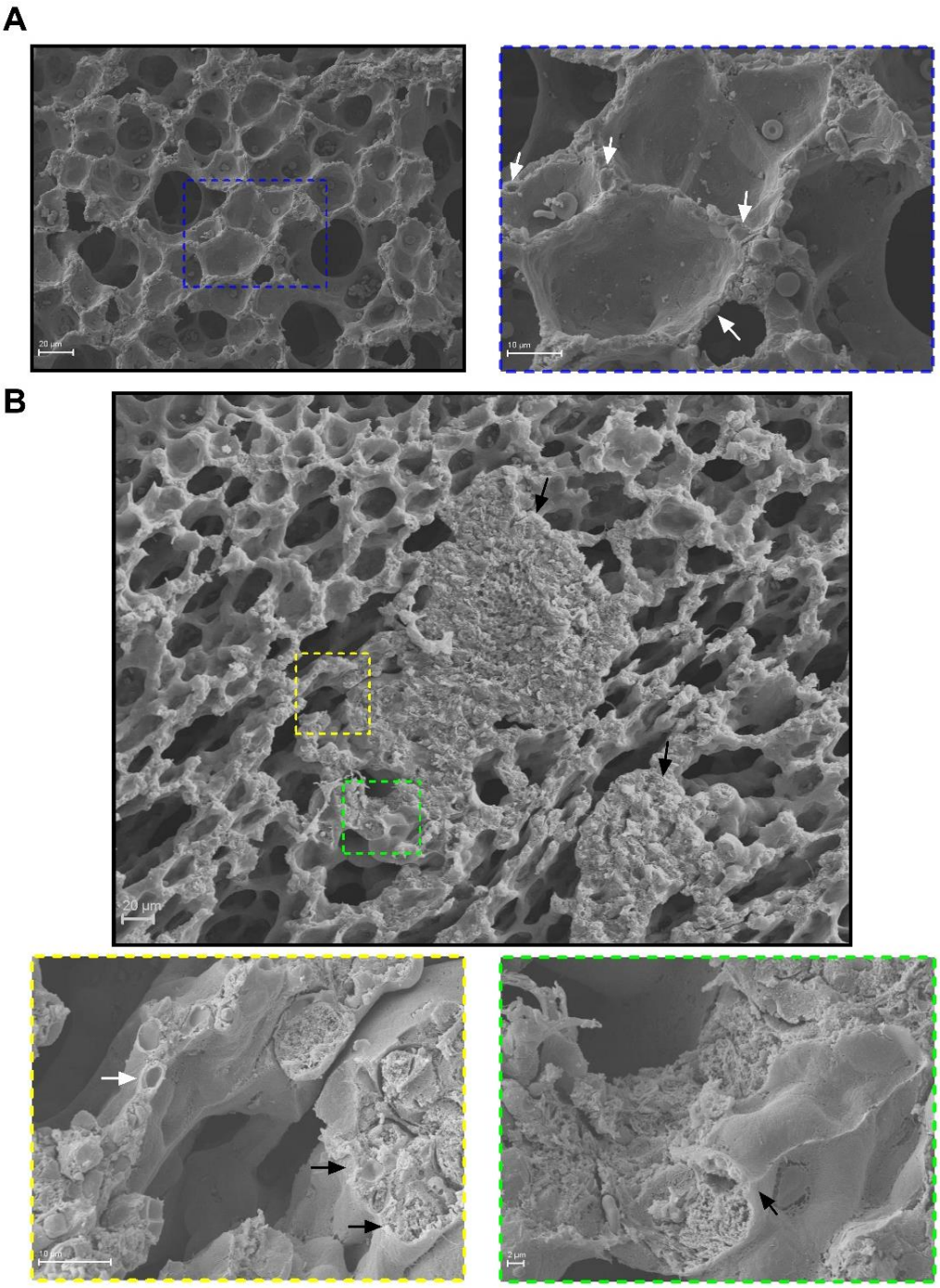

Figure 4.4. Structural characteristics of 4T1 tumor in the lung. A) Scanning electron microscopy image showing the alveoli structure. High-magnification image (*blue frame*) showing alveoli surrounded by blood capillaries (*white arrows*). B) Low-magnification image (*black frame*) showing tumor nodules (*black arrows*). High-magnification images (*colored frames*) showing tumor cells. The left picture shows small empty capillaries in healthy tissue (*white arrow*) and tumor cell-filled capillaries (*black arrows*). The right picture shows blood capillary (*black arrow*) with blocked interior.

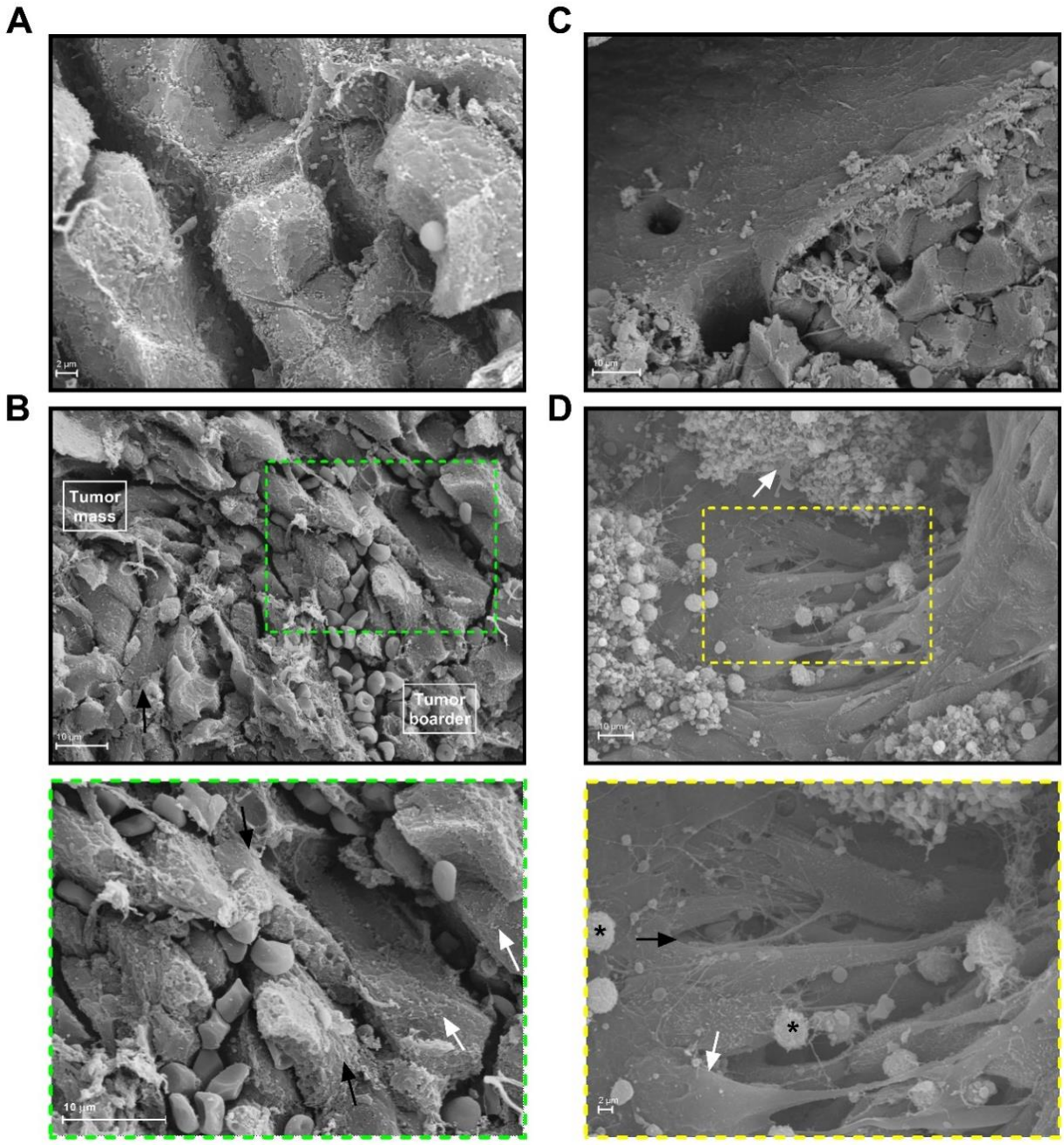

Figure 4.5. Structural characteristics of 4T1 tumor in the liver. A) Scanning electron microscopy image taken from healthy liver showing the hepatic cords and blood capillaries (sinusoids). B) Low-magnification image (*black frame*) showing tumor nodule. High-magnification image (*green frame*) showing the tumor border (*black arrows*) and two hepatic cords (*white arrows*). C) Scanning electron microscopy image showing the structure of vasculature in a healthy liver. D) Low-magnification image showing destruction of the blood vessel wall by the tumor growing underneath, and presence of blood clot (*white arrow*). High-magnification image (*yellow frame*) showing endothelial cell (*white arrow*) without cell-cell junction, a blood vessel gap (*black arrow*), and accumulation of immune cells (*black stars*).

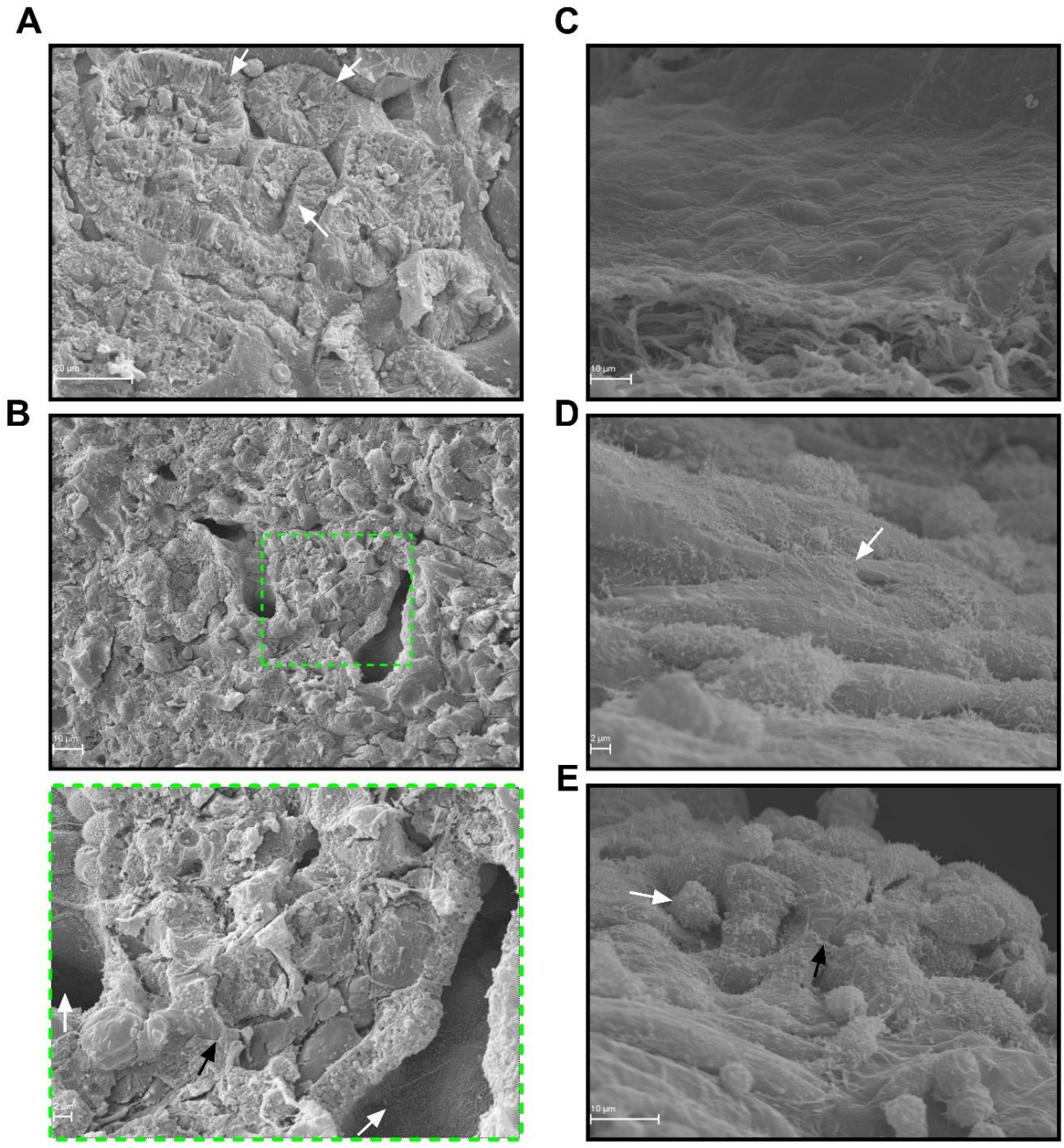

Figure 4.6. Structural characteristics of 4T1 tumor in the kidneys. A) Scanning electron microscopy image showing the structure of the renal tubules (*white arrows*) in a healthy kidney. B) Low-magnification image (*black frame*) shows tumor nodule. High-magnification image (*green frame*) showing that the area between renal tubules (*white arrows*) was infiltrated by a group of cells (*black arrow*). C) Scanning electron microscopy imaging shows the lining of a healthy renal blood vessel. D) Scanning electron microscopy image showing endothelial cell (*white arrow*) without cell-cell junction as a result of cell infiltration. E. Scanning electron microscopy image showing the proliferation of tumor cells (*black arrow*) inside the cavity of the renal vasculature, and accumulation of the immune cells (*white arrow*).

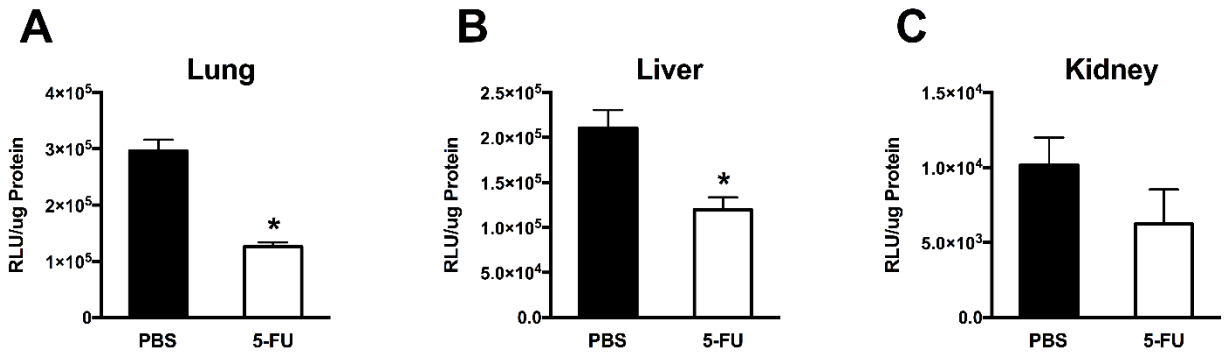

Figure 4.7. Different response of RCC tumors growing in different organs to 5-FU treatment. Balb/c mice were hydrodynamically injected with 1×10^6 Renca$^{Luc/RFP}$ cells/mouse. Seven days after cell injection, mice were injected (*i.p.*) with 20 mg/kg of 5-FU every other day for a total of 6 times. Mice were euthanized on day 18, and organs were collected and assessed. A-C) Quantification of tumor burden in the lung, liver, and kidneys, respectively, determined by luciferase activity (RLU/μg of protein). Values represent mean ± SD (n=4), **P*<0.05.

4.7. Differential Responses to Cytokine Gene Therapy

The second approach employed was gene therapy using different cytokine genes. Cytokine genes were chosen based on their unique functions, including cytotoxic activity against tumor cells (IFN-β and IL-24); activation of B cells (IL- 21); activation of T cells and NK cells (IL-2, IL-7 and IFN-β); and activation of Th1 cells (IL-12 and IL-27) [205-211]. Three days after tumor-cell injection, twenty-one tumor-bearing mice were randomly divided into seven groups, and each group received a hydrodynamic injection of a pLIVE plasmid containing one of the cytokine genes (IL-2: 2.5 μg/mouse, IFN-β: 10 μg/ mouse, other cytokines: 20 μg/mouse). Tumor growth over time was monitored using *in vivo* bioluminescence imaging on days 6 and 15. Results show that both IFN-β and IL-12 suppressed tumor growth, while other cytokines failed to show significant antitumor effects (**Figure 4.8**). A single injection of IL-12 plasmid was sufficient to prolong animal survival to 32 days, compared to other animals that showed signs of morbidity on day 18.

The suppression effect of IFN-β gene therapy on a multi-organ RCC model was further evaluated with a lower dose to avoid potential toxicity. On day 3 post tumor cell injection, 6 tumor-bearing mice were randomly divided into control and treated groups. The control group received a hydrodynamic injection of the empty pLIVE plasmid, while the IFN-β treated group received pLIVE-IFN-β (4 μg/mouse) plasmid DNA. *In vivo* bioluminescence imaging results on days 8 and 15 show that IFN-β significantly suppressed tumor growth compared to control (**Figures 4.9A** and **4.9B**). Results of the luciferase activity assessment on tumor-bearing organs indicated that tumor suppression obtained by IFN-β was due to inhibition of tumor growth in the liver, but not in the lung (**Figures 4.9C** and **4.9D**). Suppression of tumor growth was also seen in the kidneys (**Figure 4.9E**). Images of collected organs (**Figure 4.10A**) exhibit that IFN-β was highly effective in suppressing tumor growth in the liver, as observed by the absence of tumor nodules on the surface

of this organ. There was no obvious difference in the tumor load in the lung between treated and control animals. Results from histological examination of these animals are in full agreement with these conclusions (**Figure 4.10B**). These results provide direct evidence in support that the same tumor growth in different organs responds differently to the same treatment, indicating the importance of environment in determining the outcome of cancer treatment.

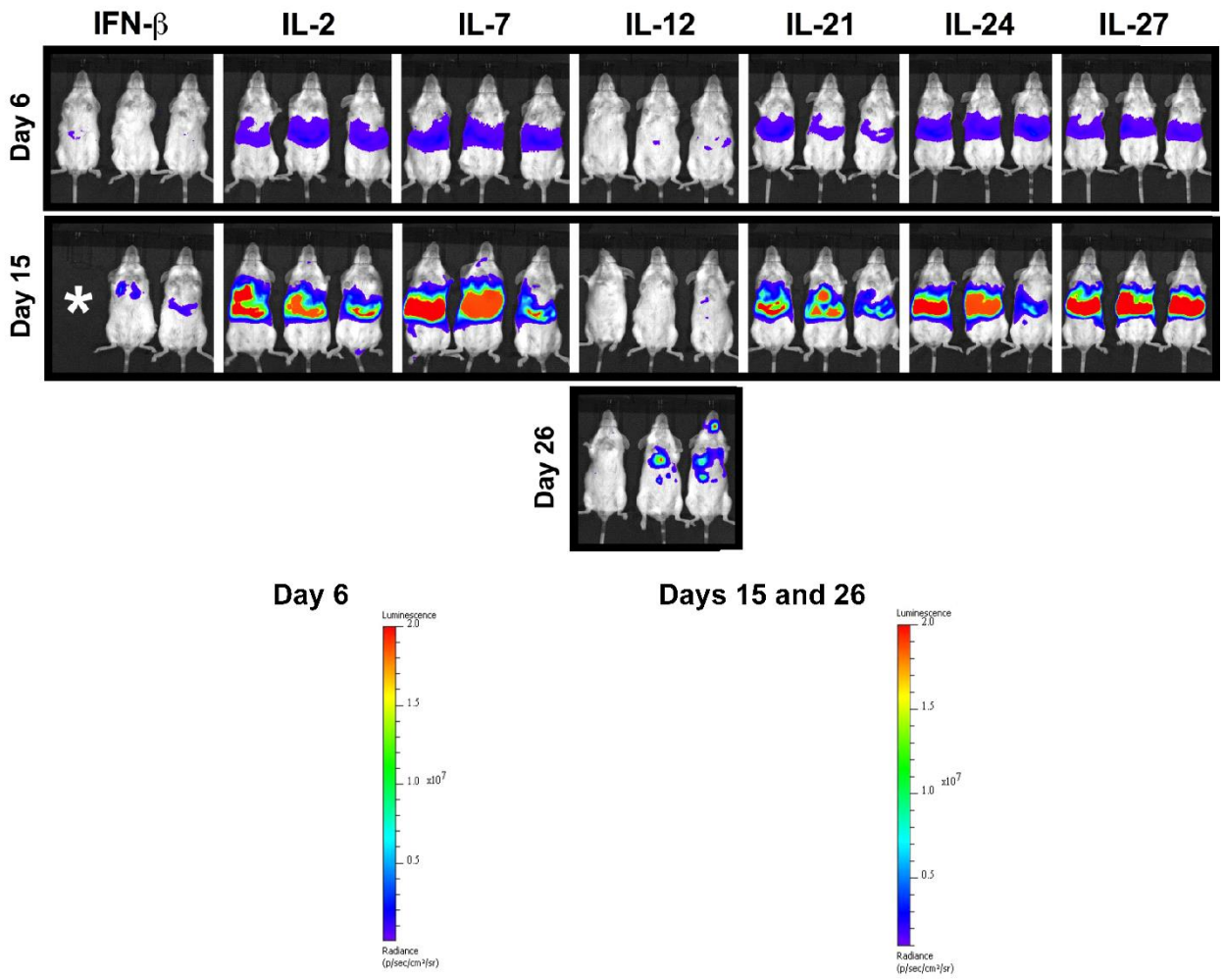

Figure 4.8. Assessment of antitumor activity of cytokine genes by hydrodynamic gene transfer. Balb/c mice were hydrodynamically injected with 1×10^6 Renca$^{Luc/RFP}$ cells/mouse. Three days after tumor injection, tumor-bearing mice were hydrodynamically injected with cytokine genes containing plasmid DNA (IFN-β: 10 μg/mouse, IL-2: 2.5 μg/ mouse, other cytokines: 20 μg/mouse). Mice were imaged using *in vivo* bioluminescence imaging on days 6 and 15 after tumor cell injection. *One mouse was lost in IFN-β group when performing bioluminescence imaging on day 15.

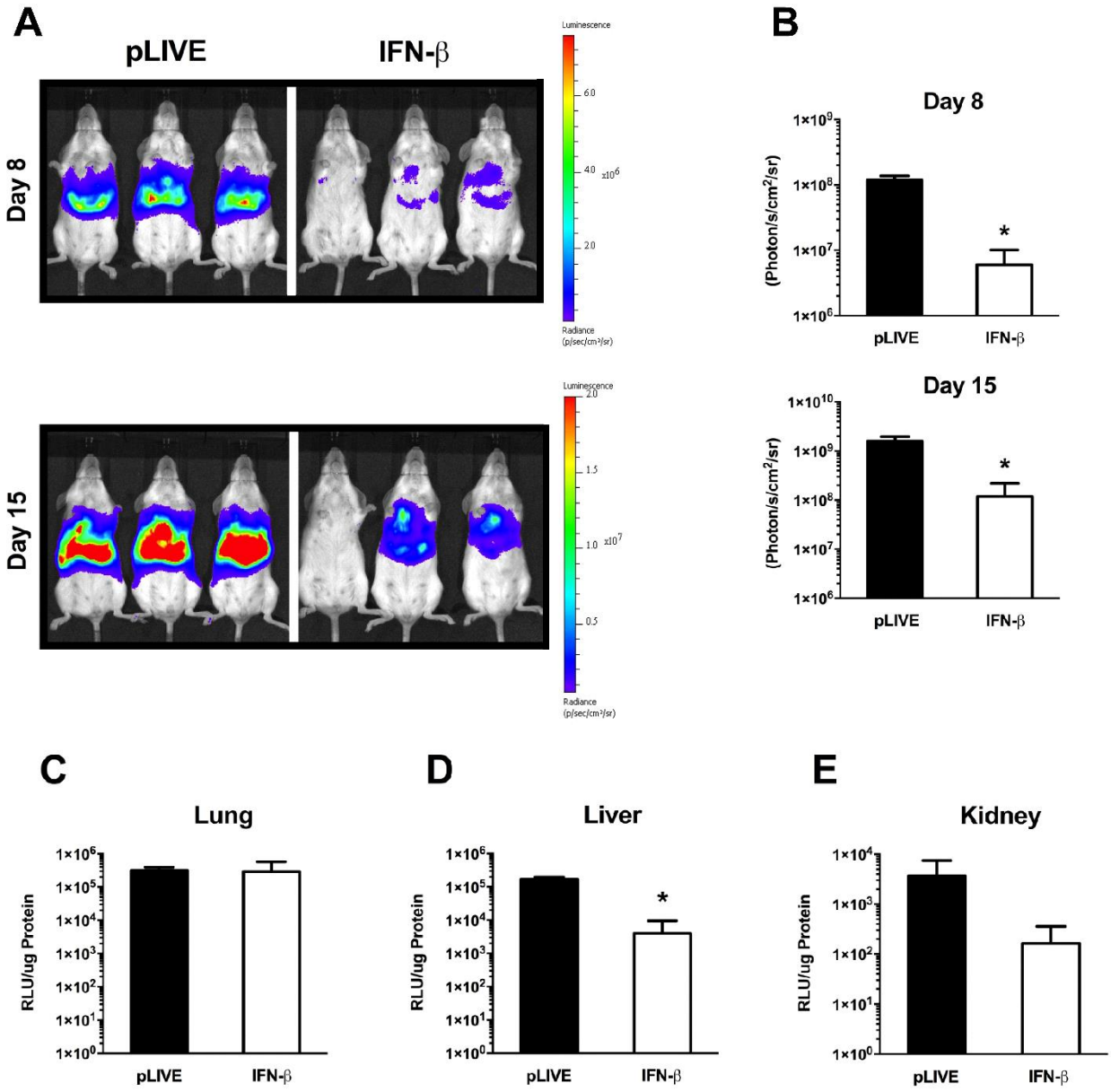

Figure 4.9. Quantitative assessment of the impact of IFN-β gene transfer on tumor growth. Balb/c mice were hydrodynamically injected with 1×10^6 Renca$^{Luc/RFP}$ cells/mouse. Three days later, animals (3 mice/group) were hydrodynamically injected with empty plasmid (control) or plasmids carrying IFN-β gene. Mice were imaged using *in vivo* bioluminescence imaging on days 8 and 15. Mice were euthanized on day 18 after cell injection and organs were collected for luciferase assay. A) *In vivo* bioluminescence images of the control and treated animals with hydrodynamic IFN-β gene transfer. B) Quantification of bioluminescence measurements for imaged areas of animals after 8 and 15 days of tumor injection, mean ± SD (n=3), **P*<0.05. C-E) Quantification of tumor burden in different organs of control and treated animals based on luciferase assay, mean ± SD (n=3), **P*<0.05.

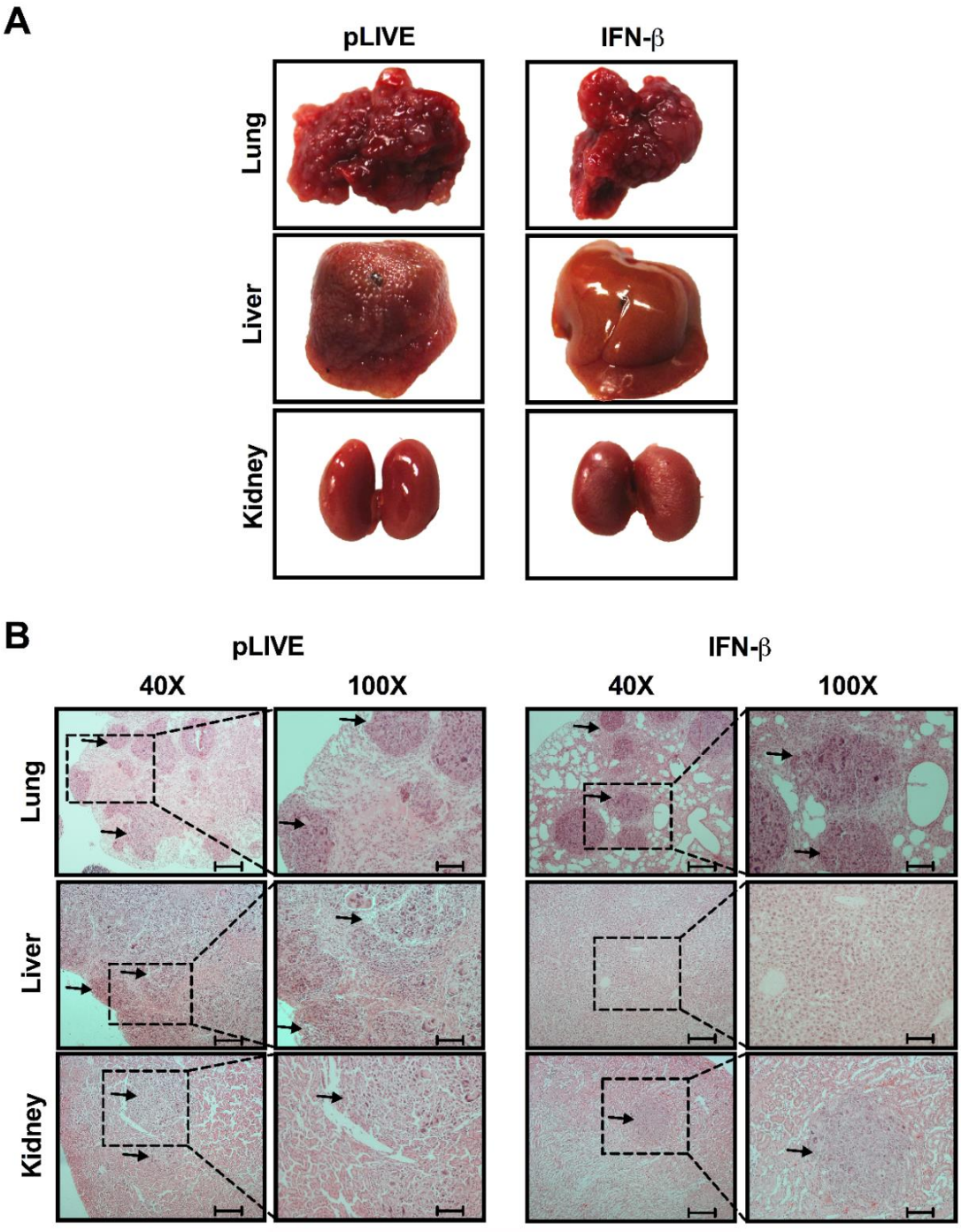

Figure 4.10. Histological examination of the impact of IFN-β gene transfer on tumor growth. Organs were collected from tumor-bearing mice 18 days after tumor cell injection and 15 days after hydrodynamic transfer of empty (control) or IFN-β gene containing plasmids. A) Representative images of tumor-bearing organs from both control and animals treated with IFN-β gene transfer. B) Representative images of H&E staining of different organs. Arrows indicate the tumor nodules in the lung and kidneys. No tumor nodules were seen in the liver of IFN-β treated mice. Scale bars represent 250 μm (40×) and 100 μm (100×).

CHAPTER 5

DISCUSSION

5.1. Principle and Potentials of the Multi-organ Tumor Model

A multi-organ tumor model for accurate preclinical drug assessment is an unmet need. In this project, we exploited hydrodynamic delivery to simultaneously implant wild-type 4T1 breast cancer cells and quantifiable Renca renal cell carcinoma into the lung, liver, and kidneys. The mechanism underlying multi-organ cell delivery by hydrodynamic injection involves the flow dynamics of the injected solution as determined by the vasculature of the inferior vena cava (IVC). When a large volume of tumor cell suspension, equal to 9% of the mouse body weight, is rapidly injected into the tail vein over 5-8 s, cardiac congestion is generated as the volume exceeds cardiac output. The cardiac congestion and presence of the large volume of solution lead to an elevation of the intravascular pressure inside the IVC. This pressure forces tumor cells to enter the liver and kidneys through the hepatic and renal veins, respectively, in retrograde. While some cells remain in the liver and kidneys once they reach these organs, the significant majority of the tumor cells go through the heart and reach the lungs when the heart regains its function and resumes regular blood flow. A phase contrast medium injected hydrodynamically and instantaneously monitored with fluoroscopic imaging in real time has confirmed this mechanism [200]. As a result of hydrodynamic cell delivery, we seeded tumor cells into three organs with different environments that are critical to tumor growth.

The multi-organ tumor model is considered an advanced *in vivo* model imitating the last stage of tumor metastasis and able to overcome the limitations of the current animal models. It

allows researchers to simultaneously evaluate the influence of the environments that existed in the visceral organs on the tumor biology while excluding the influence of the tumor cells with genetic heterogeneity [212, 213]. The results demonstrated the existence of microenvironmental heterogeneity between multiple anatomical sites after implanting genetically similar tumor cells into the lung, liver, and kidneys. Moreover, the multi-organ tumor model is user-friendly. First, the researcher can develop the model without the need for a surgical procedure to implant tumor cells or dissect the primary tumor as required in other advanced metastatic models. Second, the tumor development in these three organs is reproducible and within a short period. In this study, the lung, liver, and kidneys collected from the multi-organ tumor models of 4T1 and Renca$^{Luc/RPF}$ displayed the development of large tumor nodules within 12 and 18 days, respectively (**Figures 4.2A**, **4.2B** and **4.2C**). Therefore, it overcomes the practical challenges facing researchers dealing with the GEMM and spontaneous metastasis models, such as the asynchronous development of the tumors, the growth of tumors in unconfined sites, and the long time needed until a detectable tumor mass forms [188, 189]. Additionally, the multi-organ tumor model possesses a functional immune system. SEM images of the liver (**Figure 4.5D**) and the kidneys (**Figure 4.6E**) collected from 4T1 multi-organ tumor models showed the accumulation of immune cells in the tumor sites. The simultaneous growth of tumors in different organs provided an opportunity to assess the types and quantities of the immune cells infiltrating tumors in multiple organs in a setting resembling tumor metastasis in humans.

5.2. Factors Affecting Tumor Growth in Different Organs

Tumor growth rates vary in different organs. By using luciferase activity 1 day after injection as a baseline, the calculated activity increased 14-fold in the lung and 66-fold in the liver

on day 9, respectively, with a further increase to 322-fold in the lung and 1977-fold in the liver on day 18 (**Figures 4.3F** and **4.3G**). In the kidneys, tumor cells were below our detection limit at earlier time points but proliferated aggressively to 557-fold between days 9 to 18 post tumor injection, making their growth rate the highest compared to those of the lung and liver for the same period (**Figure 4.3H**). It appears that the kidneys offer the best environment for Renca$^{Luc/RFP}$ cells to grow, followed by the liver, with the lung being the most unfavorable among the three.

Moreover, tumor cell-stroma structural interactions were distinctive among different organs. In the lung, we found that 4T1 tumor cell growth was intravascular, as demonstrated by the clogged capillaries and enlargement of vessel diameters without any sign of tumor cell extravasation (**Figure 4.4**). A previous report using immunohistochemical staining indicated that single and small clusters of prostate cancer cells trapped in the lung capillaries soon after metastasis expressed Ki-67, reflecting active intravascular proliferation [214]. In this study, the morphological alterations on the tumor nodules at a later stage of tumor growth suggested that tumor cells followed the same intravascular growth as observed at an early stage of metastasis in the previous study. Furthermore, the similarity between the growth of breast and prostate cancer cells in both studies suggested that the tumor microenvironment of the lung was responsible for intravascular growth independent of cancer type.

In the liver and kidneys (**Figures 4.5** and **4.6**) tumor growth was extravascular, as indicated by the destruction and disorganization of hepatic cords and renal tubules, respectively. Additional evidence of the extravascular growth in this study was the tumor intravasation in the liver and kidneys. A previous intravital microscopy study performed on hepatic colon cancer metastasis demonstrated a significant decrease of blood flow in the hepatic vasculature, including the sinusoids, which were adjacent to the tumor nodules [215]. Our study and the previous one

demonstrated that the tumor extravascular growth was a feature in the liver. Both studies suggested that when tumor cells proliferate extravascularly, the tumor mass compressed the hepatic cords and slowed the circulation in the sinusoids. Excessive compression on the large vasculature causes vessel wall rupture and intravasation of the tumor mass.

While *in vivo* bioluminescence imaging and scanning electron microscopy allowed assessing tumor growth rates in visceral organs and demonstrated the structural interaction of tumor cell-stroma, these imaging techniques suffer from limitations. *In vivo* quantification of tumor growth in different organs might be affected by the anatomy and physiological status of different organs. Factors such as oxygen levels and proteolytic degradation in the microenvironment of different organs could influence the luciferase activity [216]. In addition, scanning electron microscopy images were interpreted based on the morphological characteristics of the tumor, so future investigation to the use of immunohistochemistry to confirm different types of cells in different organs is needed.

There are key factors by which the anatomical site can influence tumor growth. For example, the tumor-stroma interaction can provide a favorable or hostile microenvironment to tumor growth. The SEM images of the tumor-bearing lung indicated that tumor cells were enclosed inside the pulmonary vasculature. Intravascular tumor growth, as well as the proximity of the lung to the heart, increased the hemodynamic shear stress inside the pulmonary capillaries. Therefore, increased hemodynamic shear stress renders the lung a hostile environment for tumor cells to grow, in comparison to the liver and kidneys in which cancer cells grew extravascularly [217-219]. Additionally, the liver is considered a hypoxic organ [82]. Hypoxia is a crucial factor forcing tumor cells to undergo gene expression alterations, such as upregulation of hypoxia-inducible factor 1 (HIF-1), which augments cancer cell aggressiveness [220, 221]. Conversely, cancer cells are less

aggressive in an oxygenated environment. Therefore, the different oxygen levels in the lung, liver, and kidneys may have different impact on tumor growth in different organs.

Previous research on tumor-bearing organs demonstrated that there were other factors by which the tumor microenvironment influenced tumor growth. The organ-specific resident cells, types and quantities of myeloid and lymphoid cells recruited to different tumor-bearing organs varied, and the different metabolic characteristics of different organs contributed to tumor growth [30, 31, 81, 85, 87, 222]. Investigations to identify the impact of various factors on tumor growth in the lung, liver, and kidneys are needed. These factors can be potential targets for antimetastatic therapies instead of targeting intrinsic properties of tumor cells that are commonly susceptible to mutation [223]. We expect that organ-specific treatments can be designed based on the critical factor(s) in each organ.

5.3. Possible Mechanisms for Differential Responses to Therapy

The unique influence of each organ on tumor growth suggests that tumors' response to antitumor drugs would vary depending on the environment in which the tumor cells grow. The results in (**Figures 4.7- 4.10**) provide direct evidence in support of such a prediction. Treatment with 5-FU and by gene therapy with IFN-β and IL-12 resulted in varied response. 5-FU chemotherapy and IFN-β gene therapy exhibited better antitumor activity in the liver. Tumors in the lung were sensitive to 5-FU but not to IFN-β gene therapy. Conversely, 5-FU and IFN-β monotherapy did not produce significant tumor inhibition in the kidneys. A surprising observation in the study is that not all cytokines, even those belonging to the same family, possessed similar effectiveness. For example, while IFN-β gene therapy showed liver-specific tumor suppression, IL-12 gene therapy exerted a whole-body antitumor activity that significantly prolonged the

survival time of tumor-bearing mice. While additional studies are needed, these results suggest that the difference between alternative cytokine gene therapies is due to the various activities of the overexpressed cytokines in activating the different types of immune cells at the tumor sites.

Results in (**Figures 4.3** and **4.7**) demonstrated an inverse correlation between tumor growth rate and tumor response to 5-FU treatment. Tumors in the kidneys grew faster than tumors in other organs but demonstrated no response to 5-FU therapy. Conversely, tumors in the lung grew slower and demonstrated a higher response to 5-FU therapy. We anticipated that 5-FU should kill rapidly growing tumors more than slowly growing tumors. It is possible that the faster elimination of 5-FU and intermittent administration in this study allowed 5-FU to kill only a small fraction of the tumor cells during drug exposure [224]. Since the tumor microenvironment of the kidneys improved the proliferation capability of tumors, tumor cell proliferation in the kidneys might compensate for resulted tumor cell death by 5-FU therapy. Therefore, the different proliferation capabilities of tumors among different organs might be the key mediator of the differential response of tumors to 5-FU therapy. This conclusion does not exclude a possible influence of tumor microenvironment on the tumor cells' intrinsic mechanisms of resistance to 5-FU [225]. Future investigation of these mechanisms is needed. These results suggested that direct killing of tumor cells was not sufficient to eliminate tumors and, therefore, incorporating drugs that target the tumor microenvironment with cytotoxic drugs will improve the therapeutic outcome.

Moreover, tumor microenvironment can induce tumor resistance to therapy by altering the antitumor activity of immune cells and regulating the amount and types of immune cells infiltrating the tumor microenvironment [31]. Previous studies showed that the liver is rich with NK cells, and type I interferon activates NK cells against tumor cells [209, 226]. Results in (**Figures 4.9** and **4.10**) demonstrated that the overexpression of IFN-β using hydrodynamic gene delivery

suppressed tumor growth in the liver only. Therefore, it was likely that IFN-β activated NK cells present in the liver, which in return suppressed tumor growth. The absence of INF-β antitumor activity in the lung and kidney suggested it might be possible that various degrees of NK cell tumor infiltration might exist among the organs, and that the microenvironments in the lung and kidney were immunosuppressive. It has been previously shown that orthotopic tumors in the kidney were more immunosuppressive than subcutaneous tumors, which caused tumors in the kidney to be resistant [31]. Although IFN-β pharmacokinetics might contribute to the antitumor activity of IFN-β in the liver, the whole-body tumor suppression in the IL-12 treated group (**Figure 4.8**) suggested that the impact of the pharmacokinetics was minimum, and the differential accumulation of immune cells among tumor-hosting organs was the key mediator. Evaluation of types and amount of tumor-infiltrated immune cells in different anatomical sites is needed in the future.

In conclusion, we established multi-organ tumor models of breast cancer and renal cell carcinoma using hydrodynamic delivery. The multi-organ tumor model demonstrates differential tumor growth rates and distinctive interactions between tumor cells and the surrounding environment in different organs. This multi-organ tumor model offers an opportunity for precise preclinical evaluation of antitumor drugs against tumors simultaneously growing in multiple organs. Distinct differences in tumor growth and response to treatment in various organs stress the importance of future study to illustrate the underlying mechanisms and identify factors that play a critical role in supporting tumor progression. Our findings highlight the necessity of considering the anatomical site of metastasis as a critical factor when deciding the use of a particular therapeutic regime. Moreover, this work suggests the need for a combination therapy to eradicate tumors in various organs.

CHAPTER 6

FUTURE PERSPECTIVES

6.1. The Bottleneck of Cancer Metastasis Treatment

Although only around 0.01% of circulating tumor cells can form metastatic tumors in distant organs, metastatic tumors, once formed, become extremely difficult to eliminate for the majority of cancer patients [74]. Thus, most cancer deaths are due to cancer metastasis [12]. The tumor cell-stroma interaction is a key factor contributing to the insufficient efficacy of antimetastatic therapies. Tumors rich with non-malignant stromal cells demonstrated lower sensitivity to therapies and a higher risk of cancer recurrence [227].

The overall goal of this dissertation research was to determine the role of the stroma of different organs as a barrier for effective cancer metastasis treatment. The central hypothesis is that anatomical structure determines tumor growth and its response to therapy. The results obtained from a hydrodynamic-based tumor model confirms that tumor growing in the lung, liver and kidneys have different growth rates and responses to therapies even though the tumors originated from cells with similar genetic background. For example, renal cell carcinoma tumors in the lung and liver respond to 5-FU treatment, while those in the kidneys of the same mouse continued to progress.

Differential tumor response represents an obstacle to successful antimetastatic treatment and may explain why patients with multiple-organ metastasis have the poorest overall survival [190]. The capability to eliminate tumors in particular organs could be influenced by organ-specific tumor cell-stroma interactions. Understanding the organ-specific tumor cell-stroma

interaction is a critical step toward achieving an effective treatment of metastasis. Future research should consider metastatic tumors in different organs as different entities. Identifying the stromal mediators at the cellular and molecular levels that contribute to tumor growth and resistance to therapy in different organs will allow a better design of organ-specific therapies targeting these stromal mediators. Disruption of the organ-specific tumor cell-stroma communication could be more effective in suppressing tumor growth and progression, especially for tumors that have already metastasized into different organs.

6.2. Animal Model: a Critical Component in Anticancer Research

Establishing the right tumor model to simulate the complexity of cancer metastasis with clinically relevant anatomical, physiological, and biochemical conditions remains an important research area. Animal models have helped in studying cancer biology, developing chemical and biological entities that target cancer, and predicting the therapeutic efficacies, pharmacokinetics and toxicities of the anticancer drugs. Choosing the appropriate animal model to answer a specific question is critical for obtaining information that is closely relevant to clinical application. Four advanced animal models have been established in recent years and introduced for preclinical drug evaluation: multi-organ, GEMM, experimental and spontaneous metastasis models. These advanced tumor models help with the study of the influence of tumor cell implantation site on metastatic tumors biology and response to treatment. Preclinical research using advanced animal models may speed up the discovery of improved treatment plans for effective antimetastatic therapies. Future research to continuously re-evaluate and find new strategies to overcome the weaknesses of the current preclinical research is necessary. Until then, demand for the usage of

more than one tumor model in cancer research is promising progress to make animal data more clinically useful.

6.3. Advantages and Limitations of the Multi-organ Tumor Model

The advantages of the multi-organ tumor model are easily recognizable. The multi-organ tumor model allows for the study of tumor cell-stroma interactions that take place in the lung, liver and kidneys and how these interactions contribute to the outcome of anticancer treatments. Studies of molecular mechanisms underlying tumor growth and controlling the tumor sensitivity to a therapy may lead to new treatment strategies to eliminate organ-specific metastasis. The hydrodynamic cell delivery procedure developed to establish the multi-organ tumor model is much simpler to perform than the surgery-based procedures required for tumor cell implantation in the sites of interest. The multi-organ tumor model has a fully functional immune system, so the model can be used to assess the role of the immune system in influencing therapeutic outcomes.

Although the multi-organ tumor model possesses remarkable advantages over the other advanced animal models, the model in its current status needs further improvements to overcome its limitations. First, hydrodynamic cell delivery does not simulate the natural process of tumor cell dissemination, in which tumor cells continuously separate from the primary tumor over time. Also, the contribution of the primary tumor in the establishment of a pre-metastatic niche and the early steps of the metastasis process do not exist in the multi-organ tumor model. Therefore, the multi-organ tumor model is not suitable for preclinical evaluation of drugs that target the pre-metastatic niche formation or early steps of metastasis. In addition, the multi-organ tumor model in its current form does not imitate the intrinsic heterogeneity of the tumor of cancer patients [228]. Although we do not see any challenge to developing multi-organ tumor models in mice growing

human tumors, it is necessary to examine the feasibility of using hydrodynamic cell delivery in a mouse with an immune-compromised system. Future research should employ patient-derived cell lines that can be injected into mice and then evaluate drug response. A combination of xenograft and allograft multi-organ tumor models will allow researchers to make a better prediction of clinical outcomes of a therapeutic agent.

6.4. New Strategies for Treatment of Metastatic Tumor

The poor survival of patients with multi-organ metastasis [190] necessitates new strategies to eliminate metastatic tumors effectively. Current evidence, including the results presented in this dissertation, has demonstrated that different anatomical sites impact the tumor biology and response to therapy. These findings cast strong doubt on the current practice of using animal model with one tumor site for assessment of drug efficacy or drug discovery. To develop an effective therapeutic strategy, researchers need to select a drug or procedure based on its activity against tumors in different organs, not solely on the site of the tumor origin. For example, treatment of renal cell carcinoma with hepatic metastasis needs to consider the effectiveness of the strategy not only on the tumor growing in the kidneys but also its effectiveness in suppressing tumor growth in the liver. In addition, assessment of drug metabolism and toxicity is equally important and should be done in animal models that involve tumor growth in multiple organs. As the growth rate of tumor cells in different organs is organ-dependent, multiple therapeutic windows might exist if the treatment is sensitive to the stage of tumor progression. Efforts in searching for such therapeutic windows for various antimetastatic drugs may lead to improvements in treating tumor metastasis.

Furthermore, non-malignant stromal cells, including organ-specific resident cells and tumor infiltrating cells, are appealing drug targets. Since stromal cells support tumor cells by

improving cancer cell proliferation, rendering tumor cells resistant to therapy and suppressing antitumor immunity, targeting the stromal cells may disrupt the supportive environment on which tumors rely. Lack of a supportive environment can make tumors susceptible to cytotoxic drugs and antitumor immunity. A successful example of targeting organ-specific stromal cells is the utilization of bisphosphonates to treat bone metastatic tumors. Bisphosphonates have shown beneficial outcomes when incorporated into the treatment regimen against bone metastasis of different types of cancer [229, 230]. The bone, through its activated osteoclast, releases growth factors that promote the proliferation of metastatic tumor cells. Bisphosphonates inhibit osteoclast activity and block the release of growth factors. As a result, the bone becomes a hostile environment for the growth of metastatic tumor cells [229]. Future investigations should be directed to find the equivalents of bisphosphonates that have the same effect in other organs' metastases. Therefore, combining drugs with direct tumor-killing activity with one or more drugs targeting stromal cells may lead to a better therapeutic outcome. Future research should focus on the identification of stromal molecules in each organ essential for tumor growth.

In addition to developing new antimetastatic treatment strategies, more research is needed to develop prognostic biomarkers based on the type of cancer and the site of metastasis. Organ-specific prognostic biomarkers allow assessing the efficacy of the treatment plan and identifying tumor resistance at early stages in an organ-specific fashion. Although clinical trials depend heavily on prognostic biomarkers to design and assess antimetastatic regimens, identification and application of organ-specific biomarkers are still in an early stage of development [231, 232]. Multiple prognostic biomarkers are desirables and the multi-organ tumor model described in this dissertation offers a great opportunity to facilitate the identification of organ-specific prognostic biomarkers.

REFERENCES

1. Siegel, R.L., K.D. Miller, and A. Jemal, *Cancer Statistics, 2017.* CA Cancer J Clin, 2017. **67**(1): p. 7-30.

2. Palumbo, M.O., P. Kavan, W.H. Miller, Jr., *et al.*, *Systemic cancer therapy: achievements and challenges that lie ahead.* Front Pharmacol, 2013. **4**: p. 57.

3. American Cancer Society. *Treating bone metastasis*. 2016; cited March 27, 2017; From: https://www.cancer.org/treatment/understanding-your-diagnosis/advanced-cancer/treating-bone-metastases.html.

4. Kris, M.G., R.B. Natale, R.S. Herbst, *et al.*, *Efficacy of gefitinib, an inhibitor of the epidermal growth factor receptor tyrosine kinase, in symptomatic patients with non-small cell lung cancer: a randomized trial.* JAMA, 2003. **290**(16): p. 2149-58.

5. Fehrenbacher, L., A. Spira, M. Ballinger, *et al.*, *Atezolizumab versus docetaxel for patients with previously treated non-small-cell lung cancer (POPLAR): a multicentre, open-label, phase 2 randomised controlled trial.* Lancet, 2016. **387**(10030): p. 1837-46.

6. Brahmer, J., K.L. Reckamp, P. Baas, *et al.*, *Nivolumab versus Docetaxel in Advanced Squamous-Cell Non-Small-Cell Lung Cancer.* N Engl J Med, 2015. **373**(2): p. 123-35.

7. Charlton, P. and J. Spicer, *Targeted therapy in cancer.* Medicine, 2016. **44**(1): p. 34-38.

8. Cameron, D., J. Brown, R. Dent, *et al.*, *Adjuvant bevacizumab-containing therapy in triple-negative breast cancer (BEATRICE): primary results of a randomised, phase 3 trial.* Lancet Oncol, 2013. **14**(10): p. 933-42.

9. Aghajanian, C., B. Goff, L.R. Nycum, *et al.*, *Final overall survival and safety analysis of OCEANS, a phase 3 trial of chemotherapy with or without bevacizumab in patients with platinum-sensitive recurrent ovarian cancer.* Gynecol Oncol, 2015. **139**(1): p. 10-6.

10. Herbst, R.S., R. Ansari, F. Bustin, *et al.*, *Efficacy of bevacizumab plus erlotinib versus erlotinib alone in advanced non-small-cell lung cancer after failure of standard first-line chemotherapy (BeTa): a double-blind, placebo-controlled, phase 3 trial.* Lancet, 2011. **377**(9780): p. 1846-54.

11. Steeg, P.S., *Targeting metastasis.* Nature Reviews Cancer, 2016. **16**(4): p. 201-218.

12. Seyfried, T.N. and L.C. Huysentruyt, *On the origin of cancer metastasis.* Crit Rev Oncog, 2013. **18**(1-2): p. 43-73.

13. Yori, J.L., K.L. Lozada, D.D. Seachrist, *et al.*, *Combined SFK/mTOR inhibition prevents rapamycin-induced feedback activation of AKT and elicits efficient tumor regression.* Cancer Res, 2014. **74**(17): p. 4762-71.

14. Campbell, V.T., P. Nadesan, S.A. Ali, *et al.*, *Hedgehog pathway inhibition in chondrosarcoma using the smoothened inhibitor IPI-926 directly inhibits sarcoma cell growth.* Mol Cancer Ther, 2014. **13**(5): p. 1259-69.

15. Polychronidou, G., V. Karavasilis, S.M. Pollack, *et al.*, *Novel therapeutic approaches in chondrosarcoma.* Future Oncol, 2017. **13**(7): p. 637-648.

16. Gucalp, A., J.A. Sparano, J. Caravelli, *et al.*, *Phase II trial of saracatinib (AZD0530), an oral SRC-inhibitor for the treatment of patients with hormone receptor-negative metastatic breast cancer.* Clin Breast Cancer, 2011. **11**(5): p. 306-11.

17. Pusztai, L., S. Moulder, M. Altan, *et al.*, *Gene signature-guided dasatinib therapy in metastatic breast cancer.* Clin Cancer Res, 2014. **20**(20): p. 5265-71.

18. Hay, M., D.W. Thomas, J.L. Craighead, *et al.*, *Clinical development success rates for investigational drugs.* Nat Biotechnol, 2014. **32**(1): p. 40-51.

19. Suntharalingam, G., M.R. Perry, S. Ward, *et al.*, *Cytokine storm in a phase 1 trial of the anti-CD28 monoclonal antibody TGN1412.* N Engl J Med, 2006. **355**(10): p. 1018-28.

20. Amiri-Kordestani, L. and T. Fojo, *Why Do Phase III Clinical Trials in Oncology Fail so Often?* JNCI Journal of the National Cancer Institute, 2012. **104**(8): p. 568-569.

21. Musther, H., A. Olivares-Morales, O.J. Hatley, *et al.*, *Animal versus human oral drug bioavailability: do they correlate?* Eur J Pharm Sci, 2014. **57**: p. 280-91.

22. Adams, D.J., *The Valley of Death in anticancer drug development: a reassessment.* Trends Pharmacol Sci, 2012. **33**(4): p. 173-80.

23. Lee, E.W., Y. Lai, H. Zhang, *et al.*, *Identification of the mitochondrial targeting signal of the human equilibrative nucleoside transporter 1 (hENT1): implications for interspecies*

differences in mitochondrial toxicity of fialuridine. J Biol Chem, 2006. **281**(24): p. 16700-6.

24. Nair, A.B. and S. Jacob, *A simple practice guide for dose conversion between animals and human.* J Basic Clin Pharm, 2016. **7**(2): p. 27-31.

25. Lindhagen, E., P.-J. Vig Hjarnaa, L.E. Friberg, *et al.*, *Pharmacodynamic differences between species exemplified by the novel anticancer agent CHS 828.* Drug Development Research, 2004. **61**(4): p. 218-226.

26. Price, J.E., *Xenograft models in immunodeficient animals : I. Nude mice: spontaneous and experimental metastasis models.* Methods Mol Med, 2001. **58**: p. 205-13.

27. Ostrand-Rosenberg, S., *Immune surveillance: a balance between protumor and antitumor immunity.* Curr Opin Genet Dev, 2008. **18**(1): p. 11-8.

28. Nakasone, E.S., H.A. Askautrud, T. Kees, *et al.*, *Imaging tumor-stroma interactions during chemotherapy reveals contributions of the microenvironment to resistance.* Cancer Cell, 2012. **21**(4): p. 488-503.

29. Langley, R.R. and I.J. Fidler, *The seed and soil hypothesis revisited--the role of tumor-stroma interactions in metastasis to different organs.* Int J Cancer, 2011. **128**(11): p. 2527-35.

30. Kroesen, M., I.C. Brok, D. Reijnen, *et al.*, *Intra-adrenal murine TH-MYCN neuroblastoma tumors grow more aggressive and exhibit a distinct tumor microenvironment relative to their subcutaneous equivalents.* Cancer Immunol Immunother, 2015. **64**(5): p. 563-72.

31. Devaud, C., J.A. Westwood, L.B. John, *et al., Tissues in different anatomical sites can sculpt and vary the tumor microenvironment to affect responses to therapy.* Mol Ther, 2014. **22**(1): p. 18-27.

32. Euhus, D.M., C. Hudd, M.C. LaRegina, *et al., Tumor measurement in the nude mouse.* J Surg Oncol, 1986. **31**(4): p. 229-34.

33. Tomayko, M.M. and C.P. Reynolds, *Determination of subcutaneous tumor size in athymic (nude) mice.* Cancer Chemother Pharmacol, 1989. **24**(3): p. 148-54.

34. Patel, J.K., M.S. Didolkar, J.W. Pickren, *et al., Metastatic pattern of malignant melanoma. A study of 216 autopsy cases.* Am J Surg, 1978. **135**(6): p. 807-10.

35. Li, J., Q. Yao, and D. Liu, *Hydrodynamic cell delivery for simultaneous establishment of tumor growth in mouse lung, liver and kidney.* Cancer Biol Ther, 2011. **12**(8): p. 737-41.

36. Luo, J., N.L. Solimini, and S.J. Elledge, *Principles of cancer therapy: oncogene and non-oncogene addiction.* Cell, 2009. **136**(5): p. 823-37.

37. Loeb, L.A., *Endogenous carcinogenesis: molecular oncology into the twenty-first century--presidential address.* Cancer Res, 1989. **49**(20): p. 5489-96.

38. Doll, R. and R. Peto, *The causes of cancer: quantitative estimates of avoidable risks of cancer in the United States today.* J Natl Cancer Inst, 1981. **66**(6): p. 1191-308.

39. Marur, S., G. D'Souza, W.H. Westra, *et al., HPV-associated head and neck cancer: a virus-related cancer epidemic.* Lancet Oncol, 2010. **11**(8): p. 781-9.

40. Hanahan, D. and R.A. Weinberg, *Hallmarks of cancer: the next generation.* Cell, 2011. **144**(5): p. 646-74.

41. Hui, L. and Y. Chen, *Tumor microenvironment: Sanctuary of the devil.* Cancer Lett, 2015. **368**(1): p. 7-13.

42. SEER Training Modules. *Cancer classification*. cited May 4, 2017; From: https://training.seer.cancer.gov/disease/categories/classification.html.

43. in *Surgical Treatment: Evidence-Based and Problem-Oriented*, R.G. Holzheimer and J.A. Mannick, Editors. 2001: Munich.

44. Fidler, I.J., *Metastasis: quantitative analysis of distribution and fate of tumor emboli labeled with 125 I-5-iodo-2'-deoxyuridine.* J Natl Cancer Inst, 1970. **45**(4): p. 773-82.

45. Butler, T.P. and P.M. Gullino, *Quantitation of cell shedding into efferent blood of mammary adenocarcinoma.* Cancer Res, 1975. **35**(3): p. 512-6.

46. Husemann, Y., J.B. Geigl, F. Schubert, *et al.*, *Systemic spread is an early step in breast cancer.* Cancer Cell, 2008. **13**(1): p. 58-68.

47. Nagy, J.A. and H.F. Dvorak, *Heterogeneity of the tumor vasculature: the need for new tumor blood vessel type-specific targets.* Clin Exp Metastasis, 2012. **29**(7): p. 657-62.

48. Sitohy, B., J.A. Nagy, and H.F. Dvorak, *Anti-VEGF/VEGFR therapy for cancer: reassessing the target.* Cancer Res, 2012. **72**(8): p. 1909-14.

49. Kessenbrock, K., V. Plaks, and Z. Werb, *Matrix metalloproteinases: regulators of the tumor microenvironment.* Cell, 2010. **141**(1): p. 52-67.

50. Steeg, P.S., *Tumor metastasis: mechanistic insights and clinical challenges.* Nat Med, 2006. **12**(8): p. 895-904.

51. Amo, L., E. Tamayo-Orbegozo, N. Maruri, *et al.*, *Involvement of platelet-tumor cell interaction in immune evasion. Potential role of podocalyxin-like protein 1.* Front Oncol, 2014. **4**: p. 245.

52. Rejniak, K.A., *Circulating Tumor Cells: When a Solid Tumor Meets a Fluid Microenvironment.* Adv Exp Med Biol, 2016. **936**: p. 93-106.

53. Paget, S., *The distribution of secondary growths in cancer of the breast. 1889.* Cancer Metastasis Rev, 1989. **8**(2): p. 98-101.

54. Hart, I.R. and I.J. Fidler, *Role of organ selectivity in the determination of metastatic patterns of B16 melanoma.* Cancer Res, 1980. **40**(7): p. 2281-7.

55. Weiss, L., E. Grundmann, J. Torhorst, *et al.*, *Haematogenous metastatic patterns in colonic carcinoma: an analysis of 1541 necropsies.* J Pathol, 1986. **150**(3): p. 195-203.

56. Hess, K.R., G.R. Varadhachary, S.H. Taylor, *et al.*, *Metastatic patterns in adenocarcinoma.* Cancer, 2006. **106**(7): p. 1624-33.

57. DuBois, S.G., Y. Kalika, J.N. Lukens, *et al.*, *Metastatic sites in stage IV and IVS neuroblastoma correlate with age, tumor biology, and survival.* J Pediatr Hematol Oncol, 1999. **21**(3): p. 181-9.

58. Minn, A.J., G.P. Gupta, P.M. Siegel, *et al.*, *Genes that mediate breast cancer metastasis to lung.* Nature, 2005. **436**(7050): p. 518-24.

59. Bos, P.D., X.H. Zhang, C. Nadal, *et al.*, *Genes that mediate breast cancer metastasis to the brain.* Nature, 2009. **459**(7249): p. 1005-9.

60. Kang, Y., P.M. Siegel, W. Shu, *et al.*, *A multigenic program mediating breast cancer metastasis to bone.* Cancer Cell, 2003. **3**(6): p. 537-49.

61. Smith, H.A. and Y. Kang, *Determinants of Organotropic Metastasis.* Annual Review of Cancer Biology, 2017. **1**(1): p. 403-423.

62. Jandial, R., *Metastatic cancer : clinical and biological perspectives*. Molecular biology intelligence unit. 2013, Austin, Texas, USA: Landes Bioscience. 290 pages.

63. Aird, W.C., *Phenotypic heterogeneity of the endothelium: I. Structure, function, and mechanisms.* Circ Res, 2007. **100**(2): p. 158-73.

64. Okajima, T., S. Fukumoto, H. Ito, *et al.*, *Molecular cloning of brain-specific GD1alpha synthase (ST6GalNAc V) containing CAG/Glutamine repeats.* J Biol Chem, 1999. **274**(43): p. 30557-62.

65. Muller, A., B. Homey, H. Soto, *et al.*, *Involvement of chemokine receptors in breast cancer metastasis.* Nature, 2001. **410**(6824): p. 50-6.

66. Brown, D.M. and E. Ruoslahti, *Metadherin, a cell surface protein in breast tumors that mediates lung metastasis.* Cancer Cell, 2004. **5**(4): p. 365-74.

67. Santini, D., G. Perrone, I. Roato, *et al.*, *Expression pattern of receptor activator of NFkappaB (RANK) in a series of primary solid tumors and related bone metastases.* J Cell Physiol, 2011. **226**(3): p. 780-4.

68. Padua, D., X.H. Zhang, Q. Wang, *et al.*, *TGFbeta primes breast tumors for lung metastasis seeding through angiopoietin-like 4.* Cell, 2008. **133**(1): p. 66-77.

69. Costa-Silva, B., N.M. Aiello, A.J. Ocean, *et al.*, *Pancreatic cancer exosomes initiate pre-metastatic niche formation in the liver.* Nat Cell Biol, 2015. **17**(6): p. 816-26.

70. Valiente, M., A.C. Obenauf, X. Jin, *et al.*, *Serpins promote cancer cell survival and vascular co-option in brain metastasis.* Cell, 2014. **156**(5): p. 1002-16.

71. Sierra, A., J.E. Price, M. Garcia-Ramirez, *et al.*, *Astrocyte-derived cytokines contribute to the metastatic brain specificity of breast cancer cells.* Lab Invest, 1997. **77**(4): p. 357-68.

72. Sevenich, L., R.L. Bowman, S.D. Mason, *et al.*, *Analysis of tumour- and stroma-supplied proteolytic networks reveals a brain-metastasis-promoting role for cathepsin S.* Nat Cell Biol, 2014. **16**(9): p. 876-88.

73. Braun, S., F.D. Vogl, B. Naume, *et al.*, *A pooled analysis of bone marrow micrometastasis in breast cancer.* N Engl J Med, 2005. **353**(8): p. 793-802.

74. Luzzi, K.J., I.C. MacDonald, E.E. Schmidt, *et al.*, *Multistep nature of metastatic inefficiency: dormancy of solitary cells after successful extravasation and limited survival of early micrometastases.* Am J Pathol, 1998. **153**(3): p. 865-73.

75. Massagué, J. and A.C. Obenauf, *Metastatic colonization by circulating tumour cells.* Nature, 2016. **529**(7586): p. 298-306.

76. Oskarsson, T., S. Acharyya, X.H. Zhang, *et al.*, *Breast cancer cells produce tenascin C as a metastatic niche component to colonize the lungs.* Nat Med, 2011. **17**(7): p. 867-74.

77. Lu, X., Q. Wang, G. Hu, *et al.*, *ADAMTS1 and MMP1 proteolytically engage EGF-like ligands in an osteolytic signaling cascade for bone metastasis.* Genes Dev, 2009. **23**(16): p. 1882-94.

78. Shevde, L.A., S. Das, D.W. Clark, *et al.*, *Osteopontin: an effector and an effect of tumor metastasis.* Curr Mol Med, 2010. **10**(1): p. 71-81.

79. Contie, S., N. Voorzanger-Rousselot, J. Litvin, *et al.*, *Increased expression and serum levels of the stromal cell-secreted protein periostin in breast cancer bone metastases.* Int J Cancer, 2011. **128**(2): p. 352-60.

80. LeBleu, V.S., J.T. O'Connell, K.N. Gonzalez Herrera, *et al.*, *PGC-1alpha mediates mitochondrial biogenesis and oxidative phosphorylation in cancer cells to promote metastasis.* Nat Cell Biol, 2014. **16**(10): p. 992-1003, 1-15.

81. Nieman, K.M., H.A. Kenny, C.V. Penicka, *et al.*, *Adipocytes promote ovarian cancer metastasis and provide energy for rapid tumor growth.* Nat Med, 2011. **17**(11): p. 1498-503.

82. Arteel, G.E., R.G. Thurman, J.M. Yates, *et al.*, *Evidence that hypoxia markers detect oxygen gradients in liver: pimonidazole and retrograde perfusion of rat liver.* Br J Cancer, 1995. **72**(4): p. 889-95.

83. Jungermann, K. and T. Kietzmann, *Oxygen: modulator of metabolic zonation and disease of the liver.* Hepatology, 2000. **31**(2): p. 255-60.

84. Jungermann, K. and T. Kietzmann, *Zonation of parenchymal and nonparenchymal metabolism in liver.* Annu Rev Nutr, 1996. **16**: p. 179-203.

85. Loo, J.M., A. Scherl, A. Nguyen, *et al.*, *Extracellular metabolic energetics can promote cancer progression.* Cell, 2015. **160**(3): p. 393-406.

86. Dupuy, F., S. Tabaries, S. Andrzejewski, *et al.*, *PDK1-Dependent Metabolic Reprogramming Dictates Metastatic Potential in Breast Cancer.* Cell Metab, 2015. **22**(4): p. 577-89.

87. Chen, J., H.J. Lee, X. Wu, *et al.*, *Gain of glucose-independent growth upon metastasis of breast cancer cells to the brain.* Cancer Res, 2015. **75**(3): p. 554-65.

88. Teicher, B.A., T.S. Herman, S.A. Holden, *et al.*, *Tumor resistance to alkylating agents conferred by mechanisms operative only in vivo.* Science, 1990. **247**(4949 Pt 1): p. 1457-61.

89. McMillin, D.W., J. Delmore, E. Weisberg, *et al.*, *Tumor cell-specific bioluminescence platform to identify stroma-induced changes to anticancer drug activity.* Nat Med, 2010. **16**(4): p. 483-9.

90. Manshouri, T., Z. Estrov, A. Quintas-Cardama, *et al.*, *Bone marrow stroma-secreted cytokines protect JAK2(V617F)-mutated cells from the effects of a JAK2 inhibitor.* Cancer Res, 2011. **71**(11): p. 3831-40.

91. Flach, E.H., V.W. Rebecca, M. Herlyn, *et al.*, *Fibroblasts contribute to melanoma tumor growth and drug resistance.* Mol Pharm, 2011. **8**(6): p. 2039-49.

92. Schmidt, T., B. Kharabi Masouleh, S. Loges, *et al.*, *Loss or inhibition of stromal-derived PlGF prolongs survival of mice with imatinib-resistant Bcr-Abl1(+) leukemia.* Cancer Cell, 2011. **19**(6): p. 740-53.

93. Kim, S.W., H.J. Choi, H.J. Lee, *et al.*, *Role of the endothelin axis in astrocyte- and endothelial cell-mediated chemoprotection of cancer cells.* Neuro Oncol, 2014. **16**(12): p. 1585-98.

94. Wojtkowiak, J.W., D. Verduzco, K.J. Schramm, *et al.*, *Drug resistance and cellular adaptation to tumor acidic pH microenvironment.* Mol Pharm, 2011. **8**(6): p. 2032-8.

95. Minchinton, A.I. and I.F. Tannock, *Drug penetration in solid tumours.* Nat Rev Cancer, 2006. **6**(8): p. 583-92.

96. Muranen, T., L.M. Selfors, D.T. Worster, *et al.*, *Inhibition of PI3K/mTOR leads to adaptive resistance in matrix-attached cancer cells.* Cancer Cell, 2012. **21**(2): p. 227-39.

97. DeNardo, D.G., D.J. Brennan, E. Rexhepaj, *et al.*, *Leukocyte complexity predicts breast cancer survival and functionally regulates response to chemotherapy.* Cancer Discov, 2011. **1**(1): p. 54-67.

98. Provenzano, P.P., C. Cuevas, A.E. Chang, *et al.*, *Enzymatic targeting of the stroma ablates physical barriers to treatment of pancreatic ductal adenocarcinoma.* Cancer Cell, 2012. **21**(3): p. 418-29.

99. Upadhyay, R.K., *Drug delivery systems, CNS protection, and the blood brain barrier.* Biomed Res Int, 2014. **2014**: p. 869269.

100. Ruffell, B. and L.M. Coussens, *Macrophages and therapeutic resistance in cancer*. Cancer Cell, 2015. **27**(4): p. 462-72.

101. Huang, M., A. Shen, J. Ding, *et al.*, *Molecularly targeted cancer therapy: some lessons from the past decade.* Trends Pharmacol Sci, 2014. **35**(1): p. 41-50.

102. Wang, Y., K.J. Szretter, W. Vermi, *et al.*, *IL-34 is a tissue-restricted ligand of CSF1R required for the development of Langerhans cells and microglia.* Nat Immunol, 2012. **13**(8): p. 753-60.

103. Liu, Y. and X. Cao, *Immunosuppressive cells in tumor immune escape and metastasis.* J Mol Med (Berl), 2016. **94**(5): p. 509-22.

104. Fidler, I.J., C. Wilmanns, A. Staroselsky, *et al.*, *Modulation of tumor cell response to chemotherapy by the organ environment.* Cancer Metastasis Rev, 1994. **13**(2): p. 209-22.

105. Takebayashi, K., E. Mekata, H. Sonoda, *et al.*, *Differences in chemosensitivity between primary and metastatic tumors in colorectal cancer.* PLoS One, 2013. **8**(8): p. e73215.

106. Wu, J.M., M.J. Fackler, M.K. Halushka, *et al.*, *Heterogeneity of breast cancer metastases: comparison of therapeutic target expression and promoter methylation between primary tumors and their multifocal metastases.* Clin Cancer Res, 2008. **14**(7): p. 1938-46.

107. Molinari, F., V. Martin, P. Saletti, *et al.*, *Differing deregulation of EGFR and downstream proteins in primary colorectal cancer and related metastatic sites may be clinically relevant.* Br J Cancer, 2009. **100**(7): p. 1087-94.

108. Talmadge, J.E. and I.J. Fidler, *AACR centennial series: the biology of cancer metastasis: historical perspective.* Cancer Res, 2010. **70**(14): p. 5649-69.

109. Redig, A.J. and S.S. McAllister, *Breast cancer as a systemic disease: a view of metastasis.* J Intern Med, 2013. **274**(2): p. 113-26.

110. Guillem-Llobat, P., M. Dovizio, A. Bruno, *et al.*, *Aspirin prevents colorectal cancer metastasis in mice by splitting the crosstalk between platelets and tumor cells.* Oncotarget, 2016. **7**(22): p. 32462-77.

111. Gomis, R.R. and S. Gawrzak, *Tumor cell dormancy.* Molecular Oncology, 2017. **11**(1): p. 62-78.

112. Murray, L.J. and M.H. Robinson, *Radiotherapy: technical aspects.* Medicine, 2016. **44**(1): p. 10-14.

113. Skliarenko, J. and P. Warde, *Practical and clinical applications of radiation therapy.* Medicine, 2016. **44**(1): p. 15-19.

114. Gates, V.L., B. Atassi, R.J. Lewandowski, *et al.*, *Radioembolization with Yttrium-90 microspheres: review of an emerging treatment for liver tumors.* Future Oncol, 2007. **3**(1): p. 73-81.

115. Milenic, D.E., E.D. Brady, and M.W. Brechbiel, *Antibody-targeted radiation cancer therapy.* Nat Rev Drug Discov, 2004. **3**(6): p. 488-99.

116. Maverakis, E., L.A. Cornelius, G.M. Bowen, *et al.*, *Metastatic melanoma - a review of current and future treatment options.* Acta Derm Venereol, 2015. **95**(5): p. 516-24.

117. Jones, R., *Cytotoxic chemotherapy: clinical aspects.* Medicine, 2016. **44**(1): p. 25-29.

118. Corrie, P.G., *Cytotoxic chemotherapy: clinical aspects.* Medicine, 2008. **36**(1): p. 24-28.

119. Abraham, J. and J. Staffurth, *Hormonal therapy for cancer.* Medicine, 2016. **44**(1): p. 30-33.

120. DeVita, V.T., S. Hellman, and S.A. Rosenberg, *Cancer, principles & practice of oncology*. 7th ed. 2005, Philadelphia, PA: Lippincott Williams & Wilkins. lxxv, 2898 p.

121. Rau, K.M., H.Y. Kang, T.L. Cha, *et al.*, *The mechanisms and managements of hormone-therapy resistance in breast and prostate cancers.* Endocr Relat Cancer, 2005. **12**(3): p. 511-32.

122. Dixon, J.M., *Endocrine Resistance in Breast Cancer.* New Journal of Science, 2014. **2014**: p. 27.

123. Zhou, G. and H. Levitsky, *Towards curative cancer immunotherapy: overcoming posttherapy tumor escape.* Clin Dev Immunol, 2012. **2012**: p. 124187.

124. Mellman, I., G. Coukos, and G. Dranoff, *Cancer immunotherapy comes of age.* Nature, 2011. **480**(7378): p. 480-9.

125. Larkin, J., V. Chiarion-Sileni, R. Gonzalez, *et al.*, *Combined Nivolumab and Ipilimumab or Monotherapy in Untreated Melanoma.* N Engl J Med, 2015. **373**(1): p. 23-34.

126. Scott, S.D., *Rituximab: a new therapeutic monoclonal antibody for non-Hodgkin's lymphoma.* Cancer Pract, 1998. **6**(3): p. 195-7.

127. Tsimberidou, A.M., *Targeted therapy in cancer.* Cancer Chemother Pharmacol, 2015. **76**(6): p. 1113-32.

128. Zhang, Q., Z. Wang, J. Guo, *et al.*, *Comparison of single-agent chemotherapy and targeted therapy to first-line treatment in patients aged 80 years and older with advanced non-small-cell lung cancer.* Onco Targets Ther, 2015. **8**: p. 893-8.

129. Fisher, R.I., S.A. Rosenberg, and G. Fyfe, *Long-term survival update for high-dose recombinant interleukin-2 in patients with renal cell carcinoma.* Cancer J Sci Am, 2000. **6 Suppl 1**: p. S55-7.

130. Engelman, J.A. and J. Settleman, *Acquired resistance to tyrosine kinase inhibitors during cancer therapy.* Curr Opin Genet Dev, 2008. **18**(1): p. 73-9.

131. Bernards, N., G.J. Creemers, G.A. Nieuwenhuijzen, *et al.*, *No improvement in median survival for patients with metastatic gastric cancer despite increased use of chemotherapy.* Ann Oncol, 2013. **24**(12): p. 3056-60.

132. Tevaarwerk, A.J., R.J. Gray, B.P. Schneider, *et al.*, *Survival in patients with metastatic recurrent breast cancer after adjuvant chemotherapy: little evidence of improvement over the past 30 years.* Cancer, 2013. **119**(6): p. 1140-8.

133. Worni, M., U. Guller, R.R. White, *et al.*, *Modest improvement in overall survival for patients with metastatic pancreatic cancer: a trend analysis using the surveillance, epidemiology, and end results registry from 1988 to 2008.* Pancreas, 2013. **42**(7): p. 1157-63.

134. in *Conflict of Interest in Medical Research, Education, and Practice*, B. Lo and M.J. Field, Editors. 2009: Washington (DC).

135. Dehm, S.M. and K. Bonham, *SRC gene expression in human cancer: the role of transcriptional activation.* Biochem Cell Biol, 2004. **82**(2): p. 263-74.

136. Dunn, E.F., M. Iida, R.A. Myers, *et al.*, *Dasatinib sensitizes KRAS mutant colorectal tumors to cetuximab.* Oncogene, 2011. **30**(5): p. 561-74.

137. Trevino, J.G., J.M. Summy, D.P. Lesslie, *et al.*, *Inhibition of SRC expression and activity inhibits tumor progression and metastasis of human pancreatic adenocarcinoma cells in an orthotopic nude mouse model.* Am J Pathol, 2006. **168**(3): p. 962-72.

138. Chan, C.M., X. Jing, L.A. Pike, *et al.*, *Targeted inhibition of Src kinase with dasatinib blocks thyroid cancer growth and metastasis.* Clin Cancer Res, 2012. **18**(13): p. 3580-91.

139. Mayer, E.L., J.F. Baurain, J. Sparano, *et al.*, *A phase 2 trial of dasatinib in patients with advanced HER2-positive and/or hormone receptor-positive breast cancer.* Clin Cancer Res, 2011. **17**(21): p. 6897-904.

140. Sharma, M.R., K. Wroblewski, B.N. Polite, *et al.*, *Dasatinib in previously treated metastatic colorectal cancer: a phase II trial of the University of Chicago Phase II Consortium.* Invest New Drugs, 2012. **30**(3): p. 1211-5.

141. Miller, A.A., H. Pang, L. Hodgson, *et al.*, *A phase II study of dasatinib in patients with chemosensitive relapsed small cell lung cancer (Cancer and Leukemia Group B 30602).* J Thorac Oncol, 2010. **5**(3): p. 380-4.

142. Karhadkar, S.S., G.S. Bova, N. Abdallah, *et al.*, *Hedgehog signalling in prostate regeneration, neoplasia and metastasis.* Nature, 2004. **431**(7009): p. 707-12.

143. Varnat, F., A. Duquet, M. Malerba, *et al.*, *Human colon cancer epithelial cells harbour active HEDGEHOG-GLI signalling that is essential for tumour growth, recurrence, metastasis and stem cell survival and expansion.* EMBO Mol Med, 2009. **1**(6-7): p. 338-51.

144. Velcheti, V., *Hedgehog signaling is a potent regulator of angiogenesis in small cell lung cancer*. Med Hypotheses, 2007. **69**(4): p. 948-9.

145. Ng, J.M. and T. Curran, *The Hedgehog's tale: developing strategies for targeting cancer.* Nat Rev Cancer, 2011. **11**(7): p. 493-501.

146. Akhtar, A., *The flaws and human harms of animal experimentation.* Camb Q Healthc Ethics, 2015. **24**(4): p. 407-19.

147. Martignoni, M., G.M. Groothuis, and R. de Kanter, *Species differences between mouse, rat, dog, monkey and human CYP-mediated drug metabolism, inhibition and induction.* Expert Opin Drug Metab Toxicol, 2006. **2**(6): p. 875-94.

148. Mestas, J. and C.C. Hughes, *Of mice and not men: differences between mouse and human immunology*. J Immunol, 2004. **172**(5): p. 2731-8.

149. Xu, X., M.C. Farach-Carson, and X. Jia, *Three-dimensional in vitro tumor models for cancer research and drug evaluation.* Biotechnol Adv, 2014. **32**(7): p. 1256-68.

150. Bissell, M.J., D.C. Radisky, A. Rizki, *et al.*, *The organizing principle: microenvironmental influences in the normal and malignant breast.* Differentiation, 2002. **70**(9-10): p. 537-46.

151. Bissell, M.J., P.A. Kenny, and D.C. Radisky, *Microenvironmental regulators of tissue structure and function also regulate tumor induction and progression: the role of extracellular matrix and its degrading enzymes.* Cold Spring Harb Symp Quant Biol, 2005. **70**: p. 343-56.

152. Infanger, D.W., M.E. Lynch, and C. Fischbach, *Engineered culture models for studies of tumor-microenvironment interactions.* Annu Rev Biomed Eng, 2013. **15**: p. 29-53.

153. Lindner, D., *Animal models and the tumor microenvironment: studies of tumor-host symbiosis.* Semin Oncol, 2014. **41**(2): p. 146-55.

154. Dong, X., J. Guan, J.C. English, *et al.*, *Patient-derived first generation xenografts of non-small cell lung cancers: promising tools for predicting drug responses for personalized chemotherapy.* Clin Cancer Res, 2010. **16**(5): p. 1442-51.

155. Ocana, A., A. Pandiella, L.L. Siu, *et al.*, *Preclinical development of molecular-targeted agents for cancer.* Nat Rev Clin Oncol, 2010. **8**(4): p. 200-9.

156. Becher, O.J. and E.C. Holland, *Genetically engineered models have advantages over xenografts for preclinical studies.* Cancer Res, 2006. **66**(7): p. 3355-8, discussion 3358-9.

157. Frese, K.K. and D.A. Tuveson, *Maximizing mouse cancer models.* Nat Rev Cancer, 2007. **7**(9): p. 645-58.

158. Sikder, H., D.L. Huso, H. Zhang, *et al.*, *Disruption of Id1 reveals major differences in angiogenesis between transplanted and autochthonous tumors.* Cancer Cell, 2003. **4**(4): p. 291-9.

159. Contag, C.H., D. Jenkins, P.R. Contag, *et al.*, *Use of reporter genes for optical measurements of neoplastic disease in vivo.* Neoplasia, 2000. **2**(1-2): p. 41-52.

160. Ottewell, P.D., R.E. Coleman, and I. Holen, *From genetic abnormality to metastases: murine models of breast cancer and their use in the development of anticancer therapies.* Breast Cancer Res Treat, 2006. **96**(2): p. 101-13.

161. Francia, G., W. Cruz-Munoz, S. Man, *et al.*, *Mouse models of advanced spontaneous metastasis for experimental therapeutics.* Nat Rev Cancer, 2011. **11**(2): p. 135-41.

162. Hingorani, S.R., E.F. Petricoin, A. Maitra, *et al.*, *Preinvasive and invasive ductal pancreatic cancer and its early detection in the mouse.* Cancer Cell, 2003. **4**(6): p. 437-50.

163. Dankort, D., D.P. Curley, R.A. Cartlidge, *et al.*, *Braf(V600E) cooperates with Pten loss to induce metastatic melanoma.* Nat Genet, 2009. **41**(5): p. 544-52.

164. Talmadge, J.E., R.K. Singh, I.J. Fidler, *et al.*, *Murine models to evaluate novel and conventional therapeutic strategies for cancer.* Am J Pathol, 2007. **170**(3): p. 793-804.

165. Politi, K., M.F. Zakowski, P.D. Fan, *et al.*, *Lung adenocarcinomas induced in mice by mutant EGF receptors found in human lung cancers respond to a tyrosine kinase inhibitor or to down-regulation of the receptors.* Genes Dev, 2006. **20**(11): p. 1496-510.

166. De Raedt, T., Z. Walton, J.L. Yecies, *et al.*, *Exploiting cancer cell vulnerabilities to develop a combination therapy for ras-driven tumors.* Cancer Cell, 2011. **20**(3): p. 400-13.

167. Olive, K.P., M.A. Jacobetz, C.J. Davidson, *et al.*, *Inhibition of Hedgehog signaling enhances delivery of chemotherapy in a mouse model of pancreatic cancer.* Science, 2009. **324**(5933): p. 1457-61.

168. Hu, Y., S. Swerdlow, T.M. Duffy, *et al.*, *Targeting multiple kinase pathways in leukemic progenitors and stem cells is essential for improved treatment of Ph+ leukemia in mice.* Proc Natl Acad Sci U S A, 2006. **103**(45): p. 16870-5.

169. Rottenberg, S., J.E. Jaspers, A. Kersbergen, *et al.*, *High sensitivity of BRCA1-deficient mammary tumors to the PARP inhibitor AZD2281 alone and in combination with platinum drugs.* Proc Natl Acad Sci U S A, 2008. **105**(44): p. 17079-84.

170. Hay, T., J.R. Matthews, L. Pietzka, *et al.*, *Poly(ADP-ribose) polymerase-1 inhibitor treatment regresses autochthonous Brca2/p53-mutant mammary tumors in vivo and delays tumor relapse in combination with carboplatin.* Cancer Res, 2009. **69**(9): p. 3850-5.

171. Bearss, D.J., M.A. Subler, J.E. Hundley, *et al.*, *Genetic determinants of response to chemotherapy in transgenic mouse mammary and salivary tumors.* Oncogene, 2000. **19**(8): p. 1114-22.

172. Singh, M., S.S. Couto, W.F. Forrest, *et al.*, *Anti-VEGF antibody therapy does not promote metastasis in genetically engineered mouse tumour models.* J Pathol, 2012. **227**(4): p. 417-30.

173. Singh, M., A. Lima, R. Molina, *et al.*, *Assessing therapeutic responses in Kras mutant cancers using genetically engineered mouse models.* Nat Biotechnol, 2010. **28**(6): p. 585-93.

174. Combest, A.J., P.J. Roberts, P.M. Dillon, *et al.*, *Genetically engineered cancer models, but not xenografts, faithfully predict anticancer drug exposure in melanoma tumors.* Oncologist, 2012. **17**(10): p. 1303-16.

175. Khanna, C. and K. Hunter, *Modeling metastasis in vivo.* Carcinogenesis, 2005. **26**(3): p. 513-23.

176. Munoz, R., S. Man, Y. Shaked, *et al.*, *Highly efficacious nontoxic preclinical treatment for advanced metastatic breast cancer using combination oral UFT-cyclophosphamide metronomic chemotherapy.* Cancer Res, 2006. **66**(7): p. 3386-91.

177. Cruz-Munoz, W., S. Man, P. Xu, *et al.*, *Development of a preclinical model of spontaneous human melanoma central nervous system metastasis.* Cancer Res, 2008. **68**(12): p. 4500-5.

178. Furukawa, T., T. Kubota, M. Watanabe, *et al.*, *A novel "patient-like" treatment model of human pancreatic cancer constructed using orthotopic transplantation of histologically intact human tumor tissue in nude mice.* Cancer Res, 1993. **53**(13): p. 3070-2.

179. Kiguchi, K., T. Kubota, D. Aoki, *et al.*, *A patient-like orthotopic implantation nude mouse model of highly metastatic human ovarian cancer.* Clin Exp Metastasis, 1998. **16**(8): p. 751-6.

180. Kubota, T., *Metastatic models of human cancer xenografted in the nude mouse: the importance of orthotopic transplantation.* J Cell Biochem, 1994. **56**(1): p. 4-8.

181. Morikawa, K., S.M. Walker, J.M. Jessup, *et al.*, *In vivo selection of highly metastatic cells from surgical specimens of different primary human colon carcinomas implanted into nude mice.* Cancer Res, 1988. **48**(7): p. 1943-8.

182. Man, S., G. Bocci, G. Francia, *et al.*, *Antitumor effects in mice of low-dose (metronomic) cyclophosphamide administered continuously through the drinking water.* Cancer Res, 2002. **62**(10): p. 2731-5.

183. Francia, G., S. Man, C.J. Lee, *et al.*, *Comparative impact of trastuzumab and cyclophosphamide on HER-2-positive human breast cancer xenografts.* Clin Cancer Res, 2009. **15**(20): p. 6358-66.

184. Brodie, S.G., X. Xu, W. Qiao, *et al.*, *Multiple genetic changes are associated with mammary tumorigenesis in Brca1 conditional knockout mice.* Oncogene, 2001. **20**(51): p. 7514-23.

185. Albiges, L., F. Andre, C. Balleyguier, *et al.*, *Spectrum of breast cancer metastasis in BRCA1 mutation carriers: highly increased incidence of brain metastases.* Ann Oncol, 2005. **16**(11): p. 1846-7.

186. Mook, O., *Visualization of early events in tumor formation of eGFP-transfected rat colon cancer cells in liver.* Hepatology, 2003. **38**(2): p. 295-304.

187. Arguello, F., R.B. Baggs, and C.N. Frantz, *A murine model of experimental metastasis to bone and bone marrow.* Cancer Res, 1988. **48**(23): p. 6876-81.

188. Otsuka, T., H. Takayama, R. Sharp, *et al.*, *c-Met autocrine activation induces development of malignant melanoma and acquisition of the metastatic phenotype.* Cancer Res, 1998. **58**(22): p. 5157-67.

189. McClatchey, A.I., I. Saotome, K. Mercer, *et al.*, *Mice heterozygous for a mutation at the Nf2 tumor suppressor locus develop a range of highly metastatic tumors.* Genes Dev, 1998. **12**(8): p. 1121-33.

190. Capitanio, U., F. Abdollah, R. Matloob, *et al.*, *Effect of number and location of distant metastases on renal cell carcinoma mortality in candidates for cytoreductive nephrectomy: implications for multimodal therapy.* Int J Urol, 2013. **20**(6): p. 572-9.

191. Devaud, C., L.B. John, J.A. Westwood, *et al.*, *Cross-talk between tumors can affect responses to therapy.* Oncoimmunology, 2015. **4**(7): p. e975572.

192. Liu, F., Y. Song, and D. Liu, *Hydrodynamics-based transfection in animals by systemic administration of plasmid DNA.* Gene Ther, 1999. **6**(7): p. 1258-66.

193. Zhang, G., V. Budker, and J.A. Wolff, *High levels of foreign gene expression in hepatocytes after tail vein injections of naked plasmid DNA.* Hum Gene Ther, 1999. **10**(10): p. 1735-7.

194. Bonamassa, B., L. Hai, and D. Liu, *Hydrodynamic gene delivery and its applications in pharmaceutical research.* Pharm Res, 2011. **28**(4): p. 694-701.

195. Kamimura, K., T. Suda, W. Xu, *et al.*, *Image-guided, lobe-specific hydrodynamic gene delivery to swine liver.* Mol Ther, 2009. **17**(3): p. 491-9.

196. Suda, T., K. Suda, and D. Liu, *Computer-assisted hydrodynamic gene delivery.* Mol Ther, 2008. **16**(6): p. 1098-104.

197. Zhang, G., C.I. Wooddell, J.O. Hegge, *et al.*, *Functional efficacy of dystrophin expression from plasmids delivered to mdx mice by hydrodynamic limb vein injection.* Hum Gene Ther, 2010. **21**(2): p. 221-37.

198. Ma, Y. and D. Liu, *Hydrodynamic delivery of adiponectin and adiponectin receptor 2 gene blocks high-fat diet-induced obesity and insulin resistance.* Gene Ther, 2013. **20**(8): p. 846-52.

199. Yang, P.L., A. Althage, J. Chung, *et al.*, *Hydrodynamic injection of viral DNA: a mouse model of acute hepatitis B virus infection.* Proc Natl Acad Sci U S A, 2002. **99**(21): p. 13825-30.

200. Kanefuji, T., T. Yokoo, T. Suda, *et al.*, *Hemodynamics of a hydrodynamic injection.* Mol Ther Methods Clin Dev, 2014. **1**: p. 14029.

201. Budczies, J., M. von Winterfeld, F. Klauschen, *et al.*, *The landscape of metastatic progression patterns across major human cancers.* Oncotarget, 2015. **6**(1): p. 570-83.

202. Wisse, E., F. Braet, H. Duimel, *et al.*, *Fixation methods for electron microscopy of human and other liver.* World J Gastroenterol, 2010. **16**(23): p. 2851-66.

203. Cao, Z., Z. Zhang, Z. Huang, *et al.*, *Antitumor and immunomodulatory effects of low-dose 5-FU on hepatoma 22 tumor-bearing mice.* Oncol Lett, 2014. **7**(4): p. 1260-1264.

204. Fischer, A.H., K.A. Jacobson, J. Rose, *et al.*, *Hematoxylin and eosin staining of tissue and cell sections.* CSH Protoc, 2008. **2008**: p. pdb prot4986.

205. Chawla-Sarkar, M., D.W. Leaman, and E.C. Borden, *Preferential induction of apoptosis by interferon (IFN)-beta compared with IFN-alpha2: correlation with TRAIL/Apo2L induction in melanoma cell lines.* Clin Cancer Res, 2001. **7**(6): p. 1821-31.

206. Park, M.A., T. Walker, A.P. Martin, *et al.*, *MDA-7/IL-24-induced cell killing in malignant renal carcinoma cells occurs by a ceramide/CD95/PERK-dependent mechanism.* Mol Cancer Ther, 2009. **8**(5): p. 1280-91.

207. Kuchen, S., R. Robbins, G.P. Sims, *et al.*, *Essential role of IL-21 in B cell activation, expansion, and plasma cell generation during CD4+ T cell-B cell collaboration.* J Immunol, 2007. **179**(9): p. 5886-96.

208. Liao, W., J.X. Lin, and W.J. Leonard, *IL-2 family cytokines: new insights into the complex roles of IL-2 as a broad regulator of T helper cell differentiation.* Curr Opin Immunol, 2011. **23**(5): p. 598-604.

209. Swann, J.B., Y. Hayakawa, N. Zerafa, *et al.*, *Type I IFN contributes to NK cell homeostasis, activation, and antitumor function.* J Immunol, 2007. **178**(12): p. 7540-9.

210. Hsieh, C.S., S.E. Macatonia, C.S. Tripp, *et al.*, *Development of TH1 CD4+ T cells through IL-12 produced by Listeria-induced macrophages.* Science, 1993. **260**(5107): p. 547-9.

211. Pflanz, S., J.C. Timans, J. Cheung, *et al.*, *IL-27, a heterodimeric cytokine composed of EBI3 and p28 protein, induces proliferation of naive CD4+ T cells.* Immunity, 2002. **16**(6): p. 779-90.

212. Gould, S.E., M.R. Junttila, and F.J. de Sauvage, *Translational value of mouse models in oncology drug development.* Nat Med, 2015. **21**(5): p. 431-9.

213. Gerlinger, M., A.J. Rowan, S. Horswell, *et al.*, *Intratumor heterogeneity and branched evolution revealed by multiregion sequencing.* N Engl J Med, 2012. **366**(10): p. 883-92.

214. Zhang, Q., M. Yang, J. Shen, *et al.*, *The role of the intravascular microenvironment in spontaneous metastasis development.* Int J Cancer, 2010. **126**(11): p. 2534-41.

215. Kruskal, J.B., P. Thomas, R.A. Kane, *et al.*, *Hepatic perfusion changes in mice livers with developing colorectal cancer metastases.* Radiology, 2004. **231**(2): p. 482-90.

216. Badr, C.E., *Bioluminescence imaging: basics and practical limitations.* Methods Mol Biol, 2014. **1098**: p. 1-18.

217. Brooks, D.E., *The biorheology of tumor cells.* Biorheology, 1984. **21**(1-2): p. 85-91.

218. Egan, K., N. Cooke, and D. Kenny, *Living in shear: platelets protect cancer cells from shear induced damage.* Clin Exp Metastasis, 2014. **31**(6): p. 697-704.

219. Fidler, I.J., *The pathogenesis of cancer metastasis: the 'seed and soil' hypothesis revisited.* Nat Rev Cancer, 2003. **3**(6): p. 453-8.

220. Axelson, H., E. Fredlund, M. Ovenberger, *et al.*, *Hypoxia-induced dedifferentiation of tumor cells--a mechanism behind heterogeneity and aggressiveness of solid tumors.* Semin Cell Dev Biol, 2005. **16**(4-5): p. 554-63.

221. Yamamoto, Y., M. Ibusuki, Y. Okumura, *et al.*, *Hypoxia-inducible factor 1alpha is closely linked to an aggressive phenotype in breast cancer.* Breast Cancer Res Treat, 2008. **110**(3): p. 465-75.

222. Kang, N., G.J. Gores, and V.H. Shah, *Hepatic stellate cells: partners in crime for liver metastases?* Hepatology, 2011. **54**(2): p. 707-13.

223. Nicolson, G.L., *Tumor cell instability, diversification, and progression to the metastatic phenotype: from oncogene to oncofetal expression.* Cancer Res, 1987. **47**(6): p. 1473-87.

224. Li, S., A. Wang, W. Jiang, *et al.*, *Pharmacokinetic characteristics and anticancer effects of 5-fluorouracil loaded nanoparticles.* BMC Cancer, 2008. **8**: p. 103.

225. Zhang, N., Y. Yin, S.J. Xu, *et al.*, *5-Fluorouracil: mechanisms of resistance and reversal strategies.* Molecules, 2008. **13**(8): p. 1551-69.

226. Takeda, K., Y. Hayakawa, M.J. Smyth, *et al.*, *Involvement of tumor necrosis factor-related apoptosis-inducing ligand in surveillance of tumor metastasis by liver natural killer cells.* Nat Med, 2001. **7**(1): p. 94-100.

227. de Kruijf, E.M., J.G. van Nes, C.J. van de Velde, *et al.*, *Tumor-stroma ratio in the primary tumor is a prognostic factor in early breast cancer patients, especially in triple-negative carcinoma patients.* Breast Cancer Res Treat, 2011. **125**(3): p. 687-96.

228. Hidalgo, M., F. Amant, A.V. Biankin, *et al.*, *Patient-Derived Xenograft Models: An Emerging Platform for Translational Cancer Research.* Cancer Discovery, 2014. **4**(9): p. 998-1013.

229. Santini, D., L. Stumbo, C. Spoto, *et al.*, *Bisphosphonates as anticancer agents in early breast cancer: preclinical and clinical evidence.* Breast Cancer Res, 2015. **17**: p. 121.

230. Tolia, M., A. Zygogianni, J.R. Kouvaris, *et al.*, *The key role of bisphosphonates in the supportive care of cancer patients.* Anticancer Res, 2014. **34**(1): p. 23-37.

231. Schubert, M., K. Junker, and J. Heinzelmann, *Prognostic and predictive miRNA biomarkers in bladder, kidney and prostate cancer: Where do we stand in biomarker development?* J Cancer Res Clin Oncol, 2016. **142**(8): p. 1673-95.

232. Patel, V., Z. Wang, Q. Chen, *et al.*, *Emerging Cancer Biomarkers for HNSCC Detection and Therapeutic Intervention*, in *Contemporary Oral Oncology: Biology, Epidemiology, Etiology, and Prevention*, M.A. Kuriakose, Editor. 2017, Springer International Publishing: Cham. p. 281-308.

APPENDIX A

OVEREXPRESSION OF sPLA2G5 SUPPRESSES HFD-INDUCED BODY WEIGHT GAIN AND LEADS TO OCD-LIKE BEHAVIOR AND VISCERAL MASSES

A.1. Introduction

Obesity prevalence worldwide has substantially increased during the last three decades. [1]. In 2015, 36.5% of adults and approximately 17% of children in the United States were obese (adults: BMI≥30 ; children: BMI≥ age-specific 95th percentile) [2]. Obesity is associated with a high risk of several diseases, including cardiovascular diseases, type II diabetes, fatty liver disease, atherosclerosis, neuropsychological diseases and cancer [3-9]. Obesity-associated diseases used to be observed exclusively in adults, but they have now been reported in overweight and obese children as well [10]. Unfortunately, there is no cure for obesity, but the most effective treatment currently available is bariatric surgery that focuses on decreasing the food absorption capacity of gastrointestinal system [11, 12]. Although more desirable, safe and effective anti-obesity drugs are not available [11], which provide an incentive for research to find new approaches and strategies for a cure. In the past few years, our laboratory has used gene transfer approach to block or cure obesity by overexpressing genes that are responsible for regulation of lipid and sugar metabolism. Using a high-fat diet-induced mouse model, the lab has demonstrated effective inhibition of high-fat diet-induced obesity and insulin resistance by hydrodynamic transfer of genes such as adiponectin, IL-10, FGF-21, IL-6, IL-13, SOD3, IL-15 and NRG4 [13-20]. The objective of this project is to assess and characterize the effects of sPLA2G5 gene transfer on metabolic and physiological homeostasis in mice fed a high-fat diet.

The sPLA2G5 is a member of the secretory phospholipase a2 family (sPLA2), consisting of 11 Ca^{+2} –dependent, low molecular weight enzymes that catalyze the hydrolysis of the *sn*-2 acyl ester bond of phospholipids in the cellular and lipoproteins membranes [21]. This hydrolysis process generates free fatty acids and lysophospholipids, which are involved in numerous biological processes, such as inflammation, reproduction, metabolism, atherosclerosis, brain functions and tumorigenesis [21-24]. The diversities of physiological and pathological functions of sPLA2 enzymes is due to the different substrate specificity of each isomer and the different forms of lipid mediators generated [21]. During the last few years, research has demonstrated the involvement of IB, IIE and V isomers in obesity. In contrast to IB and IIE isomers, V isoenzyme has been indicated by recent research for its anti-obesity function [21, 25].

The Group V sPLA2 (sPLA2G5) gene is expressed in diverse cells and involved in various physiological functions [21, 26]. Alteration of sPLA2G5 expression has been linked to multiple chronic diseases, such as atherosclerosis, asthma, rheumatoid arthritis and obesity [21]. In the context of obesity, a clinical study reported an upregulation of sPLA2G5 gene expression in the placenta of obese neonates as a result of the increased levels of TNF-α and leptin [27]. A similar increase of sPLA2G5 expression has been observed in the adipose tissue of HFD-induced obese mice. sPLA2G5 knockout mice, when fed high-fat diet, exhibited an accelerated body weight gain, hepatic lipid accumulation and worsening of adipose tissue inflammation compared to HFD-induced obese wild-type mice [25]. The evidence presented by these earlier studies suggests potential involvement of sPLA2G5 in regulating metabolic homeostasis. The goal of the current study is to explore and characterize the beneficial effects of sPLA2G5 overexpression against HFD-induced obesity.

A.2. Materials and Methods

A.2.1. *Materials and Animals*

The pLIVE plasmid vector was purchased from Mirus Bio (Madison, WI). High-fat diet (60% kJ/fat, 20% kJ/carbohydrate, 20% kJ/protein) was purchased from Bio-Serv (Frenchtown, NJ, catalog number S3282). The SuperScrip III® First-Strand Synthesis System was purchased from Invitrogen (Carlsbad, CA). TRIzol reagent was obtained from Invitrogen (Carlsbad, CA). QIAquick Gel Extraction Kit was from Qiagen (Germantown, MD). Male C57BL/6 mice (6 weeks, 19-22 g) and female NCI Cr:SW and female CD-1 mice (5 weeks, 22-24 g) were purchased from Charles River Laboratories (Wilmington, MA). Animals were housed under a standard condition with a 12-hour light-dark cycle.

A.2.2. *DNA Plasmid Construction and Preparation*

Total mRNA was extracted from murine heart homogenate of C57BL/6 mice and used for reverse transcription by PCR to synthesize the first strand cDNA using oligo$(dT)_{20}$ primers to initiate reverse transcription. The PCR product was amplified with sPLA2G5 primers (synthesized by Thermo Scientific) based on the NCBI reference sequence (NM_001122954.1) as follows: a forward primer with SalI restriction site, 5'-ACAGCTGTCGACATGAAGGGTCTCCTCA-CACTG-3' and a reverse primer with XhoI restriction site, 5'-ACAGCGCTCGAGTTAG-CAGAGGAAGTTGGGGTAATA-3'. The desired PCR product was purified from a 1% agarose gel. The cDNA of the mouse sPLA2G5 gene (414 bp) was subcloned into the multiple cloning sites of the pLIVE vector using restriction enzyme digestion to yield pLIVE-sPLA2G5 plasmid. The sPLA2G5 gene sequence cloned in pLIVE-sPLA2G5 plasmid vector was verified by DNA sequencing. The plasmid was prepared by the method of cesium chloride-ethidium bromide

gradient centrifugation and kept in saline at -80°C until use. The purity and concentration of the plasmid DNA were determined by 1% agarose gel electrophoresis and $OD_{260/280}$ ratio, and OD_{260}, respectively.

A.2.3. *Animal Treatment and Body Weight Measurements*

All procedures performed on mice were approved by the Institutional Animal Care and Use Committee at the University of Georgia, Athens, Georgia (protocol number, A2011 07-Y2-A3). pLIVE-sPLA2G5 plasmid DNA was hydrodynamically injected into the mice as previously described [28, 29]. Briefly, saline solution with plasmid DNA in a volume equivalent to 9% of the mouse body weight was injected into a mouse tail vein within 5–8 seconds (20 μg plasmid DNA/mouse). Plasmid carrying secreted alkaline phosphatase reporter gene (pLIVE-SEAP) was used as a negative control (20 μg/mouse). Mice were kept on a high-fat diet during the experiment. Repeated injections with the same amount of plasmid DNA per animal were performed on weeks 3 and 6. Body weight and food intake were measured every 5 days. Body composition was determined using EchoMRI-100TM (Echo Medical Systems, Houston, TX). Mice were sacrificed at the end of 25 weeks.

Similar assessment was also performed on Cr:SW and CD-1 outbred mice. The frequency of plasmid injection was once every two weeks for a period of 5.5 months.

A.2.4. *Statistical Analysis*

GraphPad Prism software from GraphPad Software, Inc. (La Jolla, CA) was used for statistical analysis. Statistical significance was determined using an unpaired Student *t*-test. A $P<0.05$ was considered significantly different. Results are expressed as the mean ± SEM.

A.3. Results

Mice receiving a hydrodynamic injection of pLIVE-sPLA2G5 at a dose of 20 ug/mouse demonstrated significant suppression of HFD-induced body weight gain compared to the control group injected with pLIVE-SEAP in the first 5 weeks, mainly due to a lower level of fat mass, not lean mass (**Figures A.1A-A.1C**). Five-day average food intake was the same between sPLA2G5 treated and control animals (**Figure A.1D**).

Mice receiving injection of pLIVE-sPLA2G5 displayed a trend of weight loss starting from month 5. The body-weight reduction was directly proportional to decrease of the fat mass (**Figures A.1A** and **A.1B**). The sPLA2G5 treated mice, in this period, showed behavior change, grooming their nose and face continuously and picking their facial fur and whiskers (**Figures A.2A-A.2C**). The severity of the symptoms and body-weight loss were positively correlated and continued (**Figure A.1A** and **Figure A.2B**). Continuous and repetitive grooming behavior of these animal fits the definition of obsessive-compulsive disorder (OCD), a disorder manifested by obsessive thoughts and repetitive actions [30-32].

Efforts are made to explore the connection between sPLA2G5 plasmid gene transfer and OCD using outbred mice. Female NCI Cr:SW mice (n = 4) were injected with pLIVE-sPLA2G5 at weeks 0, 11, 14, and 17, while control mice (n = 4) were injected with the same doses of pLIVE-SEAP plasmid DNA. Both groups were fed a HFD. The mice injected with pLIVE-sPLA2G5 developed facial fur and whisker loss after 5 months, while the control group showed no symptoms (**Figure A.2D**). However, the self-overgrooming behavior and symptoms were less severe in these mice compared to male C57Bl/6 mice used in the previous experiment. Additionally, the NCI Cr:SW mice with the OCD symptoms demonstrated no alleviation in the symptoms after keeping the mice for 8 extra months (13 months after starting the experiment) without any additional

injection (**Figure A.2E**). Irreversible symptoms may suggest that the sPLA2G5 overexpression might have led to a permanent loss of facial fur. In addition, during the period of this 15-month experiment, all sPLA2G5 treated mice developed visceral masses seen in the lung and liver. Moreover, the fat pads of sPLA2G5 treated mice had distinctive spots (**Figure A.3**).

An additional experiment was performed to establish the link between sPLA2G5 overexpression and OCD. Both high-fat diet and regular chow were included in the experimental design with plasmid injection of pLIVE-sPLA2G5 or control plasmid (pLIVE-SEAP). Four groups of female CD-1 mice were used, including: pLIVE-SEAP/chow, pLIVE-sPLA2G5/chow, pLIVE-SEAP/HFD and pLIVE-sPLA2G5/HFD. Mice were injected once every two weeks for the entire period of 5.5 months. Unfortunately, none of the animals, regardless of diet used or the type of plasmids injected, showed OCD symptoms as seen in the previous experiments. No further experiments were performed from this point on.

A.4. Discussion

While the research demonstrated that obesity is associated with an alteration of sPLA2G5 expression [25, 27], the function of sPLA2G5 in the development of obesity was not clear. In the current study, we examined the impact of sPLA2G5 overexpression on animals fed a HFD or regular chow. **Figure A.1** demonstrated that overexpression of sPLA2G5 in mice on HFD suppressed HFD-induced body weight gain. While this observation may suggest that sPLA2G5 gene transfer can slow down body-weight gain, we have no way to correlate the effect to protein level because the only anti-sPLA2G5 antibodies commercially available were not able to show a difference between normal serum and serum from sPLA2G5-treated animals due to the high background signal of ELISA.

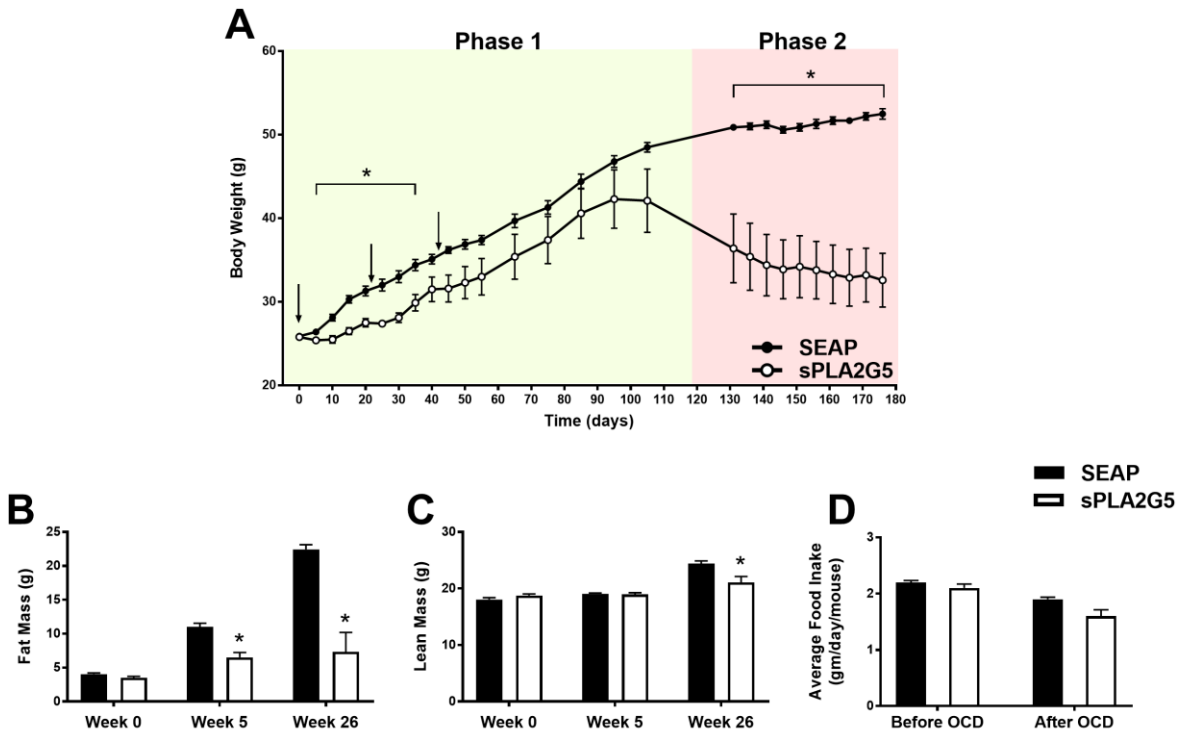

Figure A.1. sPLA2G5 overexpression suppressed body-weight gain in mice fed a HFD. **A)** Body-weight curve showing two phases: phases 1 and 2 before and after the development of OCD-like behavior, respectively; **B)** Fat mass and **C)** Lean mass at different time points; **D)** Average food intake before and after development of OCD-like behavior. Values represent mean ± SEM, ***** $p < 0.05$ (n = 5).

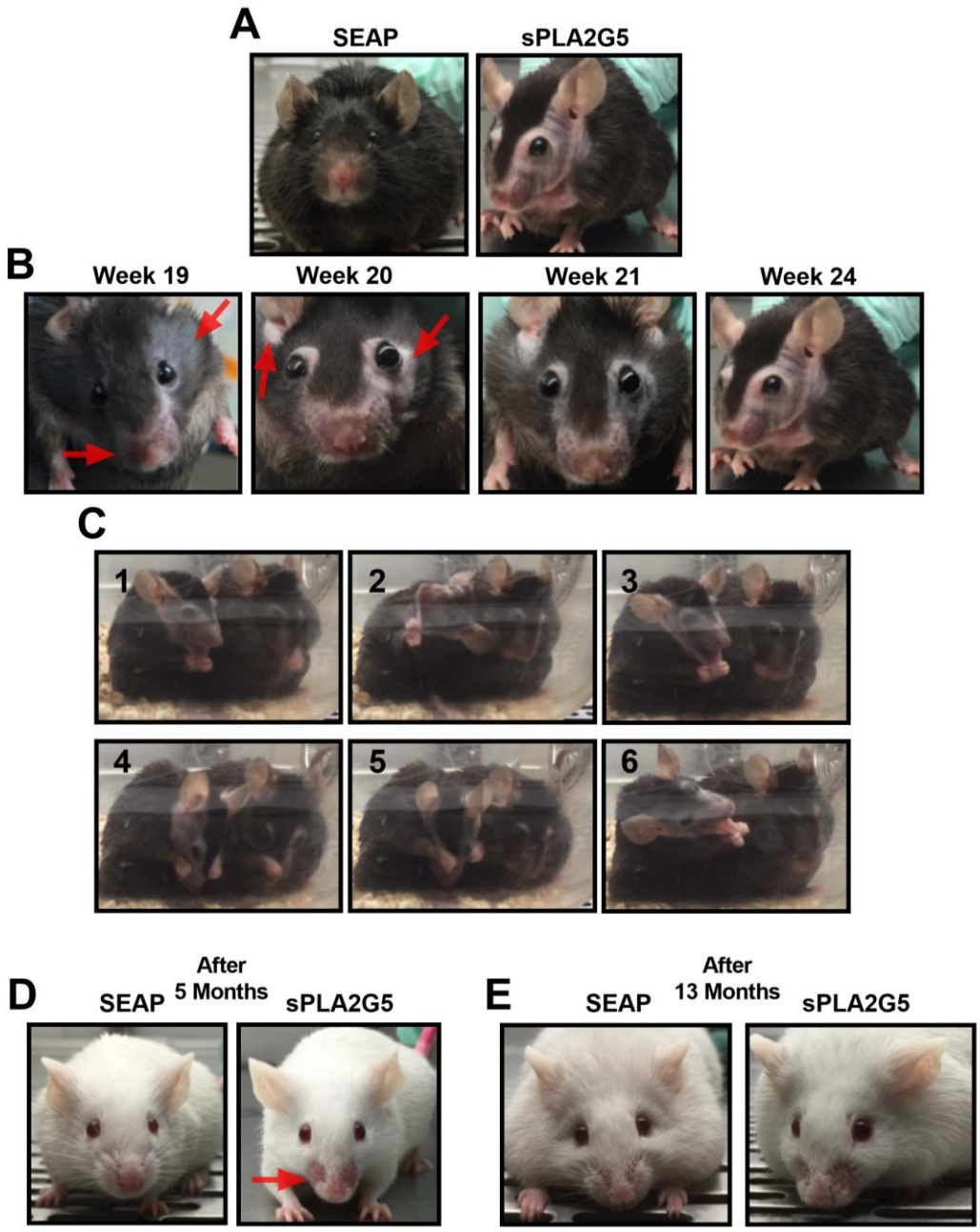

Figure A.2. sPLA2G5 overexpression led to the development of self-overgrooming in two different species of mice. A) Representative images for control and sPLA2G5-treated male C57Bl/6 mice showing loss of whiskers and facial fur as a result of excessive self-grooming; **B)** Images for the same sPLA2G5 treated mouse showing the gradual loss of facial fur and whiskers (*red arrows*) at different times; **C)** Video images showing mice picked their facial fur by themselves, with incomplete syntactic chain of self-grooming; **D** and **E)** The existence of irreversible OCD-like symptoms (*red arrow*) in the female Cr:SW mice at different times.

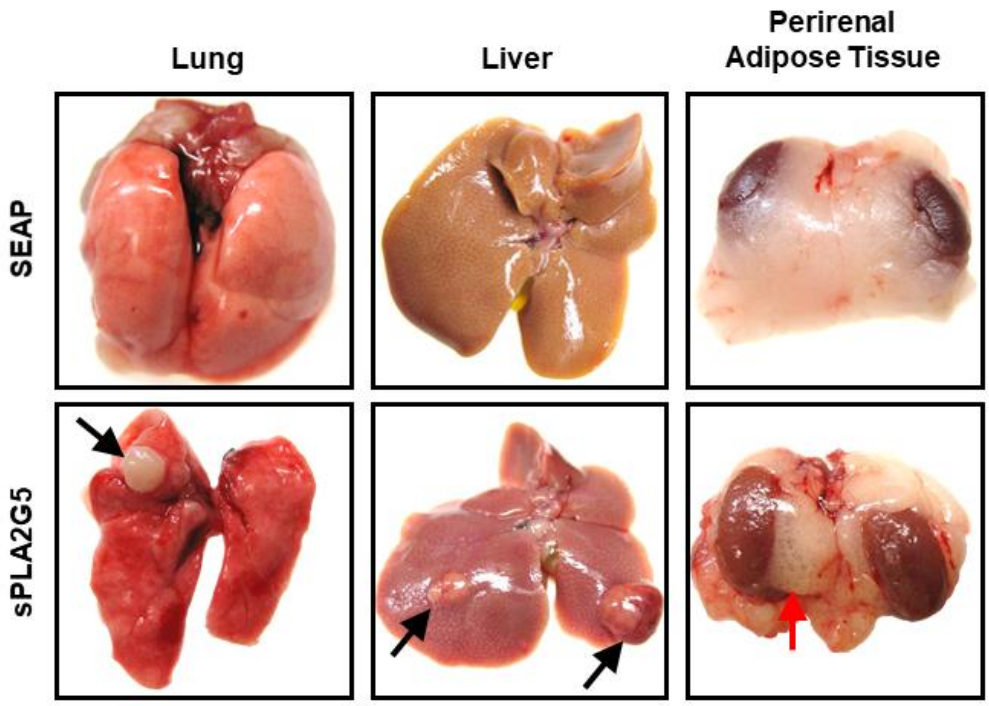

Figure A.3. sPLA2G5 overexpression led to the development of visceral masses and abnormal morphology of the fat pads. Representative images of the lung, liver, and adipose tissue collected from the control and sPLA2G5-treated female Cr:SW mice showing visceral masses (*black arrows*) in the lung and liver and the distinctive spots in the perirenal adipose tissue (*red arrow*).

sPLA2G5 gene transfer appears to have a detrimental impact on animals, showing obsessive-compulsive disorder (OCD)-like behavior and visceral masses. **Figure A.2** shows a long-term loss of facial fur and whiskers resulted from self-overgrooming. The behavior of self-overgrooming has been used to assess OCD in several mouse models [30-32]. Mice suffering from OCD display self-overgrooming with an incomplete sequential pattern and prolonged duration of grooming and imitate OCD patients with obsessive thoughts and repetitive actions. Similar to patients with OCD concerning cleaning, mice groom themselves frequently to maintain their hygiene [33]. In addition, the development of visceral masses is another observation obtained in sPLA2G5-treated mice. **Figure A.3** shows the development of visceral masses in the lung and liver of HFD-fed mice treated with sPLA2G5, but not in control mice. While it is not clear whether the visceral masses developed are tumors, the involvement of sPLA2 in cancer development has been previously reported with subtypes of IIA, III and X [24]. Future investigation to clarify the role of sPLA2G5 in tumor initiation and promotion is needed.

Hypothetically, the development of OCD-like behavior and visceral masses in sPLA2G5-treated mice might be the result of activation of a particular signal pathway triggered by lipid products of sPLA2G5-mediated reaction [21, 24, 34]. sPLA2G5 gene transfer might cause lipid homeostatic imbalance due to the extended influence of the sPLA2G5 on the lipid metabolism. The hydrolytic activity of sPLA2G5 could lead to excessive production of the active lipid mediators, such as prostaglandins, leukotrienes and lysophospholipids. Consequently, the active lipid mediators will induce chronic inflammation [22, 23, 34]. The inflammation drives the development of OCD-like behavior and initiation of the visceral tumor masses [31, 35]. Additionally, sPLA2G5 may also promotes tumor growth. An *ex vivo* study demonstrated that sPLA2G5 is capable of stimulating the secretion of proangiogenic factors, such as vascular

endothelial growth factor A (VEGF-A) and angiopoietin 1 (Ang 1), as well as antiangiogenic factor VEGF-A_{165b} [36]. Tumor growth seen in this study suggests that there might be higher levels of proangiogenic factors compared to VEGF-A_{165b}.

The observations made in this study may indicate a pathophysiological link between obesity and the development of OCD and cancer, in agreement with the results of previous studies [7-9, 21, 22, 24]. In the context of OCD, MC4R and SAPAP3 double knockout mice corrected the obesity and self-overgrooming seeing in animals with single gene knockout [37]. Future investigation will help better understand how sPLA2G5 contributes to the development of OCD-like behavior and cancer. However, it is important to point out that future work needs to keep in mind that the OCD-like behavior was only seen in some animals, not in all animals examined. In addition, while all sPLA2G5-treated female Cr:SW mice (4 out of 4) showed the development of visceral masses, this observation was not confirmed in the outbred female CD-1 mice treated with sPLA2G5.

A.5. References

1. Collaborators, G.B.D.O., *Health Effects of Overweight and Obesity in 195 Countries over 25 Years.* N Engl J Med, 2017.

2. Centers for Disease Control and Prevention CDC. *Overweight & obesity - data & statistics*. 2016; cited June 28, 2017; From: https://www.cdc.gov/obesity/data/index.html.

3. Poirier, P., T.D. Giles, G.A. Bray, *et al.*, *Obesity and cardiovascular disease: pathophysiology, evaluation, and effect of weight loss.* Arterioscler Thromb Vasc Biol, 2006. **26**(5): p. 968-76.

4. Lovren, F., H. Teoh, and S. Verma, *Obesity and atherosclerosis: mechanistic insights.* Can J Cardiol, 2015. **31**(2): p. 177-83.

5. Kahn, S.E., R.L. Hull, and K.M. Utzschneider, *Mechanisms linking obesity to insulin resistance and type 2 diabetes.* Nature, 2006. **444**(7121): p. 840-6.

6. Fabbrini, E., S. Sullivan, and S. Klein, *Obesity and nonalcoholic fatty liver disease: biochemical, metabolic, and clinical implications.* Hepatology, 2010. **51**(2): p. 679-89.

7. Lopresti, A.L. and P.D. Drummond, *Obesity and psychiatric disorders: commonalities in dysregulated biological pathways and their implications for treatment.* Prog Neuropsychopharmacol Biol Psychiatry, 2013. **45**: p. 92-9.

8. Opel, N., R. Redlich, D. Grotegerd, *et al.*, *Obesity and major depression: Body-mass index (BMI) is associated with a severe course of disease and specific neurostructural alterations.* Psychoneuroendocrinology, 2015. **51**: p. 219-26.

9. Vucenik, I. and J.P. Stains, *Obesity and cancer risk: evidence, mechanisms, and recommendations.* Ann N Y Acad Sci, 2012. **1271**: p. 37-43.

10. Gungor, N.K., *Overweight and obesity in children and adolescents.* J Clin Res Pediatr Endocrinol, 2014. **6**(3): p. 129-43.

11. Kakkar, A.K. and N. Dahiya, *Drug treatment of obesity: current status and future prospects.* Eur J Intern Med, 2015. **26**(2): p. 89-94.

12. Chang, S.H., C.R. Stoll, J. Song, *et al.*, *The effectiveness and risks of bariatric surgery: an updated systematic review and meta-analysis, 2003-2012.* JAMA Surg, 2014. **149**(3): p. 275-87.

13. Ma, Y. and D. Liu, *Hydrodynamic delivery of adiponectin and adiponectin receptor 2 gene blocks high-fat diet-induced obesity and insulin resistance.* Gene Ther, 2013. **20**(8): p. 846-52.

14. Gao, M., C. Zhang, Y. Ma, *et al.*, *Hydrodynamic delivery of mIL10 gene protects mice from high-fat diet-induced obesity and glucose intolerance.* Mol Ther, 2013. **21**(10): p. 1852-61.

15. Gao, M., Y. Ma, R. Cui, *et al.*, *Hydrodynamic delivery of FGF21 gene alleviates obesity and fatty liver in mice fed a high-fat diet.* J Control Release, 2014. **185**: p. 1-11.

16. Ma, Y., M. Gao, H. Sun, *et al.*, *Interleukin-6 gene transfer reverses body weight gain and fatty liver in obese mice.* Biochimica et Biophysica Acta (BBA) - Molecular Basis of Disease, 2015. **1852**(5): p. 1001-1011.

17. Darkhal, P., M. Gao, Y. Ma, *et al.*, *Blocking high-fat diet-induced obesity, insulin resistance and fatty liver by overexpression of Il-13 gene in mice.* Int J Obes (Lond), 2015. **39**(8): p. 1292-9.

18. Cui, R., M. Gao, S. Qu, *et al.*, *Overexpression of superoxide dismutase 3 gene blocks high-fat diet-induced obesity, fatty liver and insulin resistance.* Gene Ther, 2014. **21**(9): p. 840-8.

19. Sun, H., Y. Ma, M. Gao, *et al.*, *IL-15/sIL-15Ralpha gene transfer induces weight loss and improves glucose homeostasis in obese mice.* Gene Ther, 2016. **23**(4): p. 349-56.

20. Ma, Y., M. Gao, and D. Liu, *Preventing High Fat Diet-induced Obesity and Improving Insulin Sensitivity through Neuregulin 4 Gene Transfer.* Sci Rep, 2016. **6**: p. 26242.

21. Murakami, M., H. Sato, Y. Miki, *et al.*, *A new era of secreted phospholipase A(2).* J Lipid Res, 2015. **56**(7): p. 1248-61.

22. Farooqui, A.A. and L.A. Horrocks, *Phospholipase A2-generated lipid mediators in the brain: the good, the bad, and the ugly.* Neuroscientist, 2006. **12**(3): p. 245-60.

23. Sun, G.Y., P.B. Shelat, M.B. Jensen, *et al.*, *Phospholipases A2 and inflammatory responses in the central nervous system.* Neuromolecular Med, 2010. **12**(2): p. 133-48.

24. Brglez, V., G. Lambeau, and T. Petan, *Secreted phospholipases A2 in cancer: diverse mechanisms of action.* Biochimie, 2014. **107 Pt A**: p. 114-23.

25. Sato, H., Y. Taketomi, A. Ushida, *et al.*, *The adipocyte-inducible secreted phospholipases PLA2G5 and PLA2G2E play distinct roles in obesity.* Cell Metab, 2014. **20**(1): p. 119-32.

26. Silva-Filho, J.L., D.B. Peruchetti, F. Moraes-Santos, *et al.*, *Group V Secretory Phospholipase A2 Is Involved in Tubular Integrity and Sodium Handling in the Kidney.* PLoS One, 2016. **11**(1): p. e0147785.

27. Varastehpour, A., T. Radaelli, J. Minium, *et al.*, *Activation of phospholipase A2 is associated with generation of placental lipid signals and fetal obesity.* J Clin Endocrinol Metab, 2006. **91**(1): p. 248-55.

28. Liu, F., Y. Song, and D. Liu, *Hydrodynamics-based transfection in animals by systemic administration of plasmid DNA.* Gene Ther, 1999. **6**(7): p. 1258-66.

29. Zhang, G., V. Budker, and J.A. Wolff, *High levels of foreign gene expression in hepatocytes after tail vein injections of naked plasmid DNA.* Hum Gene Ther, 1999. **10**(10): p. 1735-7.

30. Welch, J.M., J. Lu, R.M. Rodriguiz, *et al.*, *Cortico-striatal synaptic defects and OCD-like behaviours in Sapap3-mutant mice.* Nature, 2007. **448**(7156): p. 894-900.

31. Chen, S.K., P. Tvrdik, E. Peden, *et al.*, *Hematopoietic origin of pathological grooming in Hoxb8 mutant mice.* Cell, 2010. **141**(5): p. 775-85.

32. Shmelkov, S.V., A. Hormigo, D. Jing, *et al.*, *Slitrk5 deficiency impairs corticostriatal circuitry and leads to obsessive-compulsive-like behaviors in mice.* Nat Med, 2010. **16**(5): p. 598-602, 1p following 602.

33. Kalueff, A.V., A.M. Stewart, C. Song, *et al.*, *Neurobiology of rodent self-grooming and its value for translational neuroscience.* Nat Rev Neurosci, 2016. **17**(1): p. 45-59.

34. Dennis, E.A., J. Cao, Y.H. Hsu, *et al.*, *Phospholipase A2 enzymes: physical structure, biological function, disease implication, chemical inhibition, and therapeutic intervention.* Chem Rev, 2011. **111**(10): p. 6130-85.

35. Rakoff-Nahoum, S., *Why cancer and inflammation?* Yale J Biol Med, 2006. **79**(3-4): p. 123-30.

36. Loffredo, S., F. Borriello, R. Iannone, *et al.*, *Group V Secreted Phospholipase A2 Induces the Release of Proangiogenic and Antiangiogenic Factors by Human Neutrophils.* Front Immunol, 2017. **8**: p. 443.

37. Xu, P., B.A. Grueter, J.K. Britt, *et al.*, *Double deletion of melanocortin 4 receptors and SAPAP3 corrects compulsive behavior and obesity in mice.* Proc Natl Acad Sci U S A, 2013. **110**(26): p. 10759-64.

APPENDIX B

FUTURE PERSPECTIVE: TOWARDS TARGETING AT THE CELLULAR LEVEL[1]

[1] Yahya Alhamhoom, Mohammad Alsaggar and Dexi Liu (2015) Future perspective: toward targeting at the cellular level. In "*Advances and Challenges in the Delivery of Nucleic Acid Therapeutics (Volume 2)*", Edited by Olivia Merkel and Mansoor M. Amiji, Future Medicine, London, UK, pp 2-17.

Reprinted here with permission of the publisher.

B.1. Abstract

Despite progress in the clinical use of oligonucleotides pharmaceutics for the treatment of diseases, targeted delivery of oligonucleotides to selected cells remains a major challenge. In recent years, various approaches have been taken to overcome the hurdles toward cell-specific oligonucleotide delivery. Many systems have been developed based on the principles of chemistry, cell biology and physics. Some systems have advanced to clinical trials. The objective of this chapter is to provide a brief summary of various methods of oligonucleotide delivery developed thus far. Emphasis is placed on the rationale of each system, its advantage and disadvantages, and our perspective for future improvement.

B.2. Introduction

Since their discovery in the 1970s, oligonucleotide (ON) therapeutics have emerged and progressed rapidly as a useful tool in basic research, as well as a potential drug for treatment of diseases. Diverse classes of molecules have been explored using the principle of nucleic acid base paring including antisense DNA, ribozymes, siRNA, and aptamers [1]. Advances in nucleic acid chemistry have led to the development of ONs with derivatives in phosphate backbone, sugar moieties, or nucleotide bases with more desirable properties for better function, specificity, binding affinity, nuclease resistance, and pharmacokinetics. Many ON-based therapeutics are being tested in preclinical studies, and several are already in clinical trials for treatment of cardiovascular diseases, infectious (particularly viral) diseases, inflammatory diseases and cancer. To date, three ON pharmaceutics have reached the market and received USA FDA approval, the antiviral **fomiversin** (antisense ON) and anti-angiogenic **pegaptanib** (RNA aptamer) [2] and the cholesterol-reducing **mipomersen** (antisense ON) [3]. The remaining challenge for ON research is to increase its delivery to the desired site of action and minimize the off-target effect.

Formidable research has been conducted to develop an optimized delivery system to enhance safety, efficiency and specificity of ONs. The approaches taken include the use of chemical carriers and physical methods to overcome the physiological, biochemical and cellular barriers. The primary objective of this chapter is to review the basics of ON delivery systems as well as strategies developed to meet challenges toward organ- and cell-specific delivery of ON therapeutics. It also provides a summary on the ligands that have been explored for cell-specific delivery.

B.3. Basics of ON Delivery

Being part of DNA or RNA macromolecules, ONs are large, hydrophilic compounds that are biodegradable and unable to cross the cell membrane. To preserve their biological activity in target cells, ONs need to be protected prior to reaching their target cells and intracellular target RNAs. Cell-specific ON targeting aims to bring ONs from the site of administration to the cytoplasm of cells where therapy is needed. Target-specific delivery can be divided into two steps: delivering ONs from site of administration to target cells, and delivering ONs to intracellular targets. Development of a safe and efficient method in nucleic acid delivery has been the focus of many studies in the past few years, and the approaches taken can be summarized as follows:

B.3.1. *Bringing ONs to Target Cells*

The design of cell-specific targeting is largely dependent on cell location and tissue accessibility. For epidermis in skin or airway epithelial cells in the lung, ONs can be directly applied to the skin surface, or to the lung by aerosol or pulmonary instillation [4-6]. Similarly, ONs can be brought to their target cells by intratissue injection where, for example, intraperitoneal injection would allow ONs to reach cells accessible to the peritoneal cavity. Alternatively, intratissue injection allows delivery of ONs to cells on and near the needle track of targeted tissue or other cells that are reachable by diffusion. In fact, intramuscle, intrabrain and subcutaneous injections are the most common routes for ON administration. The major advantages of tissue-specific local administration are high selectivity and dose control at the injection site. However, local administration is normally invasive and not selective at the cellular level as all cells near the injection site are exposed. To overcome these limitations, in recent years, significant effort has been placed on developing cell-specific targeting via blood, commonly referred to as systemic

delivery, through which ONs are brought to cells through blood circulation. For systemic delivery of ONs, different backbones of ONs have been employed to prevent their degradation by serum nucleases, including peptide, methoxyethyl and phosphorothioate linkage bond [7]. In addition, encapsulation of ONs into a carrier such as liposomes, nanoparticles or polymeric nanoparticles [8] is another strategy to avoid nuclease- mediated ON degradation. Studies have shown that cell-specific targeting by systemic delivery can be achieved through two mechanisms, passive and active targeting [9].

Passive targeting is defined as a process where ONs reach target cells without an active mechanism to recognize target cells. A good example of passive targeting is accumulation of ON-carrying nanoparticles or macromolecules in a tumor after intravenous administration, a phenomenon called enhanced permeability and retention (EPR). The EPR effect has been observed exclusively in tumor-bearing animals and has served as the basis for nanomedicine [10]. Successful ON and gene delivery to cells in tumors has been achieved. A critical feature for EPR-based delivery is that ON-based pharmaceutics need to remain in blood circulation long enough to reach the leaky vasculature in the tumor and be retained, which can be achieved by coating the ONs or ON carriers by PEG [11].

An alternative type of passive targeting being explored relies on the anatomic structure of the vasculature or unique function of the target cells. For example, ON-containing particles, when larger than 1 μm, tend to accumulate in the lung after intravenous injection due to the small diameter of capillaries in the lung [12]. In fact, successful gene and ON delivery to lung endothelial cells have been performed in mice by tail vein injection of ONs or plasmid DNA complexed with cationic liposomes or cationic polymers. Gene/ON transfer to lung endothelial cells is primarily due to the large aggregates formed between the cationic nucleic acid/carrier complexes and anionic

components in the blood [13]. Similar success has also been reported in gene delivery to liver endothelial cells by portal vein injection, as large aggregates are retained in liver sinusoids. Targeting to liver hepatocytes requires smaller size ON-carrying particles in order to take advantage of liver fenestrae, with a diameter of less than 100 nm [12]. It has been shown in tumor-bearing mice that liposomes with long blood resident time primarily accumulate in the liver with a size below 80 nm, in the tumor at 90–200 nm, and in the spleen at greater than 300 nm [14]. Large-sized liposomes appear to be filtered by the meshwork in the spleen. This mechanism has been explored in delivery of an antigen to spleen cells to enhance immune response [15]. Targeted delivery to liver Kupffer cells using non-PEG-coating nanoparticles/liposomes and liver endothelial cells by adding acetyl modification of proteins or drug carriers has also been established.

Active targeting is a process, by which, cell-specific delivery is achieved by a targeting ligand linked covalently or noncovalently to ONs. Active targeting stresses the importance of specific markers on the cell surface. As expected, a variety of molecules have been studied as a targeting ligand for cell-specific delivery. **Table B.1** provides a summary of molecules that have been employed for target-specific ON delivery, including antibodies, ligands (hormones or growth factors) to cell-specific receptors, sugar moieties, aptamers and protein-derived peptides. In most cases, active targeting requires linking ON to a target ligand directly or indirectly. For direct linkage, the target ligand or proteins are directly conjugated to the oligonucleotide through a linker. This delivery system requires chemically modified ONs that are resistant to serum nucleases. ONs can also be delivered without direct conjugation to target ligands. For example, lipid particles or liposomes have been commonly employed for nucleic acid delivery. Gene or ONs can be encapsulated in the aqueous core of the liposomes in its native form, and the targeting ligands are

linked to the outer surface of the lipid bilayer via conjugation to lipids or other amphipathic molecules that are part of the lipid bilayer. Again, PEGylation of liposome surface with targeting ligands conjugated to the distal end of PEG molecules has been the most commonly used strategy in cell-specific delivery. For ON delivery, cationic lipids or polymers have been included in the liposome-based system to increase encapsulation efficiency. Other forms of particle-based carriers such as micelles, emulsion, ionic crystals, quantum dots, gold particle and polymer-based nanoparticles have been explored in cell-specific delivery [7, 16-19]. The success of active targeting via systemic administration depends on the accessibility of target cells in the blood, because diffusion of particle-based carriers beyond the cell layer with direct contact to blood is difficult or prohibitive.

Table B.1. Ligands employed for targeted oligonucleotide delivery.

Targeting Ligand	Target	Target Cells	Reference
Small molecules			
Folic acid	Folate receptor	Tumor cells	[20]
EC17, 20 and 145	Folate receptor	Tumor cells	[21]
Anisamide	Sigma-1 and 2 receptor	Tumor cells	[22]
Haloperidol	Sigma-1 and 2 receptor	Tumor cells	[23]
SV119	Sigma-2 receptors	Tumor cells	[24]
SCH221153	$\alpha_v\beta_3$ & $\alpha_v\beta_5$ integrins	Tumor endothelium	[25]
Cholesterol	Cholesterol receptors	Hepatocytes	[26]

Carbohydrates

Galactose	Lectins	Epithelial cells of GIT	[20]
Galactose	Asialoglycoprotein receptor	Hepatocytes	[27, 28]
Galactosylated lipids	Asialoglycoprotein receptor	Hepatocytes	[27]
Lactosylated lipoprotein	Asialoglycoprotein receptor	Hepatocytes	[27]
Lactosylated polymers	Asialoglycoprotein receptor	Hepatocytes	[27]
Mannose	Mannose receptor	Macrophages	
Mannose-6-phosphate	Mannose 6-phosphate/IGF II (M6P/IGF-II) receptor	Hepatic stellate cells with liver fibrosis	[27]
Lactose	Lactose receptor	Healthy & cystic fibrosis airway epithelial cells	[27]
Oligosaccharide	Selectins	Endothelial cells in inflamed/tumor tissue	[27]

Aptamers

Anti-TN-C aptamer	TN-C	Tumor extracellular matrix	[29]

FB4 aptamer	Transferrin receptor	Tumor cells and lysosomal storage diseases	[29]
MUC1 aptamer	MUC1	Tumor cells	[29, 30]
AS1411 aptamer	Nucleolin	Tumor cells	[29]
A9 & A10 anti-PSMA aptamers	PSMA	$PSMA^+$ prostate cancer cells	[29, 31]
Anti-EGFR aptamer	EGFR	Tumor cells	[29]
Anti-CD30 RNA aptamer	CD30	$CD30^+$ ALCL	
Anti-CD4 aptamer	CD4	$CD4^+$ T lymphocytes	
Anti-gp120 aptamer	gp120	HIV infected cells	[29, 31]
sgc8c aptamer	PTK7	Acute lymphoblastic leukemia	[31]
TD05 aptamer	Immunoglobin heavy Mu chain	B-cell lymphoma	[31]
Antibodies			
Anti-CD19 Ab	CD19 antigen	B cell lymphomas	
Anti-HER-2 Ab	HER-2 receptor	$HER2^+$ breast cancer	[26, 32]
Anti-CD33 mAb	CD33 (Gp67)	AML	[28]
J591 mAb	PSMA	$PSMA^+$ prostate cancer	[33]

RI7217	Transferrin receptor	Blood-brain barrier	[28]
Anti-gp120 Ab	gp120	$gp120^+$ cells	[32]
Anti-ErbB2 Ab (Herceptin™)	ErbB2	$ErbB2^+$ cells	[32, 34]
34A mAb	Aminopeptidase P	Pulmonary endothelium	
PR81 mAb	MUC-1 receptor	Breast cancer cells	
		B-lymphocyte antigen CD20	[34]
Gemtuzumab ozogamicin (Mylotarg™)	CD33	Acute myeloid leukemia	[35]
Alemtuzumab (Campath™)	CD52	Chronic lymphocytic leukemia	[35]
Avastin™	VEGFR-2	Tumor endothelium	[34]
Anti-VCAM-1 mAb	VCAM-1	Tumor endothelium	[34]
Anti-human MT1-MMP mAb	MT1-MMP	Tumor extracellular matrix	
Cetuximab (Erbitux™)	Epidermal growth factor receptor	Metastatic colorectal cancer	[34]
Peptides			
RGD	$\alpha_v\beta_3$ & $\alpha_v\beta_5$ integrins	Tumor endothelium	[36, 37]

RGD4C	$\alpha_v\beta_3$	Tumor endothelium	[37]
NGR	Aminopeptidase N/CD13	Dendritic cells and cancer cells	[36, 37]
Leptin30	Leptin receptor	Neurological disease	[37]
AHNP	ErbB2	Tumor cells	[36]
DV1 and DV3	CXCR4	$CXCR4^+$ Cancer cells	[36]
PEGA	Proline-specific aminopeptidase P	Tumor cells	[36]
CREKA	Clotted plasma proteins	Extracellular tumor matrix	[36]
Pep42	GRP78	Tumor cells	[36]
F3	Nucleolin	Tumor cells	[36, 37]
Tet1	G_{T1b}	Primary motor neurons and dorsal root ganglion cells,	[37]
RVG	Neural acetylcholine receptor	Neuronal cells	[37]
IGF II	Mannose-6-phosphate receptor	Tumor cells	[34]
MC11	FGFR	Tumor cells	[37]
GE11	HER1	Prostate and pancreatic cancer	[37]

YSA peptide	EphA2 receptor	$EphA2^+$ ovarian cancer cells	[37]
B6	Transferrin receptors	Tumor cells	[37]
LHRH	LHRH receptors	Tumor cells	[28, 37]
Peptide E	ICAM-1	Pulmonary epithelial cells	[37]
Peptide Y	NR	Pulmonary epithelial cells	[37]
Tenascin	$\alpha_9\beta_1$ integrin	Pulmonary epithelial cells	[37]
Secretin	Secretin receptor	Pulmonary epithelial cells	[37]
Molossin	$\alpha_v\beta_3$ and $\alpha_5\beta_1$ integrins	Corneal epithelial cells	[37]

ALCL: anaplastic large-cell lymphoma; AML: Acute myeloid leukemia; GRP78: Glucose-regulated protein 78; LHRH: Luteinizing hormone releasing hormone; PTK7: Protein tyrosine kinase 7; TN-C: Tenascin-C

Replication-deficient viruses, commonly used for gene therapy, have also been employed as a carrier for ONs [38]. At experimental level, the coding sequence for a short RNA is cloned into the viral genome. Once delivered, the desirable RNA fragments are made available in cells by transcription of the inserted coding sequence. Cell-specific targeting can be achieved by making a

fusion protein between the viral capsid protein and part or whole of protein ligand using techniques of recombination. For example, the attachment protein of lentiviral vectors has been replaced with a glycoprotein derived from Lyssavirus resulting in the production of a viral vector with specific targeting to neurons [39]. Another example of viral vector mediated delivery involves the use of the protein that binds to the CD40 receptor which is expressed on dendritic cells. Experimentally, the targeting protein was fused to the coxsackievirus-adenovirus receptor protein, and the receptor–ligand complex allowed adenoviral vectors to target dendritic cells [40]. In principle, any protein or peptide can be incorporated into a viral vector to achieve nucleic acid transfer to selected cells. However, it is important to note that the insertion of a fragment of protein into a viral protein could lead to alteration of viral function critical for gene delivery.

B.3.2. *Endosomal Escape and Intracellular Delivery*

Since ONs cannot easily permeate the cell membrane, a mechanism to ensure that ONs reach their interior target of cells is necessary. Success of ON internalization is dependent, to a large degree, on the properties of cells and selected target ligands. It can also be facilitated or enhanced using physical or chemical methods. In most cases, cell-targeted ONs or gene delivery relies heavily on the cellular function of endocytosis, which is a process in which cells absorb and internalize large molecules or particles. A natural process of endocytosis comprises three stages. The early endosome represents the early stage of endocytosis where proton-ATPase in endosome starts decreasing the pH inside the endosome. The late endosome is a later stage of endocytosis where the pH in endosomes becomes more acidic (pH ~4.5–5.5). The last stage involves fusion of enzyme-carrying lysosome with late-stage endosome and degradation of the content internalized. While endocytosis is a common property of cells, some cells appear more active than others, which

significantly affects the outcome of cell-targeted delivery. Studies have shown that the majority of delivered ON is degraded in the lysosome, making endocytosis an inefficient pathway for intracellular delivery. Approaches taken to overcome endocytosis-mediated degradation include the use of chemical structures that can neutralize the low pH in the early endosome, inclusion of pH-sensitive lipids into liposomes to induce membrane fusion before reaching the late endosome, or the use of cationic polymers or viral proteins capable of inducing the release of the delivered substance into the cytoplasm before being degraded. Evidently, target ligands capable of inducing endocytosis are preferred in order to warrant intracellular delivery. However, an additional mechanism is needed to achieve intracellular delivery without delivering ONs to lysosomes for degradation. It is also important to note that not all cells actively endocytose, especially under physiological conditions. This would explain, at least in part, why passive targeting of drug-carrying nanoparticles to tumor sites does not always yield significant therapeutic benefits in cancer therapy.

Various approaches have been taken in enhancing intracellular delivery once ONs reach the surface of target cells. For example, an electric pulse has been applied to tissues where nucleic acids have been injected. The technique of electroporation has been employed in treatment of melanoma in clinical trials [41]. Successful gene transfer to lung epithelial cells has also been reported in pigs where electric pulses are applied to the chest, while plasmid DNA was instilled into the lung via the airways [42]. These results suggest that this approach can be effectively applied to the delivery of oligonucleotides to cells in different tissues. As an extracorporeal stimulus, ultrasound, another physical method employed to enhance intracellular transfer, can noninvasively and transiently compromise cell membrane permeability, thereby, delivering ON-based therapeutics to cells and tissue in a site- and tissue- specific manner. The principle of

hydrodynamic gene delivery, the most effective method for gene delivery to mice livers via tail vein injection [43], has been utilized to enhance peptide-based gene and ON delivery *in vivo* [44]. As expected, approaches that combine passive with active targeting have been employed for ON or gene delivery with success [45], especially for targeted drug delivery in treatment of cancer where a tumor-specific ligand or antibody has been employed to enhance the binding and increase drug internalization, once reaching the tumor site via the EPR effect.

B.4. Future Perspectives

Despite the promising therapeutic potential for ON technology in the treatment of human diseases, several barriers often limit ON delivery to the intracellular site of action. Thus, the focus of future work is not only on ONs with better affinity and specificity, but also on issues of efficient delivery and targeting. Given recent advances accomplished thus far, technologies for targeted delivery will potentially drive future developments of ON therapeutics.

To elicit therapeutic effects, systemically administered ONs should survive in circulation and reach their target tissue, where they are internalized by target cells, released from endosomes and hybridize with target mRNA to inhibit its translation. However, this process is truly challenging, as there are various physiological and cellular barriers encountered by ONs that limit their delivery and hence, their therapeutic value. In fact, the impacts of the barriers are more prominent to the delivery of plasmid DNA coding for therapeutic ONs than those of synthetic ONs. This is because ONs are typically less than 30 nt or bp, while DNA plasmids are usually greater than 5 kb. In addition, the synthetic nature of ONs allows large-scale production of purematerials, and also enables introduction of chemical modifications to improve metabolic stability, bioavailability and cell-targeting potential [46].

During the process of delivery to target tissue, ONs travel across various physiological compartments that limit the amount delivered to target cells. Among these physiological barriers are serum and tissue nucleases, elimination of ONs by metabolism and/or excretion, and extravasation through vascular endothelium. Serum and tissue nucleases are the first barriers encountered by systemically administeredONs, accounting for the relatively short half-life of ONs in circulation. Several strategies have been developed to improve ON stability against nucleases, including chemical modifications of sugar moieties at 2′-OH group, replacement of oxygen by sulfur to form phosphorothioate ONs and chemical complexation with nonviral vectors. ONs associated with nanocarriers suffer size and charge-related hepatic clearance and RES uptake. Prolonged circulation of ONs can be achieved by careful optimization of the size and charge of ON carriers using PEG-coating technologies to impart a protective sheath surrounding the final complex. Moreover, size optimization will also help escaping glomerular filtration of 5 nm or smaller nanocarrier systems, thereby avoiding loss through the renal route. One more barrier is presented by vascular endothelium, as ONs and their carriers have to traverse across tightly adhered endothelial cells to reach cells of interest. The endothelial barrier can be overcome using physical methods of gene transfer that translocate ON pharmaceuticals directly into target cells, or by the use of cell penetrating peptides, along with targeting ligands to pass through tight intracellular junctions [47].

Barriers encountered after reaching target cells include cell entry and endosomal escape. Although nonviral vectors greatly enhance cell entry, the cationic nature of these complexes renders them nonspecific, as being attracted to ubiquitously available nontarget anionic membranes. Targeting ligands discussed earlier assist in reducing nonspecific cell uptake. At the cellular level, the fate of internalized ON carriers is either to be returned to the cell surface, as in

the case of recycling endosomes, or proceed via late endosomes to the degrading lysosomes. Failure to escape from the endosome results in a significant reduction in intracellular bioavailability of ONs and an inability to reach the actual intracellular target. Incorporation of fusogenic lipids or peptides, in forming pores and eventually rupturing lysosomal membranes, became the most widely used strategy to facilitate endosomal escape. Likewise, the use of carrier systems with a high buffering capacity or osmolytic agents, such as polyethylinimine and chloroquine, respectively, results in disruption of the endosomal membrane and release of ONs into the cytoplasm.

In addition to systemic and intracellular barriers to ONs delivery, clinical application of ON therapeutics could also be hindered by the innate and adaptive immune responses to ONs and/or the carriers. It has been shown that immune response against viral vectors diminishes the activity of subsequently injected viral vectors. Immune responses to DNA sequences with unmethylated CpG motifs, an innate immune response of ONs mediated by a set of TLR [48] on macrophages, have been reported [49]. Therefore, future work should consider chemical modifications of ONs in enhancing immune evasion. Indeed, 2′-OH methylation, originally proposed to overcome nuclease stability, was accompanied by decreased immunogenic potential. Alternatively, less immunogenic viral vectors, CpG-depleted plasmids and less toxic nanocarrier systems will also drive the future of ON therapeutics toward an enhanced safety profile and more sustained therapeutic effects of ONs.

While ON therapeutics must overcome barriers for future success, significant advances have taken place in ON technologies, bringing the field to the verge of success. New delivery systems that address various related challenges, and breakthroughs in delivery technology are constantly underdevelopment and will pave the way for clinical application of ONs for disease

treatment. Novel chemistries for structural modifications and ligand conjugation to maximize potency while minimizing off-target toxicity and immunogenicity of ONs are particularly promising. Given the solid progress in preclinical and early clinical trials accomplished thus far, ON therapeutics have reached an exciting stage and become a forefront in biomedical research.

B.5. Summary

- Clinical progress of oligonucleotide ON therapeutics is challenged by inefficient delivery and off-target effects.
- Various systems have been developed for ON targeted delivery, aiming at overcoming delivery barriers, and minimizing systemic toxicity.
- Passive targeting relies on exploiting the anatomy of the body and/or physiological status of the pathological tissue to target a specific organ or tissue.
- Active targeting, involving both viral and non-viral carriers, utilizes a targeting ligand with specificity toward a receptor preferentially expressed in specific cells or tissue.
- Cellular endocytosis and lysosome escape are rate-limiting steps to achieve successful intracellular delivery. Local injection and physical methods of ON delivery have great potential for rapid progress, as they avoid various ON delivery barriers.

Key Terms

Oligonucleotide Delivery: bringing therapeutic ONs to the site of action.

Cell-specific Targeting: tailored delivery of ONs to a particular tissue or cell type, along with minimum exposure of nontarget cells.

Nanocarrier: specialized delivery systems, with nanoscale size, function as shuttles for ONs to reach the target.

Intracellular Delivery: delivering therapeutic ONs into cell cytoplasm untouched, or with minimal dose loss, by overcoming various intracellular barriers.

Financial & Competing Interests Disclosure

The authors have no relevant affiliations or financial involvement with any organization or entity with a financial interest in or financial conflict with the subject matter or materials discussed in the manuscript. This includes employment, consultancies, honoraria, stock ownership or options, expert testimony, grants or patents received or pending or royalties.

No writing assistance was utilized in the production of this manuscript.

B.6. References:

1. Goodchild, J., *Therapeutic oligonucleotides.* Methods Mol Biol, 2011. **764**: p. 1-15.

2. Kole, R., A.R. Krainer, and S. Altman, *RNA therapeutics: beyond RNA interference and antisense oligonucleotides.* Nat Rev Drug Discov, 2012. **11**(2): p. 125-40.

3. Thomas, G.S., W.C. Cromwell, S. Ali, *et al.*, *Mipomersen, an apolipoprotein B synthesis inhibitor, reduces atherogenic lipoproteins in patients with severe hypercholesterolemia at high cardiovascular risk: a randomized, double-blind, placebo-controlled trial.* J Am Coll Cardiol, 2013. **62**(23): p. 2178-84.

4. Mehta, R.C., K.K. Stecker, S.R. Cooper, *et al.*, *Intercellular Adhesion Molecule-1 Suppression in Skin by Topical Delivery of Anti-Sense Oligonucleotides.* Journal of Investigative Dermatology, 2000. **115**(5): p. 805-812.

5. Podolska, K., A. Stachurska, K. Hajdukiewicz, *et al.*, *Gene therapy prospects--intranasal delivery of therapeutic genes.* Adv Clin Exp Med, 2012. **21**(4): p. 525-34.

6. Zarogouldis, P., N.K. Karamanos, K. Porpodis, *et al.*, *Vectors for inhaled gene therapy in lung cancer. Application for nano oncology and safety of bio nanotechnology.* Int J Mol Sci, 2012. **13**(9): p. 10828-62.

7. Guzman-Villanueva, D., I.M. El-Sherbiny, D. Herrera-Ruiz, *et al.*, *Formulation approaches to short interfering RNA and MicroRNA: challenges and implications.* J Pharm Sci, 2012. **101**(11): p. 4046-66.

8. David, S., B. Pitard, J.P. Benoit, *et al.*, *Non-viral nanosystems for systemic siRNA delivery.* Pharmacol Res, 2010. **62**(2): p. 100-14.

9. Torchilin, V.P., *Passive and active drug targeting: drug delivery to tumors as an example.* Handb Exp Pharmacol, 2010(197): p. 3-53.

10. Matsumura, Y. and H. Maeda, *A new concept for macromolecular therapeutics in cancer chemotherapy: mechanism of tumoritropic accumulation of proteins and the antitumor agent smancs.* Cancer Res, 1986. **46**(12 Pt 1): p. 6387-92.

11. van Vlerken, L.E., T.K. Vyas, and M.M. Amiji, *Poly(ethylene glycol)-modified nanocarriers for tumor-targeted and intracellular delivery.* Pharm Res, 2007. **24**(8): p. 1405-14.

12. Song, Y.K., F. Liu, S. Chu, *et al.*, *Characterization of cationic liposome-mediated gene transfer in vivo by intravenous administration.* Hum Gene Ther, 1997. **8**(13): p. 1585-94.

13. Liu, F., H. Qi, L. Huang, *et al.*, *Factors controlling the efficiency of cationic lipid-mediated transfection in vivo via intravenous administration.* Gene Ther, 1997. **4**(6): p. 517-23.

14. Liu, D., A. Mori, and L. Huang, *Role of liposome size and RES blockade in controlling biodistribution and tumor uptake of GM1-containing liposomes.* Biochimica et Biophysica Acta (BBA) - Biomembranes, 1992. **1104**(1): p. 95-101.

15. Liu, D.X., A. Wada, and L. Huang, *Potentiation of the humoral response of intravenous antigen by splenotropic liposomes.* Immunol Lett, 1992. **31**(2): p. 177-81.

16. Guo, S., Y. Huang, Q. Jiang, *et al.*, *Enhanced Gene Delivery and siRNA Silencing by Gold Nanoparticles Coated with Charge-Reversal Polyelectrolyte.* ACS Nano, 2010. **4**(9): p. 5505-5511.

17. Han, H., J. Zylstra, and M.M. Maye, *Direct Attachment of Oligonucleotides to Quantum Dot Interfaces.* Chemistry of Materials, 2011. **23**(22): p. 4975-4981.

18. Cutler, J.I., D. Zheng, X. Xu, *et al.*, *Polyvalent Oligonucleotide Iron Oxide Nanoparticle "Click" Conjugates.* Nano Letters, 2010. **10**(4): p. 1477-1480.

19. Qin, B., Z. Chen, W. Jin, *et al.*, *Development of cholesteryl peptide micelles for siRNA delivery.* J Control Release, 2013. **172**(1): p. 159-68.

20. Vasir, J., M. Reddy, and V. Labhasetwar, *Nanosystems in Drug Targeting: Opportunities and Challenges.* Current Nanoscience, 2005. **1**(1): p. 47-64.

21. Low, P.S. and S.A. Kularatne, *Folate-targeted therapeutic and imaging agents for cancer.* Curr Opin Chem Biol, 2009. **13**(3): p. 256-62.

22. Li, S.D. and L. Huang, *Targeted delivery of antisense oligodeoxynucleotide and small interference RNA into lung cancer cells.* Mol Pharm, 2006. **3**(5): p. 579-88.

23. Vilner, B.J. and W.D. Bowen, *Sigma receptor-active neuroleptics are cytotoxic to C6 glioma cells in culture.* Eur J Pharmacol, 1993. **244**(2): p. 199-201.

24. Kashiwagi, H., J.E. McDunn, P.O. Simon, Jr., *et al.*, *Selective sigma-2 ligands preferentially bind to pancreatic adenocarcinomas: applications in diagnostic imaging and therapy.* Mol Cancer, 2007. **6**: p. 48.

25. Kumar, C.C., M. Malkowski, Z. Yin, *et al.*, *Inhibition of angiogenesis and tumor growth by SCH221153, a dual alpha(v)beta3 and alpha(v)beta5 integrin receptor antagonist.* Cancer Res, 2001. **61**(5): p. 2232-8.

26. Guo, P., O. Coban, N.M. Snead, *et al.*, *Engineering RNA for targeted siRNA delivery and medical application.* Adv Drug Deliv Rev, 2010. **62**(6): p. 650-66.

27. Zhang, H., Y. Ma, and X.L. Sun, *Recent developments in carbohydrate-decorated targeted drug/gene delivery.* Med Res Rev, 2010. **30**(2): p. 270-89.

28. Trapani, G., N. Denora, A. Trapani, *et al.*, *Recent advances in ligand targeted therapy.* J Drug Target, 2012. **20**(1): p. 1-22.

29. Ray, P. and R.R. White, *Aptamers for Targeted Drug Delivery.* Pharmaceuticals, 2010. **3**(6): p. 1761-1778.

30. Rahn, J.J., L. Dabbagh, M. Pasdar, *et al.*, *The importance of MUC1 cellular localization in patients with breast carcinoma: an immunohistologic study of 71 patients and review of the literature.* Cancer, 2001. **91**(11): p. 1973-82.

31. Li, X., Q. Zhao, and L. Qiu, *Smart ligand: aptamer-mediated targeted delivery of chemotherapeutic drugs and siRNA for cancer therapy.* J Control Release, 2013. **171**(2): p. 152-62.

32. Ikeda, Y. and K. Taira, *Ligand-targeted delivery of therapeutic siRNA.* Pharmaceutical Research, 2006. **23**(8): p. 1631-1640.

33. Liu, H., A.K. Rajasekaran, P. Moy, *et al.*, *Constitutive and antibody-induced internalization of prostate-specific membrane antigen.* Cancer Res, 1998. **58**(18): p. 4055-60.

34. Muro, S., *Challenges in design and characterization of ligand-targeted drug delivery systems.* Journal of Controlled Release, 2012. **164**(2): p. 125-137.

35. Schrama, D., R.A. Reisfeld, and J.C. Becker, *Antibody targeted drugs as cancer therapeutics.* Nat Rev Drug Discov, 2006. **5**(2): p. 147-59.

36. Svensen, N., J.G. Walton, and M. Bradley, *Peptides for cell-selective drug delivery.* Trends Pharmacol Sci, 2012. **33**(4): p. 186-92.

37. Levine, R.M., C.M. Scott, and E. Kokkoli, *Peptide functionalized nanoparticles for nonviral gene delivery.* Soft Matter, 2013. **9**(4): p. 985-1004.

38. Bouard, D., D. Alazard-Dany, and F.L. Cosset, *Viral vectors: from virology to transgene expression.* Br J Pharmacol, 2009. **157**(2): p. 153-65.

39. Desmaris, N., A. Bosch, C. Salaun, *et al.*, *Production and neurotropism of lentivirus vectors pseudotyped with lyssavirus envelope glycoproteins.* Mol Ther, 2001. **4**(2): p. 149-56.

40. Pereboev, A.V., J.M. Nagle, M.A. Shakhmatov, *et al.*, *Enhanced Gene Transfer to Mouse Dendritic Cells Using Adenoviral Vectors Coated with a Novel Adapter Molecule.* Molecular Therapy, 2004. **9**(5): p. 712-720.

41. Daud, A.I., R.C. DeConti, S. Andrews, *et al.*, *Phase I trial of interleukin-12 plasmid electroporation in patients with metastatic melanoma.* J Clin Oncol, 2008. **26**(36): p. 5896-903.

42. Dean, D.A., M. Barravecchia, B. Danziger, *et al.*, *Use of Electroporation for Efficacious Gene Delivery to the Lungs.* 2011: p. 167-177.

43. Suda, T. and D. Liu, *Hydrodynamic Gene Delivery: Its Principles and Applications.* Molecular Therapy, 2007. **15**(12): p. 2063-2069.

44. Fernandez, C.A., N.J. Baumhover, J.T. Duskey, *et al.*, *Metabolically stabilized long-circulating PEGylated polyacridine peptide polyplexes mediate hydrodynamically stimulated gene expression in liver.* Gene Ther, 2011. **18**(1): p. 23-37.

45. Master, A.M. and A. Sen Gupta, *EGF receptor-targeted nanocarriers for enhanced cancer treatment.* Nanomedicine (Lond), 2012. **7**(12): p. 1895-906.

46. Yu, B., X. Zhao, L.J. Lee, *et al.*, *Targeted delivery systems for oligonucleotide therapeutics.* AAPS J, 2009. **11**(1): p. 195-203.

47. Juliano, R., M.R. Alam, V. Dixit, *et al.*, *Mechanisms and strategies for effective delivery of antisense and siRNA oligonucleotides.* Nucleic Acids Res, 2008. **36**(12): p. 4158-71.

48. Robbins, M., A. Judge, and I. MacLachlan, *siRNA and innate immunity.* Oligonucleotides, 2009. **19**(2): p. 89-102.

49. Scheule, R., *The role of CpG motifs in immunostimulation and gene therapy.* Advanced Drug Delivery Reviews, 2000. **44**(2-3): p. 119-134.